Doctoral Dissertation

博士論文

Development of Muscle Function Evaluation and Training Support System for Slowing the Progress of Frailty

March 2020

令和 02 年 3 月

XU Taojin

徐 涛金

Graduate School of Sciences and Technology for Innovation

Yamaguchi University

山口大学 大学院創成科学研究科

Content

Abstract

Frailty is a common geriatric disease among elderly people, including mental frailty, social frailty and physical frailty. Physical frailty can seriously affect oral function, mobility function and upper limb function of the elderly, and ultimately lead to a decline in quality of daily life. Moreover, frailty is a dynamic process from healthy to disability and incorporates multiple stages. People in apparently vulnerable and mildly frail stage are more likely to enter the next stage. Recognizing physical frailty at its early stage, choosing the appropriate intervention treatment and routine exercise are important for slowing the progress of frailty.

Recently, evaluation of physical frailty mainly focus on oral function, mobility and upper limb function. Muscle strength, exercise control ability, and exercise tolerance are related to muscle function and are closely related to daily life and activities. Considerable evidence suggests that the ability to perform a physical task is determined by a threshold level of muscular strength and endurance. Individuals lacking the requisite muscular strength may not be able to perform various activities of daily living that are important determinants of independence. At present, the Japanese version of the Cardiovascular Health Study (J-CHS) criteria is commonly used for assessing frailty in japan from five aspects which are walking speed, muscular strength (hand grip strength), low activity, weight loss and exhaustion. Even there are some descriptive evaluation methods available for evaluation of frailty based on questionnaire, quantitative evaluation methods are not yet fully established. Therefore, means and methods for assessing frailty are highlights of recent research.

The main purpose of this paper is to develop a muscle function evaluation and training support system for the purpose of slowing the progress of frailty. Firstly, an analytical muscle model was established to estimate muscular states and a motion capture system was established to measure upper limb movement. Later, the muscle model is used

to establish the criteria of normal people which is used as a reference standard for assessing frailty level. Finally, a training support system was established for helping trainee perform the appropriate exercise while recording the training dose and frailty state.

This doctoral dissertation contains 6 chapters:

In Chapter 1, the aging society and the prevalence of frailty were reviewed, conceptual and intuitive images about the frailty were presented, means and methods of frailty evaluation were introduced, and finally, the purpose and research outline of this manuscript were drawn.

In Chapter 2, we use the method of musculoskeletal modeling to estimate muscle state during exercise. An evaluation method for quantifying function of a specific muscle during upper limb exercise training was proposed. A detailed three-dimensional model of the upper extremity, including major muscles make up the elbow flexor and extensor, was built base on public references and database. The modeling process and principle were introduced in detail. At last, the exercise of biceps curl to lift a dumbbell was simulated to verify the effect of each muscle.

In Chapter 3, the development of muscle function measurement and evaluation system are described in detail. The system incorporates an acceleration and a gyro sensor, a load cell, a camera and a personal computer for data collection and display. Forearm movement is measured using a wireless transmission module and gyro sensor. The force during resistance training is measured by attaching a load cell to Thera-Band. Posture changes are estimated using camera and OpenPose. A segmentation algorithm is proposed segment the data in to small segments. At last, indexes for quantifying fatigue and recovery ability, muscle motion control ability and exercise tolerance were proposed to assess muscle function.

In Chapter 4, based on indexes proposed in Chapter 3, the physical frailty of subject is evaluated from the perspective of muscle strength, motion control ability and endurance.

We firstly show how to assess frailty level based on muscle strength. The muscle model is used to establish a reference standard for assessing frailty level. Later, we use the quotient of acceleration and deceleration time during flexing stage to quantify motion control ability of elbow flexor. The coefficient of variation of force data during holding phase was used to quantify exercise tolerance. A larger quotient means a longer acceleration phase and a stronger ability of subject to control his flexor muscle, and a bigger coefficient of variation means a bigger fluctuation in force, which means a low ability of subject in keeping the force at a constant value. By using those indexes, the physical frailty state of subject can be determined.

Chapter 5 describes the application of our system in the field of muscle rehabilitation. The muscle model established in Chapter 2 is used to estimate muscular states during elbow flexor resistance training for bedridden patient. The fatigue and recovery indexes proposed in Chapter 3 were used to monitor subjects' fatigue state in the training. At last, a support system was established to encourage trainee to continue training while recording the training dose and frailty state.

The conclusion is drawn and the future work is discussed in Chapter 6.

要旨

虚弱（フレイル）には、精神的虚弱と社会的虚弱、身体的虚弱があり、高齢者化の進行に伴う老人性疾患である。フレイルは、高齢者の口腔機能、運動機能および上肢機能に深刻な影響を及ぼし、最終的には日常生活の質の低下につながる。また、フレイルは健康から障害までの動的なプロセスであり、明らかに脆弱で軽度の段階にある人は、次の中度・重度の段階に入っていく。フレイルの状態を早期に認識し、介入治療または日常予防を適切に取り組むことで、その進行を遅らせることが可能である。

身体フレイルの評価は、主に口腔機能、運動性および上肢機能に焦点を当てている。評価量として、咬合力、筋肉量、歩行速度、握力、身体活動状況などが上げられる。筋力、運動制御能力、および運動耐性は筋肉機能に関わるもので、日常生活・活動と密接に関連する。現在、日本におけるフレイルの評価方法に、日本版 CHS 基準（Cardiovascular Health Study）が適用され、歩行速度、筋力（握力）、活動性低下、体重減少、倦怠感・易疲労感の 5 項目を指標にしている。アンケート設問による評価を中心としており曖昧さが残るものの、フレイルを定量的に評価する方法はまだ十分に確立されていないため、フレイルの評価手段、評価方法等は、近年に注目されている研究課題である。

本論文では、上肢機能を対象とし、上肢の運動をウェアラブル加速度センサ、ロードセル、カメラなどで計測する簡便なシステムを構築することと、上肢筋力の解析モデルに基づき上腕の運動量から筋力の強度を評価する方法を開発する。また、筋力解析モデルに基づきフレイルに関する評価指数を提案する。さらに、筋力低下の進行を遅らせることを目指して、フレイルの状態を記録・表示しつつ、適切な運動を行える筋力トレーニング支援システムを考案し開発する。

本論文は緒論・ 結言を含め 6 章から構成されている 。

第 1 章では、フレイルの概念、高齢化に伴うフレイルの社会問題、フレイルの

状態を早期認知し予防することの重要性を述べ、現在フレイルの評価方法と基準化の取り組みを紹介するとともに、本論文の目的と取組を紹介する。

第 2 章では、筋骨格モデリングを使用して運動中の筋肉の状態を推定し、上肢運動トレーニングによる特定の筋肉の作用と、機能を定量化するための上肢筋力解析モデルを提示する。上肢の肘関節運動は、主に肘の屈筋と伸筋の作用によるもので、これらの 3 次元筋力モデルを、パブリックリファレンスとデータベースに基づいて構築し、その解析方法を提示する。例としてダンベルを持ち上げるための上腕７つの筋力シミュレーションを行い、各筋肉の作用効果ならびに解析モデルの妥当性を検証する。

第 3 章では、筋力機能の測定および評価システムの開発について説明する。本システムは、加速度センサ・ジャイロセンサ、ロードセル、カメラと、データ収集と表示のための PC から構成される。上腕の運動を無線加速度センサとジャイロセンサで計測し、上腕運動時にかかる負荷は、Thera-Band にロードセルを取り付けて計測する。姿勢変化等は、カメラで計測し OpenPose 技術を用いて推定する。具体的に、肘の曲げ伸ばし運動を行う際に、ロードセルによる抵抗力を記録、加速度・ジャイロセンサによる肘の運動を計測、得られたデータに対して上肢の各運動状態に分割、疲労および回復能力、筋肉運動能力、運動耐性を評価する解析アルゴリズムを開発し、筋力・運動機能を評価する方法を提案する。

第 4 章では、第 3 章で提案した筋力と運動機能の評価方法とアルゴリズムを用い、筋肉強さの観点から身体の脆弱性を評価することを検討する。複数の被験者に対して、肘の曲げ伸ばし運動実験を実施し、屈筋の運動能力と運動耐性を評価することを試みる。曲げまたは伸ばし各段階における加速区間の時間と減速区間の時間の比を用いて、肘屈筋の運動制御能力を定量化する。比が大きいと、加速段階が長くなり、被験者が屈筋を制御する能力が強いことを示す。保持フェーズ中の力変動係数を使用して、運動耐性を定量化する。変動係数が大きいほど、被験者が力を一定値に保つ能力が低いことを意味する。これらのパラメータを定量化することで、フレイルの状態を把握可能と考えられる。さらに、移動機能に関わる歩行障害の出現が、プレフレイルの段階から身体機能障害の発生に関連することに着目し、杖な

どを使用して歩行支援するために必要な上肢筋力を算出して、上肢筋力を計測・評価する手法を提案するとともに、上腕筋力によるプレフレイルやフレイルの評価基準値を検討する。

第 5 章では、筋力リハビリテーションへの応用を目指すためトレーニングシステムを構築する。第 3 章の計測と評価システムを改良し、第 2 章で提案した筋力解析モデルを組み込んだ、上肢トレーニングシステムを構築する。上腕の運動状態と筋力強度の状況をモニタリングしながら、目標値を設定してトレーニングするハードウェア並びにソフトウェアを開発する。

第 6 章では、この研究の結論と今後の展望について述べる。

Chapter 1

Introduction and Literature Review

This chapter clarify the main purpose and organization of this doctoral dissertation. We firstly talk about the healthy and unhealthy life expectancy, show the prevalence of frailty among elderly people. And then, present the conceptual and intuitive images about the frailty to give readers a clear understanding of frailty. Meanwhile, quantitative criteria for evaluation of physical function of frail elderly are introduced for choosing the right exercise intervention for treatment of frailty. Finally, the purpose and research outline of this manuscript is drawn.

1. Research background

1.1 Healthy and Unhealthy life expectancy

Initiated in 2013, one of the main purpose of the Health Japan 21 (the second term) [1], a health policy established by the Minister of Health, Labour, and Welfare of Japan, is to extend people's healthy life expectancy, and finally, to save social health care expenditure. The healthy life expectancy is the average period during which people can live independently and healthily. The Average life expectancy is the expectation of how many years a person can live at the age of 0. The difference between healthy life expectancy and average life expectancy is the unhealthy life expectancy. According to a data from Ministry of Health, Labour and Welfare of Japan [3] (Figure 1.1), the healthy life expectancy is about 71.19 years for male subjects and about 74.21 years for female subjects. Moreover, the unhealthy life expectancy is about 9.02 years for male subjects and 12.4 years for female subjects. After getting into the unhealthy state, people's ability to perform daily tasks slowly erodes until, at some stage, they become dependent on others for home help, or possibly residential care or long-term care in a hospital. That is why those people are high frequency users of health care systems, like hospital, nursing home, and rehabilitation center. This will places a very heavy burden on the

social health care system and medicare. Therefore, to save social health care expenditure, we need extend people's healthy life expectancy and shorten people's unhealthy life expectancy.

People's average life expectancy is usually the same, but the healthy life expectancy is inhibited by various diseases. According to a survey performed by the Ministry of Health, Labour and Welfare of Japan [3], it reveals that the frailty is the third leading factor that inhibits people's healthy life expectancy, following the Stroke and Cognitive disorder. Therefore, to extend people's healthy life expectancy, research on slowing the progress of frailty it is important and necessary.

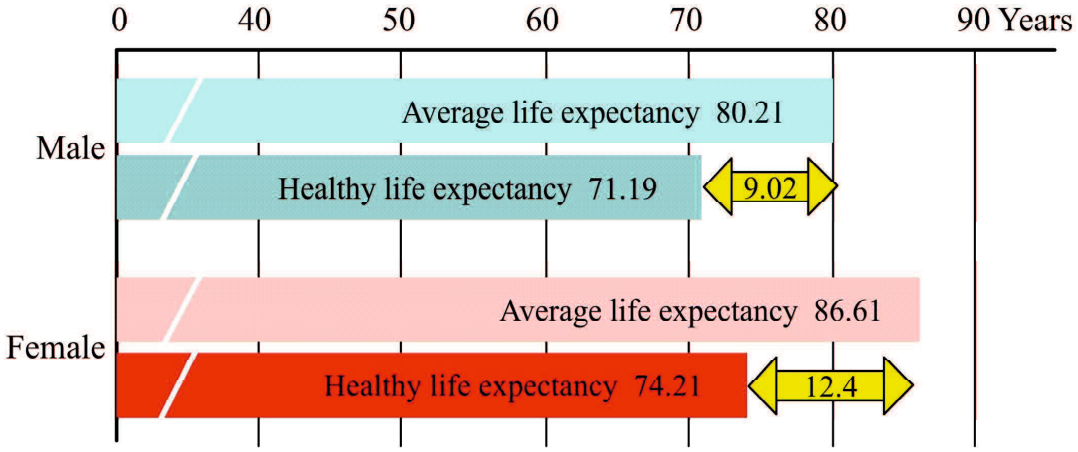

Figure 1.1 Difference between Average and Healthy life expectancy. Data obtained from the Ministry of Health, Labour and Welfare of Japan [3].

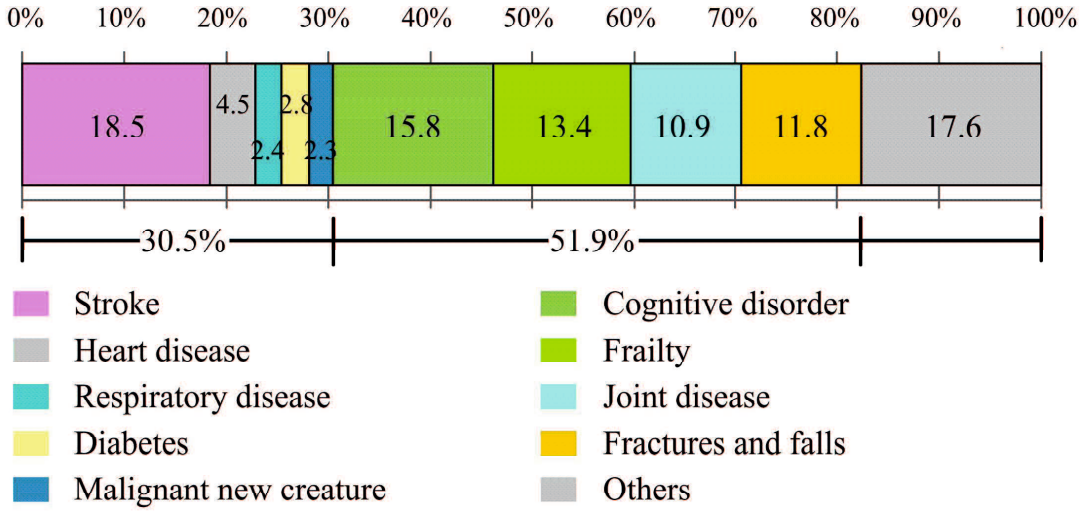

Figure 1.2 Factors that inhibit healthy life expectancy. Among those factors, the stroke, heart disease, respiratory disease, diabetes and malignant new creature are diseases associated with lifestyle habits, which counted for 30.5% of the total factors. The cognitive disorder, frailty, joint disease, fracture and falls are diseases related to geriatric diseases, which counted for 51.9% [3].

1.2 The prevalence of frailty among the elderly

The world's population is aging, albeit at different rates in different countries. Data from the Department of Economic and Social Affairs in the United Nations reveals that the population aged 60 years or over numbered 962 million in 2017, more than twice as large as in 1980 when there were 382 million older persons worldwide [4]. By 2050, the elderly population is expected to double again, with an estimated total of nearly 2.1 billion, accounting for 21.5% of the global population [5]. Although the population aging is a global phenomenon, virtually every country in the world will experience a substantial increase in the size of the population aged 60 years or over, however, there is a huge difference between the ageing rate and the current social age structure [6,7], especially in developed countries like Japan and Korea.

In Japan, the aging population is particularly serious, and it is now experiencing a pronounced aging population. Researchers even use the term of “super-aging” society [8] to express the severity of the situation. As illustrated in Figure 1.3, Japan has the highest proportion of elderly adults in the world [8,9,10], now with over 28.4% of the population aged 65 and over [11] and the number will reach 40% by 2050 [8]. Rapid declines in mortality and baby booms after World War II contributed to the population aging in Japan, and the critical contributor to population aging is the rapidly declining fertility. Because the elderly people are often cognitively impaired or limb function disabled, they are high-frequency users of community resources, hospitalization, and nursing homes. The rapidly growing old population drives increasing long-term care costs and work force shortages, and thus poses a challenge for health care and social services [12]. The situation will get worse when the second baby boomers reach their 65s. It is critical to develop and strengthen support systems for those elderly people, especially for those with limited physical and cognitive function [7].

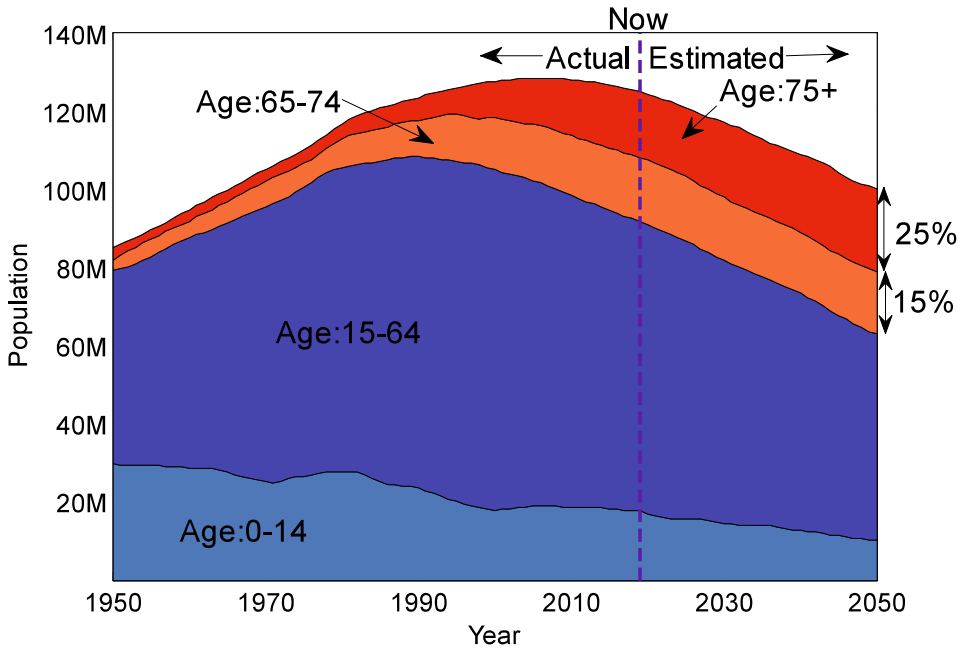

Figure 1.3 Population proportion of Japan between 1950 and 2050 [8]. Notes: The data from 1950 to 2010 are based on the census. The data from 2010 to 2050 are based on medium estimates. Source: National Institute of Population and Social Security Research.

Human aging is associated with a progressive decline in skeletal muscle mass, muscle strength and force generating capacity, referred to as sarcopenia [**13**,**14**]. Literature shows that there is a decline in thigh muscle cross sectional area of 25-40% over the lifespan [**15**,**16**] and this seems to be in line with other studies reporting about reduction in leg muscle mass [**17**]. At the age of 80, the muscle force generating capacity is on average approximately 60% of that at the age of 20-30 [**18**]. The progressive decline in muscle mass and muscle force generating capacity is presumed to be a significant contributor to increase vulnerability for falls, and result in an impaired capacity to perform daily activities, like feeding himself and dressing himself [**14**,**19**,**20**,**21**]. The dependent life-style and a state of vulnerability for adverse health outcomes are major frailty symptoms which are the most problematic expression of population ageing [**21**,**23**].

Frailty is considered highly prevalent among elderly people and to confer high risk for falls, disability, hospitalization, and mortality [**24**]. Investigators assessed the prevalence of frailty in a recent systematic review [**25**]. 21 community-based cohort studies of 61500 elderly people were identified and a prevalence of from 4.0% to 17.0% (mean 9.9%) of

physical frailty was found. Women (9.6%) were almost twice as likely as men (5.2%) to be frail. Frailty increased steadily with age: 65 - 69 years 4%; 70 - 74 years 7%; 75 - 79 years 9% and 80 - 84 years 16% [**22**], and the prevalence of frailty is markedly increased in persons older than 80 [**26**]. Between a quarter and half of people older than 85 years are estimated to be frail, and these people have a substantially increased risk of falls, disability, long-term care, and death [**22**].

1.3 Concepts of frailty

The concept of frailty has been present in geriatric literature for many years and we are witnessing an explosion of articles published on this topic recently [**29**]. A PUBMED search made by Hogan and colleagues found that the number of publications containing the term "frail elderly" had increased exponentially over the last 30 years [**30**]. However, although there have been a large number of articles published on the topic of frailty in elderly people and many definitions of frailty have been proposed, none is considered "Gold Standard". This is probably because that frailty develops as a consequence of age-related decline in many physiological systems, which collectively results in subject's vulnerability to sudden health status changes triggered by minor stressor events [**22**]. Although there are many controversies about the operational definition of the frailty symptom, the frailty is an important medical syndrome with biological bases.

According to consensus opinions of experts involved in the Frailty Consensus Conference hold by 6 major international, European, and US societies [**26**], the frailty is literally defined as a clinical state in which there is an increase in an individual's vulnerability for developing increased dependency and/or mortality when exposed to a stressor event. Chronic and acute diseases, and/or the physiological decline in the neuromuscular, metabolic, and immune system that occurs during the aging process frequently contribute to the frailty symptom. To vividly explain this literal definition, a diagram is drawn and shown in Figure 1.2. As illustrated in the diagram, the neuromuscular, metabolic and immune systems serve as three walls to protect patients from diseases. Due to aging and disease, some holes appear and

grow on the wall, thus increasing the chance of the disease pass through the walls. Although a single hole on the wall carries no obvious or imminent threat of mortality, the deficits contribute cumulatively to an increased risk of disability. More and bigger holes on the wall means subjects have low reserve to protect them from diseases and increasing their vulnerability to frailty. To some extend, the frailty reflects the deficits and reserves of elderly people's physiological system. Therefore, we have to think not only of plugging the holes smaller at each level, but also of making sure that they do not line up.

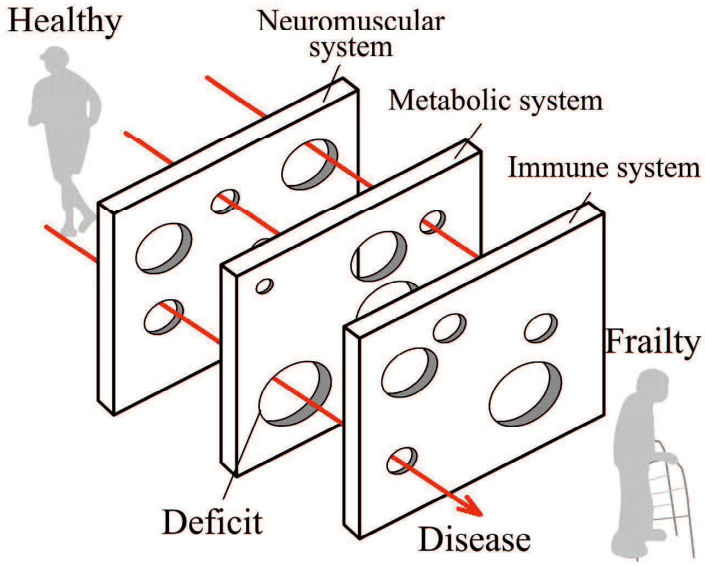

Figure 1.4 The diagram explains the literal meaning of frailty. More deficits in the neuromuscular, metabolic, and immune system will increase the possibility of disease pass through the walls, and consequently increase subjects' vulnerability to frailty.

Even there is no single generally accepted clinical definition of frailty, but one phenotype model named the Fried Criteria has become popular to screen those who are in pre-frail or frailty state so as to effectively target care [**26**,**29**]. In the 1990s, Fried and colleagues did a secondary analysis of data obtained from a prospective cohort study of 5210 men and women aged 65 years and older [**24**] and established the frailty phenotype model with five variables: unintentional weight loss, self-reported exhaustion, low energy expenditure, slow gait speed, and weak grip strength. This screening instrument was developed to identify frail persons at high risk of adverse health-related outcomes in the clinical setting and the screening criteria are presented in Table 1.1 [**27**]. People with 1~2 frailty criteria are classified as pre-frail and more than 3 frailty criteria are classified as frailty. This operational definition of frailty was

based on a conceptual paradigm and was later validated by showing its ability to predict physical disability, hospitalization, and mortality in a sample of community-dwelling older persons.

Table 1.1 The Fried Frailty screening criteria.

Criteria	Definition and parameters
Weight loss	Loss of 10 pounds unintentionally in past year or weight at examination ≤ 10% of age 60 weight;
Self-reported exhaustion	Self-report of fatigue or felt unusually tired or weak in the past month;
Physical inactivity	Frequency and duration of physical activities (walking, doing strenuous household chores, doing strenuous outdoor chores, dancing, bowling, exercise);
Low walking speed	Walking 4 m ≥ 7 s if height ≤ 159 cm or ≥ 6 s if height ≥ 159 cm.*
Low hand grip strength	Grip strength, stratified by sex and body-mass index.

* Data for older women (lowest 20th percentile).

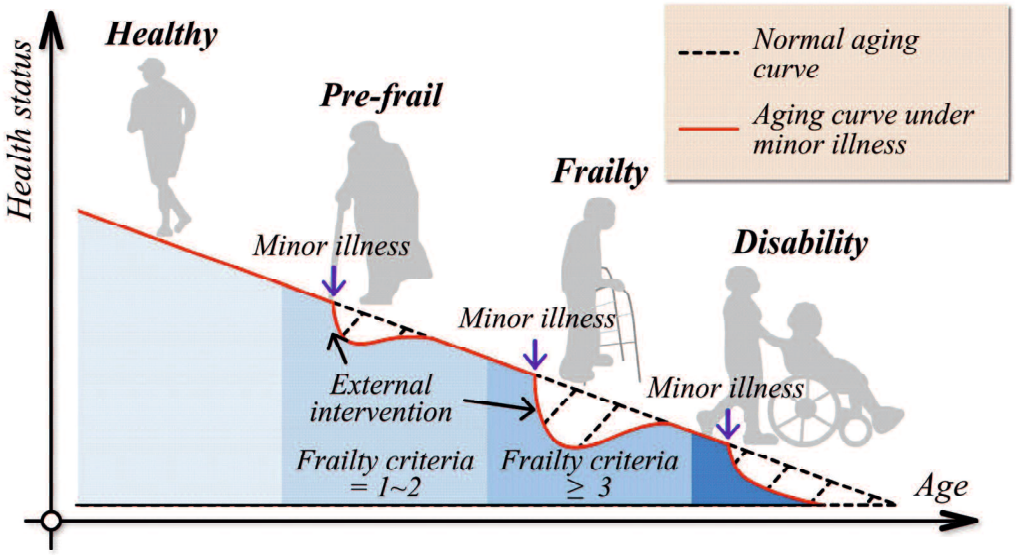

Figure 1.5 The continuous gradual process of frailty. The diagram shows the disproportion in the time of recovery and the degree of decline of health status during different stages. Four stages are included in the frailty process. Presence of 1-2 frailty criteria is defined as pre-frail stage and frailty criteria more than 3 is defined as frailty stage.

Although the frailty and disability show some of the same symptoms, but the frailty is different from disability. Figure 1.5 gives a visual representation of the disproportionate decline of health status when facing a minor illness. As illustrated in the picture, the health status of the subject continues to decline with age, and his health status can be roughly divided into four stages: the healthy state, the pre-frail state, the frailty state, and last the disability state. The pre-frail and frailty state appear to be transitional states in the dynamic process from healthy to disability [**31**]. In the pre-frail, frailty and disability state, an

apparently minor illness will results in a striking and disproportionate change in health state. The health status in the pre-frail and frailty state recovers to the normal curve through external intervention or self-recovery after a period of time. But there is a difference in the recovery time and the decline degree due to difference in the impairment of subject's physiological systems. Moreover, after entering the disability stage, the impairment of physiological systems reach to a crucial threshold that subject's health status irreversibly deteriorates after a minor illness, resulting in a significant reduction in life expectancy. That is after entering the disability stage, the health status of subject will not recover to the normal level after a minor illness.

1.4 Common physical frailty syndromes

The frailty concepts mentioned above are literal definitions and conceptual images about the frailty. However, for people without a medical background, they may not be able to obtain an intuitive image about the frailty from its literal meaning. However the frailty syndrome does happen among elderly people and affect their daily lives widely. Therefore, to successfully combat frailty and arouse people's attention about this prevalent geriatric syndrome, some common physical frailty syndromes in activities of daily life are illustrated here to depict an intuitive image about the frailty.

In addition, frailty has multifaceted characteristic and is a dynamic process from healthy to disability. Generally, the frailty can be divided into three parts: the **physical frailty**, **mental frailty** and **social frailty**. The sarcopenia is the common illness of physical frailty and the cognitive disorder is the common illness of mental frailty. The loneliness and geriatric depression are common illnesses of social frailty. The mental frailty and social frailty are combined effect of social, psychological, physiological and environmental factors, which are not research content of this thesis. The research scope of this thesis mainly focuses on the physical domain of frailty and those people in apparently vulnerable and mildly frail stage, since we believe that the physical frailty can be treated through exercise interventions. The physical frailty is closely related to the muscle wasting and weakness and is a common

phenomenon among elderly people. The decline in force generating capacity, muscle mass and strength will finally result in functional limitations of human limbs like walking, feeding himself and shopping.

The common physical frailty syndromes among elderly people were reviewed from the Fried Frailty screening criteria [**24**], the Japanese version of the Cardiovascular Health Study (J-CHS) criteria [**32**,**33**,**34**], the Kihon checklist for assessing frailty status [**35**,**36**] and the functional test for upper and lower extremity [**37**,**38**,**39**]. Those common physical frailty syndromes are shown in Figure 1.6, Figure 1.7 and Figure 1.8 vividly. Those physical frailty symptoms were classified into oral dysfunction, mobility dysfunction and upper limb dysfunction.

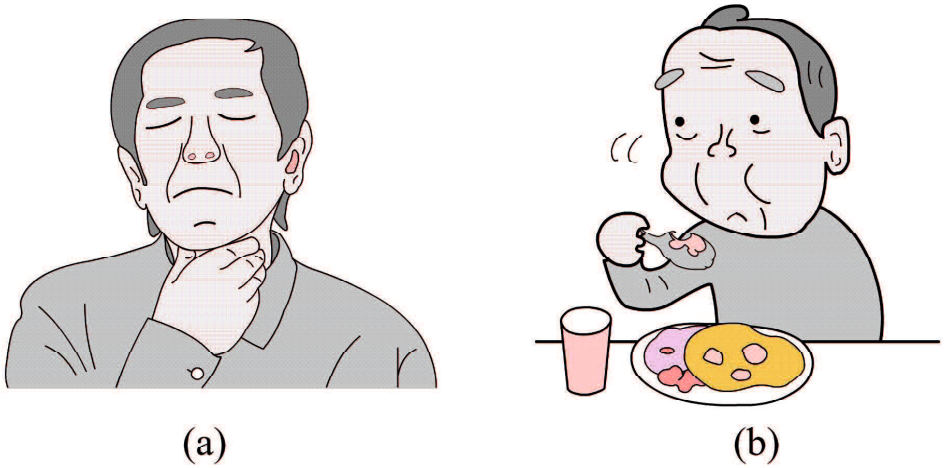

Figure 1.6 Common physical frailty symptoms related to oral function in daily life. (a) Swallow difficulty; (b) Low bite force.

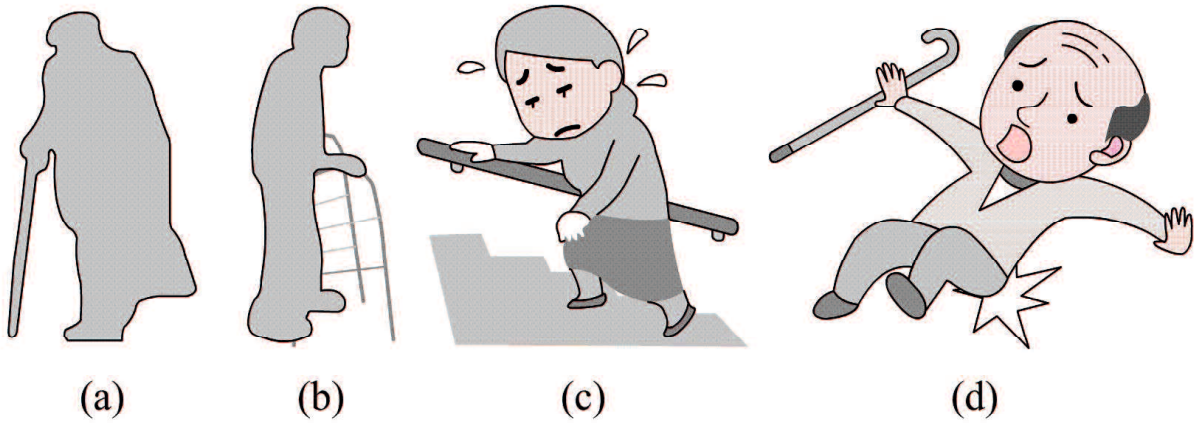

Figure 1.7 Common physical frailty symptoms in daily life related to mobility dysfunction. (a) Need a walking stick when walking. (b) Need a four-legged walker when walking. (c) Need to use handrails or walls when climbing stairs. (d) Often falls or worry about falling.

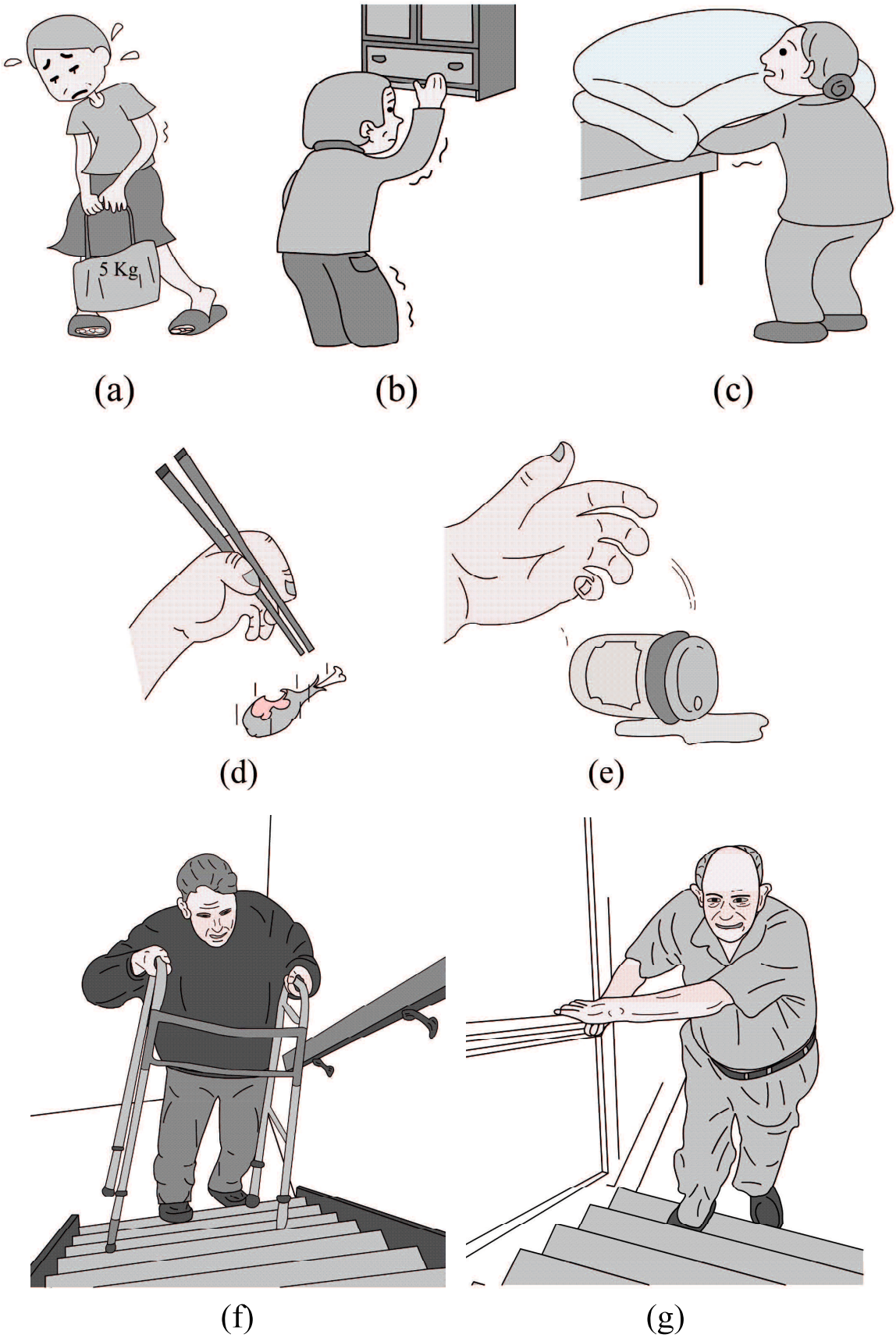

Figure 1.8 Common physical frailty symptoms in daily life related to upper limb function. (a) Having trouble lifting and carrying a shopping bag of 5 kg or more; (b) Unable to do things at or above shoulder height; (c) Having difficulty in normal housework (such as lifting a quilt); (d) Having difficulty with a knife, fork, spoon or

chopsticks (situation like the food picked up with chopsticks often falls off); (e) Water glasses often fall from his hands. (f) Having difficulty with climbing stairs while carrying a four leg walker. (g) Feel exhausted while climbing stairs.

Figure 1.6, Figure 1.7 and Figure 1.8 show some common physical frailty symptoms in daily life related to oral dysfunction, mobility dysfunction and upper limb dysfunction, respectively. Oral muscle degeneration will result in decline in oral function like swallow difficulty and low bite force. The decrease in force generating capacity of lower limb muscles will result in decline in mobile ability, such as needing a walking stick or four-legged walker while walking, needing to use handrails or walls when climbing stairs, and often falls or worrying about falling. Similarly, the decline in muscle force of upper limb muscles will result in decline in functional limitations of upper limb, such as having trouble lifting and carrying a shopping bag of 5 kg or more; unable to do things at or above shoulder height; having difficulty in normal housework (such as lifting a quilt); having difficulty with a knife, fork, spoon or chopsticks (situation like the food picked up with chopsticks often falls off) and having difficulty with holding a cup.

In addition, the upper-limbs play an important role in the process of walking and affect elderly people's mobile ability. For example, when the elderly people are walking with a four-legged walker (shows in Figure 1.8 (f)), a cane (shows in Figure 1.9) and holding a handrail to climb the stairs (shows in Figure 1.8 (g)), the upper-limbs need to bear part of the body weight, move the walker and cane forward, and maintain their body balance. Jebsen [40] and colleagues initially made the assumption that canes may be used to support 20% to 25% of body weight and canes of ideal length produce 20° to 30 ° of elbow flexion, in which case elbow extensors act as shock absorbers. Later studies using an instrumented cane proved that axial loading on the cane varies between 15% to 40% of body weight [41,42]. It is illustrated in Figure 1.9 that the elbow extensor and flexor muscles are recruited to bear part of the body weight during the support phase of walking and the flexor muscles are recruited to move the walker and cane forward during the swing phase alternately. During the swing phase, the elbow flexor need to withstand the weight of the Cane. Even the muscle strength of lower limbs are very weak, the elderly people can still walk a certain distance with the help from

their upper limbs. Therefore, it is necessary to evaluate the upper-limb function when evaluating elderly people's mobile ability.

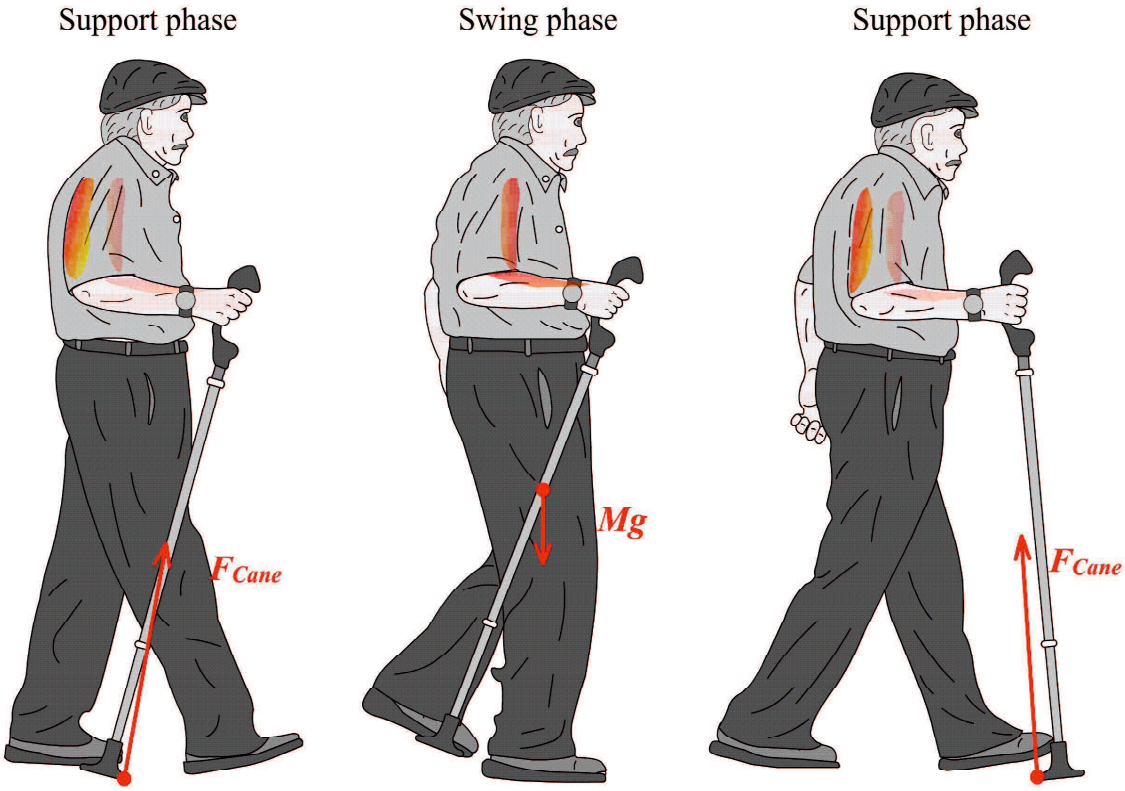

Figure 1.9 An elderly man walks with the help of a Cane. Both the elbow extensor and flexor muscles are recruited to bear part of the body weight and keep the elbow joint stable during the support phase of walking. The extensor muscles play dominate role in this process. The flexor muscles are recruited to move the walker and cane forward during the swing phase alternately. During the swing phase, the elbow flexor need to withstand the Cane weight. The axial loading on the cane varies between 15% to 40% of body weight [41,42].

1.5 Current research about physical frailty

As we have mentioned in previous sections, the research scope of this thesis mainly focuses on the physical domain of frailty and those people in apparently vulnerable and mildly frail stage. To the best of the author's knowledge, four criteria are commonly used for screening of physical frailty. They are the Fried Frailty screening criteria [**24**], the Japanese version of the Cardiovascular Health Study (J-CHS) criteria [**32**,**33**,**34**], the Kihon checklist for assessing frailty status [**35**,**36**] and the functional test for upper and lower extremity [**37**,**38**,**39**]. The Fried Frailty screening criteria is a well-known, phenomenon-based, widely accepted and commonly used frailty screening criteria world-wide, established by Fried and

his colleagues. But the experimental population in their experiments were recruited from European countries that the frailty screening value may not suitable for Asian people. Therefore, the Japanese version of the Cardiovascular Health Study criteria and the Kihon checklist were established to screen frailty among Japanese elderly people. The functional test of upper and lower extremity is a commonly used criteria for testing of upper-limb and lower-limb function.

Generally, the physical frailty can be assessed from three aspects: the oral dysfunction; the mobility dysfunction and the upper limb dysfunction. The frailty symptoms of oral dysfunction include swallowing difficulty and low bite force (As shown in Figure 1.6). The swallowing difficulty is assessed through questionnaire [**36**, **43**] and the bite force was measured by using Digital Bite Force Sensor (As shown in Figure 1.10) [**44**]. The frailty symptoms of mobility dysfunction include low walking speed, abnormal walking posture and fall (As shown in Figure 1.7). The walking speed can be assessed by walking test (As shown in Figure 1.11) [**33**,**36**,**45**]. The abnormal walking posture and fall of elderly are closely relate to their muscle amount. As illustrated in Figure 1.12, elderly people's muscle amount can be simply checked by measuring the calf circumference [**46**]. The frailty symptoms of upper limb dysfunction were vividly illustrated in Figure 1.8. Among those symptoms, the hand dysfunction can be assessed by measuring their hand grip strength [**24**,**32**,**33**,**35**]. Figure is the commonly used Digital Hand Dynamometer Grip Strength Measurement Meter for measuring subject's hand grip strength.

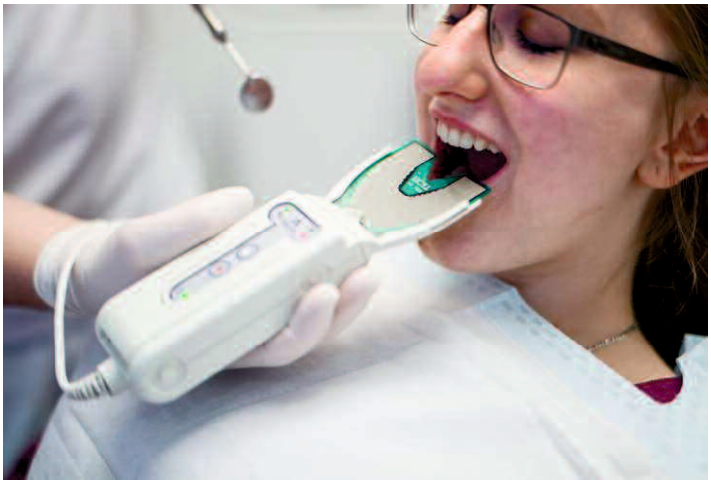

Figure 1.10 Measuring bite force by using Digital Bite Force Sensor.

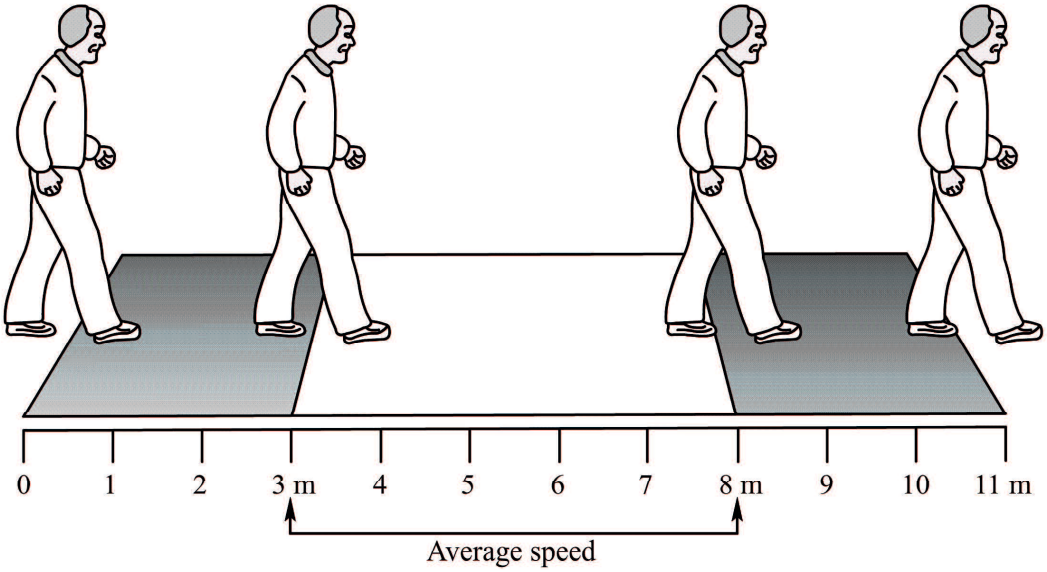

Figure 1.11 The 5 meters walking test for assessing frailty in elderly people [3,28,33].

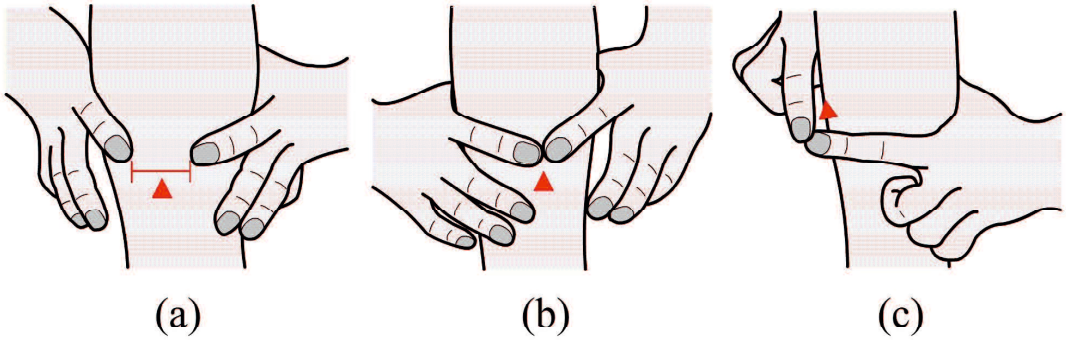

Figure 1.12 Simply checking of muscle amount by measuring the calf circumference. (a) The index finger ring can't circle the calf; (b) The index finger ring just covers the calf; (c) The index finger ring is significantly larger than the circumference of the calf.

Figure 1.13 Digital Hand Dynamometer Grip Strength Measurement Meter used for measuring hand grip strength.

Since different reader may have different understanding from the qualitative description of frailty introduced in the previous section. Quantitative indicators are necessary and important to establish an operational screening criteria of frailty. There are quantitative and operational indicators available for the screening of slowness and hand strength weakness. Table 1.2 are the quantitative value of walking time to screen slowness in a 4 m walking test [**24**,**33**,**36**,**45**] and Table 1.3 are quantitative value of grip strength to screen hand weakness [**33**,**36**,**43**]. Form the tables, we can see that the screening value is different for people with different height, body weight and gender, especially for the Fried criteria. The Fried criteria provide more detailed screening criteria for people with different body types and other two criteria provide more simpler and rougher indicators.

Table 1.2 Quantitative value of walking time to screen slowness in a 4 m walking test.

	Fried Criteria [**24,45**]	J-CHS Criteria [**33**]	Kihon checklist [**36**]
For female subjects	≥ 7s if height ≤ 159cm ≥ 6s if height ≥ 159cm	≥ 8.8s	Normal walking speed <1.0 m/s
For male subjects	≥ 7s if height ≤ 173 cm ≥ 6s if height ≥ 173cm	≥ 10s	

Table 1.3 Quantitative value of grip strength to screen weakness. BMI is the Body Mass Index.

	Fried Criteria [**45**]	J-CHS Criteria [**33**]	Kihon checklist [**36**]
For female subjects	≤ 17 kg for BMI ≤ 23 ≤ 17.3 kg for BMI 23.1-26 ≤ 18 kg for BMI 26.1-29 ≤ 21 kg for BMI ≥ 29	≤ 19 kg	≤ 18 kg
For male subjects	≤ 29 kg for BMI ≤ 24 ≤ 30 kg for BMI 24.1-26 ≤ 30 kg for BMI 26.1-28 ≤ 32 kg for BMI ≥ 28	≤ 29 kg	≤ 26 kg

After reviewing all those common frailty symptoms, we can see that current researches about physical frailty mainly focus on the oral dysfunction and mobility dysfunction. Physical frailty researches on the upper limb dysfunction only include measuring hand grip strength and there are quantitative value to screen hand weakness. According to the frailty criteria mentioned above, there are no adequate quantitative value available for the evaluation of upper limb dysfunction besides the hand grip strength. However, the upper limb functions related to elbow joint and shoulder joint play a significant and functional role in daily life of

elderly people, like lifting and carrying a shopping bag, like normal housework, like ambulatory locomotion with cane or walker, like getting up from a wheelchair. Moreover, as we have mentioned above, the upper-limbs also play an important role in the process of walking and affect elderly people's mobile ability. The upper-limbs need bear parts of the body weight. All this explains why this doctoral dissertation choice the upper-limb as the research object to study physical frailty.

Besides, considerable evidence suggests that the ability to perform a physical task is determined by a threshold level of muscular strength and endurance [**47**,**48**]. Individuals lacking the requisite muscular strength may not be able to perform various activities of daily living that are important determinants of independence. For healthy athletes, as illustrated in Figure 1.14, the elbow flexor muscle strength is an important parameter measured by using equipment like dynamometers. The main purpose of measuring elbow flexor muscle strength in healthy athletes is to screen strong athletes. However, for elderly people, the measurement of elbow flexor muscle strength is to evaluate frailty and the measuring system needs to be simple, safe and reliable. The dynamometers and the criteria designed for healthy athletes may not be suitable for screening frailty among senior subjects. Consequently, it is important and necessary to design and establish measuring system and screening criteria for upper-limb dysfunction which are suitable for senior subjects.

Figure 1.14 Dynamometers for assessing elbow flexor strength of the athletes. The Biodex System 4 [**49**].

2. Aim and organization of this thesis

In summary, as the society ages, the number of elderly people in frailty state or have a risk of being in frailty state increases exponentially, highlighting the importance of assessing frailty and choosing the appropriate intervention for slowing the progress of frailty. Figure 1.15 illustrates the core idea of the process of frailty level assessment used in this thesis. Suppose there is an elderly subject and we want to evaluate his frailty level. A specific exercise, such as walking or lifting a dumbbell, is provided and the sensor signal is recorded to evaluate the subject's performance in the exercise. Since we dose not know whether the subject is frail or not. We want know how a normal person will perform in the same exercise and compare the sensor signal to the reference value of a normal person. With the comparison results and frailty criteria, the subject's frailty level is consequently assessed. To get the reference value of a normal person, the muscle model is built to simulate the performance of normal person in the provided exercise. Demographic data, like age and body weight, of the elderly subject and public experimental data of normal people were entered into the muscle model as input parameters. Therefore, the output of simulation results are the reference value of normal person. There are there most important parts in the assessment process: 1. establishment of the muscle model to get the reference value of normal person; 2. establishment of the measurement system; 3. establishment of the frailty evaluation criteria.

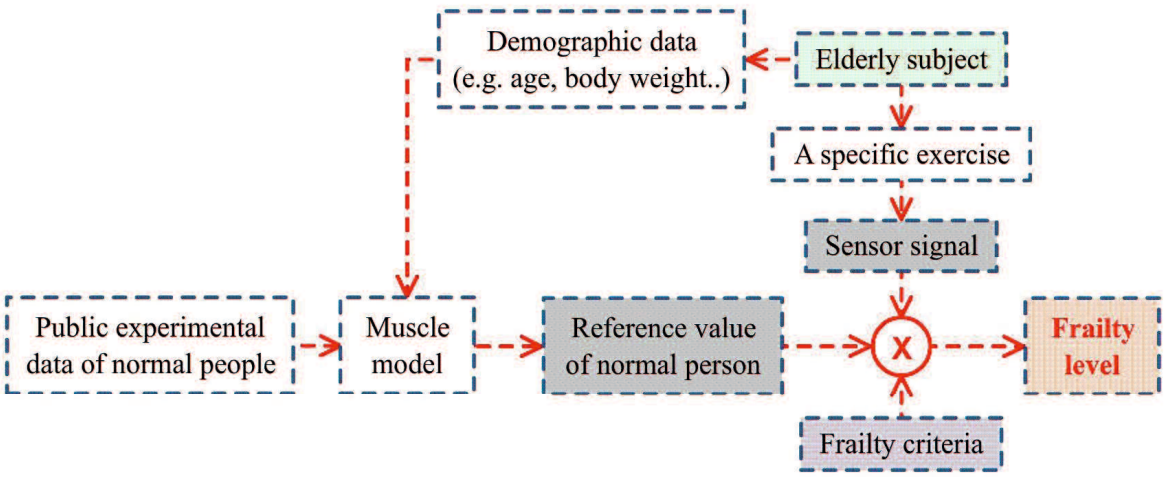

Figure 1.15 General process of assessment of frailty level.

The main object of this thesis is to develop a muscle function evaluation and training support system for the purpose of slowing the progress of frailty. The system has the ability to record and monitor the exercise dosage, evaluate muscle function and estimate muscular states during the training. In the following, the contents in each chapter will be described in detail.

In chapter 1, we firstly talk about the aging society and the prevalence of frailty among elderly people. And then the conceptual and intuitive images about the frailty are presented to give readers a clear image of frailty. Meanwhile, some quantitative criteria for evaluation of frailty are introduced. Finally, we introduce the purpose and research outline of the present manuscript.

Chapter 2 describes the concept of using musculoskeletal modeling to estimate muscular states during exercises, and to quantify and evaluate the training effect of exercise on a specific muscle. A detailed three-dimensional model of the upper extremity, including major muscles make up the elbow flexor and extensor, was built base on public references and database. The modeling process and principle were introduced in detail and the exercise of biceps curl to lift a dumbbell was simulated. The simulation results provide physiotherapists with instructions on designing training exercise.

Chapter 3 is the development of muscle function measurement and evaluation system. Firstly, we built up a motion capture system to recognize and record movements of trainee when perform rehabilitation exercises based on inertial and visual sensing. The inertial sensor has the ability to effectively and accurately recognize movement of trainee, however the gyroscope shows poor performance in long-term measurements of body motion and the accelerometer can usually measure only one degree of freedom with one sensor. A custom-made Thera-Band was designed and made to help subject do biceps curl exercise and record the resistance force. Later, a force data segmentation algorithm was proposed to segment the force data into small segments corresponding to different contraction phases. And at last, with the preprocessed data, indexes for quantifying fatigue and recovery ability,

muscle motion control ability and exercise tolerance were proposed to assess muscle function.

In chapter 4, based on the segmentation algorithm and indexes proposed in Chapter 3, we evaluate physical frailty from the perspective of muscle function. An experiments of 6 subjects was carried out and the muscle motion control ability and exercise tolerance of their elbow flexor were evaluated. We use the quotient of acceleration and deceleration time during flexing stage to quantify motion control ability of elbow flexor. A bigger quotient means a longer acceleration phase, which indicates the subject possesses a stronger ability to control his flexor muscle. The coefficient of variation of force data during holding phase were used to quantify exercise tolerance. A bigger coefficient of variation means a bigger fluctuation in force, indicating a low ability of subject in keeping the force at a constant value.

Chapter 5 describes the application of our system in the field of rehabilitation. Firstly, by using the musculoskeletal model built in Chapter 1, we estimated muscular states during elbow flexor resistance training for bedridden patient and the results revealed the contribution of each muscle in the flexing process. Later, the fatigue and recovery indexes were used to monitor fatigue state during biceps curl exercise. Finally, a support system for dumbbell lifting exercise is designed to help trainee record their training sets automatically.

In chapter 6, the conclusions of this study and future work are presented.

3. References

[1] Health Japan 21 (the second term), National Institute of Health and Nutrition, 2019. Available at, https://www.nibiohn.go.jp/eiken/kenkounippon21/en/about/index.html

[2] 健康日本 21, 2000~2019. Available at, http://www.kenkounippon21.gr.jp/. Accessed in 2019.12.16.

[3] フォーラム「健康寿命を延ばそう～フレイルを予防して～」の開会挨拶, 関 淳一. 2016. https://www.japan-who.or.jp/library/2018/book6603.pdf. Accessed in 2019.12.16.

[4] United Nations, Department of Economic and Social Affairs. "World population ageing 2017: highlights." (2017).

[5] United Nations, Department of Economic and Social Affairs, Population Division (2017). World Population Prospects: The 2017 Revision, Key Findings and Advance Tables. Working Paper No. ESA/P/WP/248.

[6] Kapteyn A. What can we learn from (and about) global aging?[J]. Demography, 2010, 47(1): S191-S209.

[7] Chen, Brian K., et al. "Forecasting trends in disability in a super-aging society: adapting the future elderly model to Japan." The Journal of the Economics of Ageing 8 (2016): 42-51.

[8] Muramatsu, Naoko, and Hiroko Akiyama. "Japan: super-aging society preparing for the future." The Gerontologist 51.4 (2011): 425-432.

[9] 高齢化の進展, Ministry of Internal Affairs and Dommunications. 2016. http://www.soumu.go.jp/johotsusintokei/whitepaper/ja/h25/html/nc123110.html. Accessed in 2019.12.16.

[10] Chen, Brian K., et al. "Forecasting trends in disability in a super-aging society: adapting the future elderly model to Japan." The Journal of the Economics of Ageing 8 (2016): 42-51.

[11] Population estimates by age (Five-year groups) and sex. Portal Site of Official Statistics of Japan. http://www.stat.go.jp/english/data/jinsui/tsuki/index.html. Accessed in 2019.10.25.

[12] Stuck, Andreas E., et al. "A trial of annual in-home comprehensive geriatric assessments for elderly people living in the community." New England Journal of Medicine 333.18 (1995): 1184-1189.

[13] Fielding, Roger A., et al. "Sarcopenia: an undiagnosed condition in older adults. Current consensus definition: prevalence, etiology, and consequences. International working group on sarcopenia." Journal of the American Medical Directors Association 12.4 (2011): 249-256.

[14] Ballak, Sam B., et al. "Aging related changes in determinants of muscle force generating capacity: a comparison of muscle aging in men and male rodents." Ageing research reviews 14 (2014): 43-55.

[15] Nilwik, Rachel, et al. "The decline in skeletal muscle mass with aging is mainly attributed to a reduction in type II muscle fiber size." Experimental gerontology 48.5 (2013): 492-498.

[16] Klitgaard, Henrik, et al. "Function, morphology and protein expression of ageing skeletal muscle: a cross-sectional study of elderly men with different training backgrounds." Acta Physiologica Scandinavica 140.1 (1990): 41-54.

[17] Janssen, Ian, et al. "Skeletal muscle mass and distribution in 468 men and women aged 18–88 yr." Journal of applied physiology 89.1 (2000): 81-88.

[18] Doherty, Timothy J. "Invited review: aging and sarcopenia." Journal of applied physiology 95.4 (2003): 1717-1727.

[19] Roubenoff, Ronenn, and Virginia A. Hughes. "Sarcopenia: current concepts." The Journals of Gerontology Series A: Biological Sciences and Medical Sciences 55.12 (2000): M716-M724.

[20] Kamel, Hosam K. "Sarcopenia and aging." Nutrition reviews 61.5 (2003): 157-167.

[21] Visser, Marjolein, and Laura A. Schaap. "Consequences of sarcopenia." Clinics in geriatric medicine 27.3 (2011): 387-399.

[22] Clegg, Andrew, et al. "Frailty in elderly people." The lancet 381.9868 (2013): 752-762.

[23] Cesari, Matteo, et al. "Frailty syndrome and skeletal muscle: results from the Invecchiare in Chianti study." The American journal of clinical nutrition 83.5 (2006): 1142-1148.

[24] Fried L P, Tangen C M, Walston J, et al. Frailty in older adults: evidence for a phenotype[J]. The Journals of Gerontology Series A: Biological Sciences and Medical Sciences, 2001, 56(3): M146-M157.

[25] Collard, Rose M., et al. "Prevalence of frailty in community-dwelling older persons: a systematic review." Journal of the American Geriatrics Society 60.8 (2012): 1487-1492.

[26] Morley, John E., et al. "Frailty consensus: a call to action." Journal of the American Medical Directors Association 14.6 (2013): 392-397.

[27] 健康日本 21, 2000~2019. Available at, http://www.kenkounippon21.gr.jp/. Accessed in 2019.10.25.

[28] フレイルを知って健康長寿を延ばす, 葛谷 雅文, 2016. Available at, https://www.japan-who.or.jp/library/2018/book6603.pdf. Accessed in 2019.10.25.

[29] Van Kan, G. Abellan, et al. "The IANA Task Force on frailty assessment of older people in clinical practice." The Journal of Nutrition Health and Aging 12.1 (2008): 29-37.
[30] Hogan D B. Models, definitions, and criteria for frailty[M]//Conn's Handbook of Models for Human Aging. Academic Press, 2018: 35-44.
[31] Kristjansson S R, Rønning B, Hurria A, et al. A comparison of two pre-operative frailty measures in older surgical cancer patients[J]. Journal of Geriatric Oncology, 2012, 3(1): 1-7.
[32] Shimada H, Makizako H, Doi T, et al. Combined prevalence of frailty and mild cognitive impairment in a population of elderly Japanese people[J]. Journal of the American Medical Directors Association, 2013, 14(7): 518-524.
[33] 佐竹 昭介. フレイルの進行に関わる要因に関する研究(25-11). 国立長寿医療研究センター, 2015. Available at, https://www.ncgg.go.jp/ncgg-kenkyu/documents/25-11.pdf. Accessed in 2019.10.25.
[34] Shimada H, Suzuki T, Suzukawa M, et al. Performance-based assessments and demand for personal care in older Japanese people: a cross-sectional study[J]. BMJ open, 2013, 3(4): e002424.
[35] Satake S, Senda K, Hong Y J, et al. Validity of the Kihon Checklist for assessing frailty status[J]. Geriatrics & gerontology international, 2016, 16(6): 709-715.
[36] 佐竹昭介. "基本チェックリストとフレイル." 日本老年医学会雑誌 55.3 (2018): 319-328.
[37] Toosizadeh N, Wendel C, Hsu C H, et al. Frailty assessment in older adults using upper-extremity function: index development[J]. BMC geriatrics, 2017, 17(1): 117.
[38] Quinn T J, McArthur K, Ellis G, et al. Functional assessment in older people[J]. Bmj, 2011, 343: d4681.
[39] Bravini E, Franchignoni F, Giordano A, et al. Classical Test Theory and Rasch Analysis Validation of the Upper Limb Functional Index in Subjects With Upper Limb Musculoskeletal Disorders[J]. Archives of physical medicine and rehabilitation, 2015, 96(1): 98-104.
[40] Jebsen, Robert H. "Use and abuse of ambulation aids." Jama 199.1 (1967): 5-10.
[41] Kumar, Rajeswari, Meng Cheng Roe, and Oscar U. Scremin. "Methods for estimating the proper length of a cane." Archives of physical medicine and rehabilitation 76.12 (1995): 1173-1175.
[42] Ely, Douglas D., and Gary L. Smidt. "Effect of cane on variables of gait for patients with hip disorders." Physical Therapy 57.5 (1977): 507-512.
[43] 転ばぬ先の歯と口の健康 - 埼玉県歯科医師会. 2016. http://www.saitamada.or.jp/wp-content/themes/saitamada/pdf/go8020/2016-fureiru.pdf. Accessed in 2019.12.28.
[44] Iwasaki, M., et al. "A 5‐year longitudinal study of association of maximum bite force with development of frailty in community‐dwelling older adults." Journal of oral rehabilitation 45.1 (2018): 17-24.
[45] Xue Q L. The frailty syndrome: definition and natural history[J]. Clinics in geriatric medicine, 2011, 27(1): 1-15.
[46] 飯島 勝矢. 東京大学 高齢社会総合研究機構. 口腔機能・栄養・運動・社会参加を総合化した複合型健康増進プログラムを用いての新たな健康づくり市民サポーター養成研修マニュアルの考案と検証, 2016. http://www.iog.u-tokyo.ac.jp/wp-content/uploads/2016/04/h27_rouken_team_iijima.pdf. Accessed in 2020.01.02.
[47] Fukagawa, Naomi K., et al. "The relationship of strength to function in the older adult." The Journals of Gerontology Series A: Biological Sciences and Medical Sciences 50.Special_Issue (1995): 55-59.
[48] Buchner, David M., et al. "Effects of physical activity on health status in older adults II: Intervention studies." Annual review of public health 13.1 (1992): 469-488.

[49] Dynamometers, Biodex System 4.https://www.biodex.com/physical-medicine/products/dynamometers. Accessed in 2020.01.03.

Chapter 2

Analytical Model of Upper-limb Muscle Function

1. Background of musculoskeletal modeling

Musculoskeletal modeling is a powerful tool to research mechanical behavior of human muscles and its interaction with human nervous system from the viewpoint of mechanics and neuroscience by using the methods of mechanics [1]. This method quantifies the mechanical and physiological properties of each muscle through parametric modeling, enabling researchers to quantify muscle differences and gain insight into the states (usually refer to mechanical states like muscle-tendon length changes, muscle fiber force and velocity) of each muscle during the movement. Muscle's mechanical behaviors, like force-length-velocity-activation relationships, are determined by anatomical features of skeletal system (e.g. anthropometric properties and muscle paths [1]) and muscle's architecture parameters (e.g. optimal fiber length, peak force, tendon slack length and pennation angle [2, 3]), enables researchers to quantify mechanical properties and behavior of muscles via mathematical modeling. More delightedly, with recent development in image-based musculoskeletal modeling [4, 5] and physiological-phenomena-based optimization method [6], highly individualized musculoskeletal model (MSM) and more realistic prediction of muscle force can be achieved, leading to a great potential of its application in clinical test and, of course, in the estimation of muscle-level stimuli of resistance training.

With regard to musculoskeletal modeling of the upper limbs, researchers can build muscle models based on public databases or use generic models provided by open source or commercial software such as OpenSim (https://simtk.org/home/opensim) and AnyBody (http://www.anybodytech.com/). Garner and his colleagues built a kinematic model of human upper limb using high-resolution medical images obtained from the National

Library of Medicine's Visible Human Project (VHP) dataset [7]. The muscle model is a detailed three-dimensional model of human upper-limb, including major muscles cross the elbow joint and shoulder joint [8]. Information about the joint kinematics and muscle architecture of the muscle model are provided in references [7, 9]. The obstacle-set method for representing muscle paths is described in detail in reference [10]. In addition, open source or commercial software such as OpenSim [11,12] and AnyBody [13] provides users with generic models to build upper limb models in a simple and convenient way. The calculation results of these software are often used as a gold standard for evaluating the muscle models built by researchers themself.

Moreover, the optimization method used in solving the muscle recruitment problem in the inverse dynamics approach is another important question in musculoskeletal modeling. In the past two decades, a number of muscle-force prediction methods have been presented based on the Optimality principle [14, 15] that represent performance criteria on which the neuromuscular system optimizes the activation of muscle forces. Static optimization methods, dealing with isometric and relatively slow motions, predict redundant muscle forces by minimizing a cost function, comprising the sum of muscular stress or force raised to a power, subject to force/torque constraints associated with a given task. The biggest advantage is that the muscle force prediction is mathematically formulated and can be numerically solved, enabling a prediction for relatively complex tasks involving multiple joints such as walking and running. There are still arguments and criticism on the neurological background of this optimization; however, the effectiveness of this approach for predicting stereotyped motor performances has been reported in many papers [16, 17].

Therefore, in this section, we will firstly talk about the computational methods used in musculoskeletal modeling and a detailed three-dimensional analytical musculoskeletal model of human upper-limb, including major muscles make up the elbow flexor and extensor, will be built to estimate muscular states during elbow flexor resistance training. The technical details of the calculation will be described in detail to create an intuitive and detailed impression of musculoskeletal modeling for the reader. And later, the muscle

activation patterns were estimated in AnyBody when forearm flexing to lifting a dumbbell with different pronation and supination angle. The estimated result could be treated as an important reference standard for physiotherapists to evaluate the training effect of the exercise on individual muscle and choose the appropriate training movement with specific purpose. This section mainly focus on the computational aspects of estimating muscle activation patterns base on musculoskeletal modeling and the clinical aspects will not be investigated.

2. Musculoskeletal modeling of the upper extremity

This section introduces the technical details of the common process of building a generic upper limb muscle model and estimation of muscular states. The muscle model incorporates the main muscles or muscle parts that make up the elbow flexor and extensor. The elbow flexor and extensor are dominated in the concentric and eccentric movements of upper limb when forearm flex or extend to lift or drop a shopping bag. According to the anatomical descriptions of human upper-limb [20], as illustrated in Figure 2.1, elbow flexor and extensor primary include 7 parts of muscles. In this paper, a three-dimensional Musculoskeletal model (MSM) of human upper-limb was established base on public data of skeletal coordinates and muscle architecture [18, 19] and by using the obstacle-set method [17] to model the muscle path. The MSM consists of 3 bones (Figure 2.1), 5 joints (Table 2.2) and 7 parts of muscles (Table 2,1). Table 2.1 shows architectural properties of each muscle or muscle parts. Additional details regarding the MSM are available in references mentioned above [18, 19].

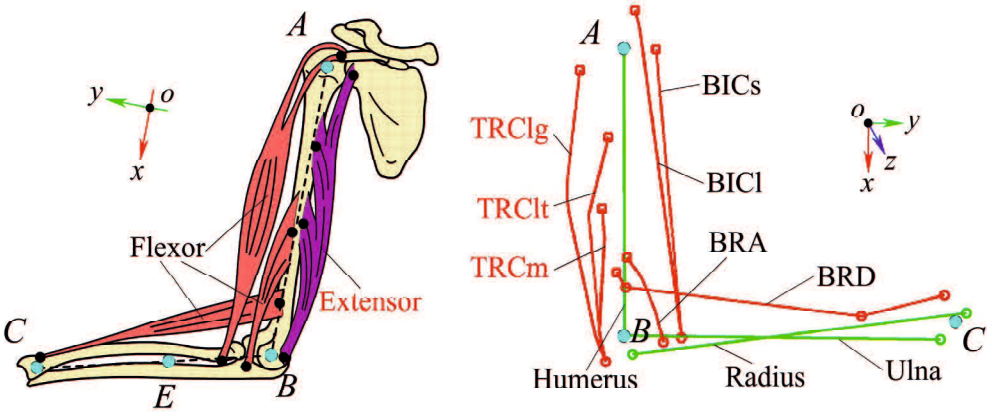

(a) (b)

Figure 2.1 (a) Extensor and flexor of human upper-limb in sagittal plan. (b) Three-dimensional MSM illustrates bones (green lines) and muscles (red lines) across elbow joint.

Table 2.1. Architectural properties of each musculotendon actuator of elbow extensor and flexor.

	Muscles	Abbr.	PCSA (cm^2)	l_0^m (cm)	v_0^m (cm/s)	l_S^t (cm)	F_0^M (N)	φ (deg)
Extensor	1.Triceps brachii(long)	TRClg	19.07	15.24	152.4	19.05	629.21	15.00
	2.Triceps brachii(lateral)	TRClt	38.45	6.17	61.7	19.64	1268.87	15.00
	3.Triceps brachii(medial)	TRCm	18.78	4.90	49.0	12.19	619.67	15.00
Flexor	4.Brachialis	BRA	25.88	10.28	102.8	1.75	853.90	15.00
	5.Brachioradialis	BRD	3.08	27.03	270.3	6.04	101.58	5.00
	6.Biceps brachii(long)	BICl	11.91	15.36	153.6	22.93	392.91	10.00
	7.Biceps brachii(short)	BICs	13.99	13.07	130.7	22.98	461.76	10.00

Table 2.2 Shoulder joint and elbow joint in the muscle model.

Shoulder joint	Flexion/Extension
	Abduction/Adduction
	External/Internal Rotation
Elbow joint	Flexion/Extension
	Pronation/Supination

2.1 Modeling of muscle geometry

Modeling muscle path is an inevitable issue in musculoskeletal modeling for muscle path plays an essential role by determining muscle length, moment arm and force-sharing of muscle-tendon force (MTF). Two different methods are commonly used in modeling muscle path in MSM: straight-line and centroid-line methods. The straight-line method is easy to implement but has many significant shortcomings. Centroid-line method can represent muscle path more accurately but application of this model is limited by the fact that location of muscle cross-sectional centroids are difficult to obtain for even a single configuration of joint. In this paper, a compromising computational method, called obstacle-set method, was used to model the joint-configuration-depended muscle path [21]. As illustrated in Figure 2.2, this method use some regular-shaped rigid bodies, like cylinder, to serve as obstacles fixed on and move with skeleton to force muscles wrap on it for all joint configurations. In the obstacle-set method, muscles were treated as mass-less, friction-less cables that follow shortest path between origin point and insertion point. The action line of MTF is determined by fixed or obstacle via points, origin and insert points.

Garner [21] presented the detailed descriptions of the algorithms and formulas about this method.

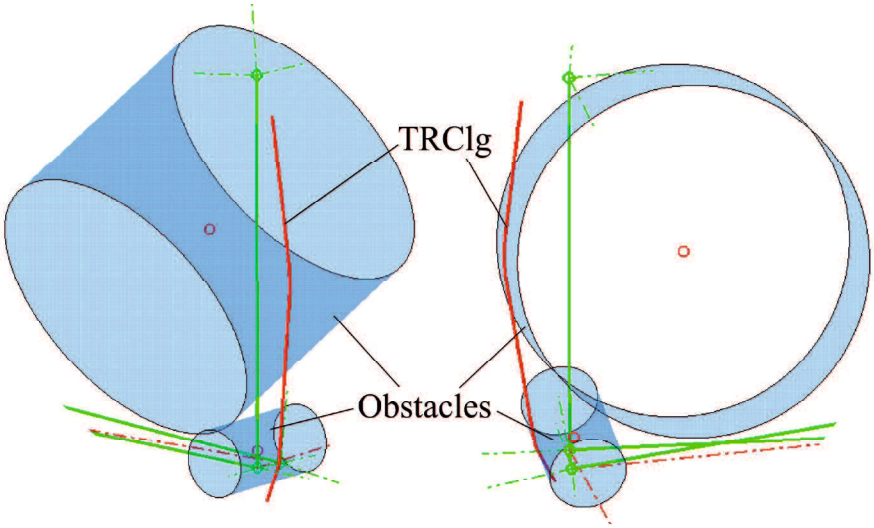

Figure 2.2 Two cylinders were modeled to force TRClg wrap on their surfaces.

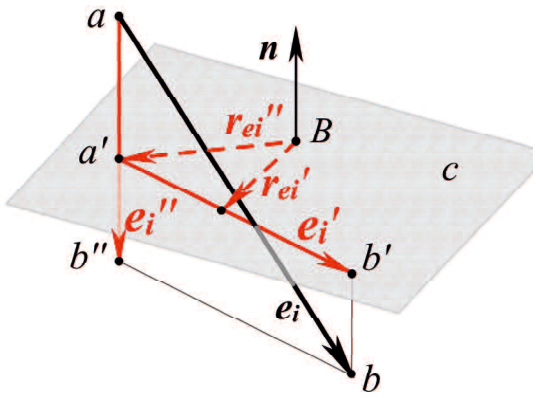

Figure 2.3 Algorithm used to project a vector into a specific plane.

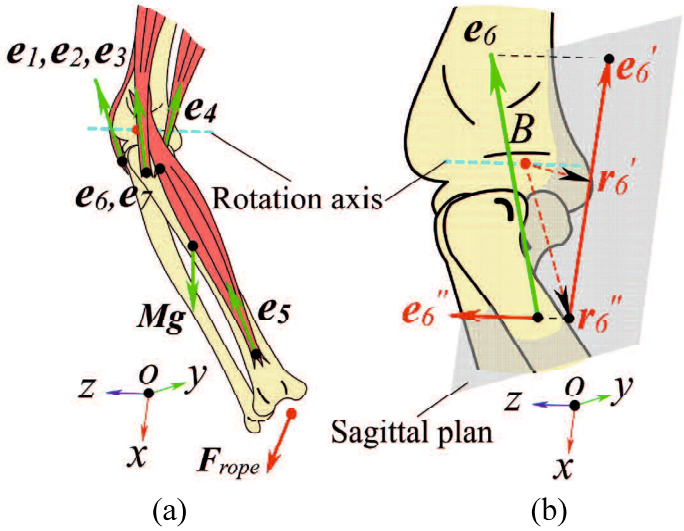

Figure 2.4 (a) Force-sharing of MTF across elbow joint. $\boldsymbol{e_i}(i=1\sim7)$ denotes action line of MTF; (b) The action line of $\boldsymbol{e_6}$ was projected into sagittal plan ($\boldsymbol{e_6}'$) and along rotation axis ($\boldsymbol{e_6}''$). $\boldsymbol{r_6}'$ and $\boldsymbol{r_6}''$ are their moment arm.

In the obstacle-set method mentioned above, shortest-path of muscle wrapping is computed analytically and muscle tendon length is calculated as sum of straight-line segments and wrapping segments. Different from the tendon displacement method [22], we classically defined moment arm as distance between muscle's action line and joint's axis of rotation [23]. Figure 2.3 illustrates algorithm used in estimating moment arm of a specific muscle with respect to a specific rotation axis. Point *a'* and *b'* is projection of point *a* and *b* in plane *c*. $\boldsymbol{r_{ei}}'$ is the moment arm of $\boldsymbol{e_i}'$ and $\boldsymbol{r_{ei}}''$ is moment arm of $\boldsymbol{e_i}''$. *B* is rotation center. For specific muscle modeled in MATLAB, coordinates of *a*, *b*, *B* and $\boldsymbol{n}$ are known and its moment arm about $\boldsymbol{n}$ can be calculated base on some simple geometric calculation. The MSM is a detailed three-dimensional model and action line of muscles usually not in the sagittal plane. As illustrated in Figure 2.4 (b), we project their action line into sagittal plan to calculate moment arm base on geometric calculation.

2.2 Optimization process

Another important issue about musculoskeletal modeling is optimization method used in estimation of MTF. As illustrated in Figure 2.4 (a), the human musculoskeletal system is usually characterized by redundant muscles and load sharing is closely related to action line of MTF and rotation axis. The static optimization method is usually used to solve this redundant problem. In the past two decades, a number of force prediction methods have been presented based on the Optimality principle [24] that represent performance criteria on which the neuromuscular system optimizes activation of motor unit. The static optimization is a computationally efficient method used in predicting redundant MTF by minimizing a cost function subject to force/torque constraints associated with a given task [24, 25]. Equilibrium equations include components in sagittal plane and along rotation axis, constructed two constraint equations in optimization. MTF is also constrained to between zero and maximum MTF by an inequality constraint. The objective function is

expressed as sum of muscle stress squared. Gravity of forearm is another contributor to the resultant moment about elbow joint. Static optimization is formulated as follows:

$$\text{Minimize} \sum_{i=1}^{n}\left(\frac{F_i^{mt}}{A_i}\right)^2 \tag{1}$$

$$\text{Subject to} \begin{cases} \sum_{i=1}^{n} F_i^{mt} \cdot \boldsymbol{r_i}' \times \boldsymbol{e_i}' + \boldsymbol{M}' = [\boldsymbol{I}] \cdot \boldsymbol{\alpha} \\ 0 \le F_i^{mt} \le F_{0i}^{M} \end{cases} \tag{2}$$

Where F_i^{mt} is magnitude of MTF; A_i is physiological cross-sectional area (PCSA); $\boldsymbol{e_i}'$ is sagittal projection of action line and $\boldsymbol{r_i}'$ is sagittal moment arm; $\boldsymbol{M}$ is resultant joint moment of gravity, resistance force, passive muscle fiber force and joint reaction moment, and $\boldsymbol{M}'$ is its projection in sagittal plane; $[\boldsymbol{I}]$ is inertia mass matrix of forearm; $\boldsymbol{\alpha}$ is angular acceleration at elbow joint (In this study, angular acceleration is relatively small and is assumed as 0); F_{0i}^{M} is the maximum isometric muscle fiber force.

2.3 Estimation of muscular states

In this section, we talk about the algorithm used in estimation of muscular states. Figure 2.5 is the flow chart of the estimation process. The musculoskeletal model and static dynamics are introduced in previous chapters and this section mainly on the description of Muscle-tendon model and the algorithm used in estimation of muscular states.

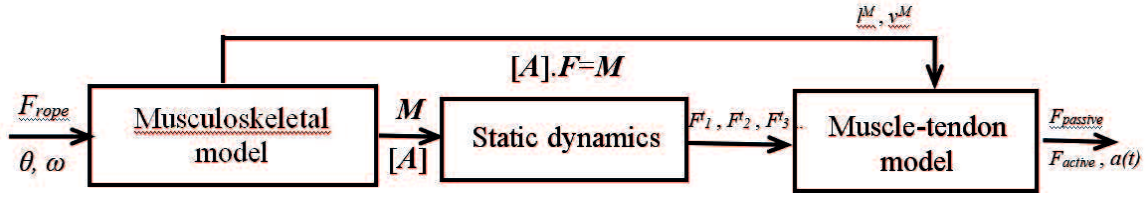

Figure 2.5 Flow chart of the estimation process.

2.3.1 Muscle-tendon model

A Hill-type muscle model was utilized to represent intrinsic mechanical properties of human muscles. As illustrated in Figure 2.6, each musculotendon actuator is represented as

a 3-element muscle in series with an elastic tendon. The instantaneous length of the actuator is determined by the length of muscle, the length of tendon, and the pennation angle of muscle. In this model, pennation angle is assumed to remain constant as muscle length changes [26].

For a specific muscle *i*, general form of function of Hill-type muscle model is given by:

$$\begin{aligned} F^{mt}(t) &= F^{t} \\ &= [F_A{}^{m} + F_P{}^{m}]\cos(\varphi) \\ &= [f_A(l) f(v) a(t) F_0{}^{M} + f_P(l) F_0{}^{M}]\cos(\varphi) \end{aligned} \tag{3}$$

Where $F^{mt}(t) = F^{t}$ is the time-varying MTF; $F_A{}^{m}$ and $F_P{}^{m}$ is the active and passive muscle fiber force; $l = l^{m}/l_0{}^{m}$ is the normalized muscle fiber length; $v = v^{m}/v_0{}^{m}$ is the normalized fiber velocity; $l_0{}^{m}$ is optimal fiber length; $v_0{}^{m}$ is maximal fiber velocity; $a(t)$ is time varying muscle activation; φ is muscle pennation angle; $f_A(l)$ and $f_P(l)$ are normalized active and passive force-length relationships; $f(v)$ is normalized curve of velocity-dependent muscle fiber force. $f_A(l)$, $f_P(l)$ and $f(v)$ are nonlinear formulas characterize material properties of muscle tissue. In this model, we use curves created by cubic spline interpolation of points defined on the Gordon Curve [27, 28]. As illustrated in Figure 2.7 and Figure 2.8 are the normalized force-length and force-velocity curves. Curves were normalized for force, length and velocity. Maximum muscle fiber contraction velocity of all muscles was assumed to be $v_0{}^{m}=10 l_0{}^{m}$ [29].

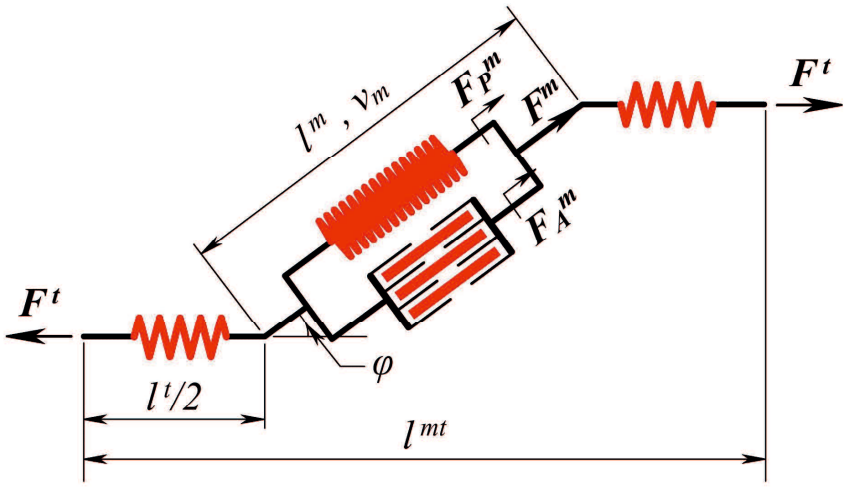

Figure 2.6 The three-parameter Hill-type muscle model used in modeling muscle force-generating characteristics

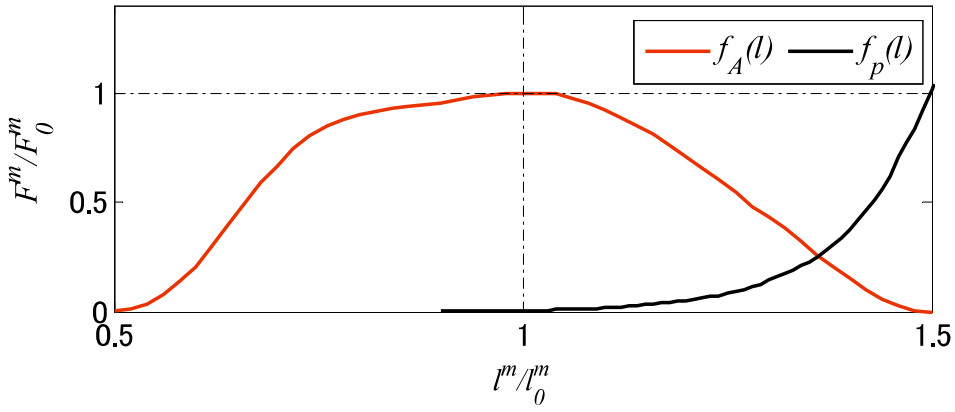

Figure 2.7 The normalized curve of active and passive force-length relationships [27].

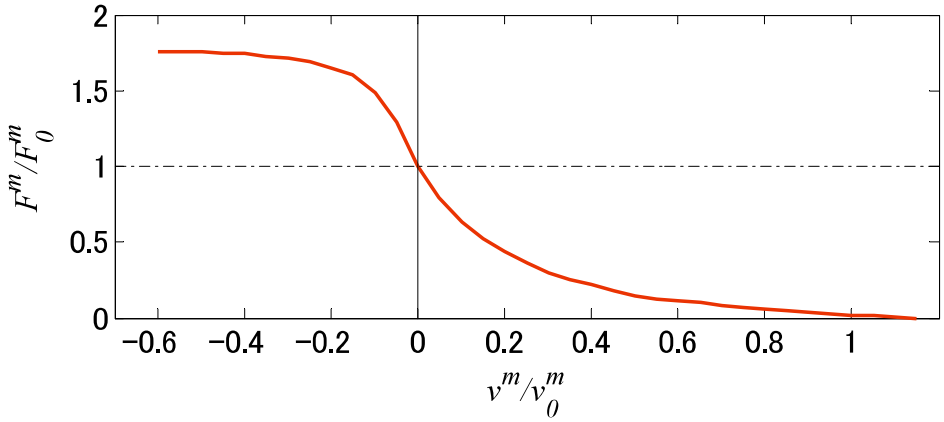

Figure 2.8 The normalized curve of force-velocity relationship of active muscle fiber.

2.3.2 Estimating muscular states

According to (3), muscle fiber length and fiber velocity is needed in estimation of

passive and active muscle fiber force. For a specific muscle, we approximate muscle-tendon length as a function of θ:

$$l^{mt} = \Psi_4(\theta) \tag{4}$$

The muscle tendon length includes two parts: tendon length l^t and fiber length l^m.

$$l^{mt} = l^t + l^m \cos(\varphi) \tag{5}$$

Suppose the change of muscle-tendon length is mainly result from the change of fiber length, we have:

$$\frac{dl^{mt}}{dt} = \frac{d\Psi_4(\theta)}{dt} = \Psi_5(\theta, w) = -v^m \cos(\varphi) \tag{6}$$

Where v^m is the fiber velocity and $v^m > 0$ means muscle is shortening; $v^m < 0$ means muscle is lengthening. Figure 2.9 illustrates algorithm used in estimation of muscular states.

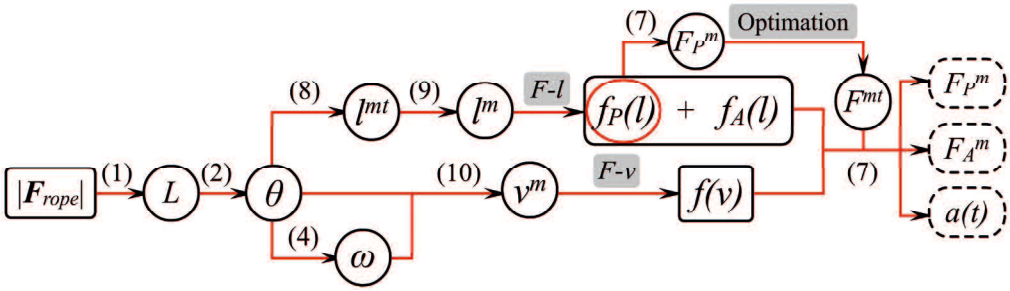

Figure 2.9 Block-diagram of algorithm used to estimate muscular states.

3. Estimating training effect on specific muscle based on AnyBody

As we have reviewed in Chapter 1, the suitable exercise intervention for treatment of frailty is different during pre-frail and frailty stage. In order to avoid unnecessary injuries to the frailty people, the exercise intervention need to be prescribed. Before choosing the exercise for frailty people, physiotherapists need to evaluate the potential training effect of exercise on patient, especially for those people who need adjust their muscle activation

patterns in an appropriate manner. As shown in Figure 2.10, when the subject performs the bicep curling exercise to lift a dumbbell, the weight of the dumbbell is the same, but the muscle activation pattern is different as a consequence of difference in the pronation and supination angle of forearm rotation.

The previous section shows that the musculoskeletal modeling provides a considerable method to gain an insight into the muscular states during exercise training and the computational methods were described in detail. However, the calculation results in previous section are closely related to the optimization method used in inverse dynamic analysis and the architectural properties of muscles in the model. To obtain a more reliable estimated result, the AnyBody is used to calculate the muscle activation patterns during biceps curl to lifting a dumbbell in this section. This section mainly focus on the building process of the musculoskeletal model, and some simulation results and discussion will be presented.

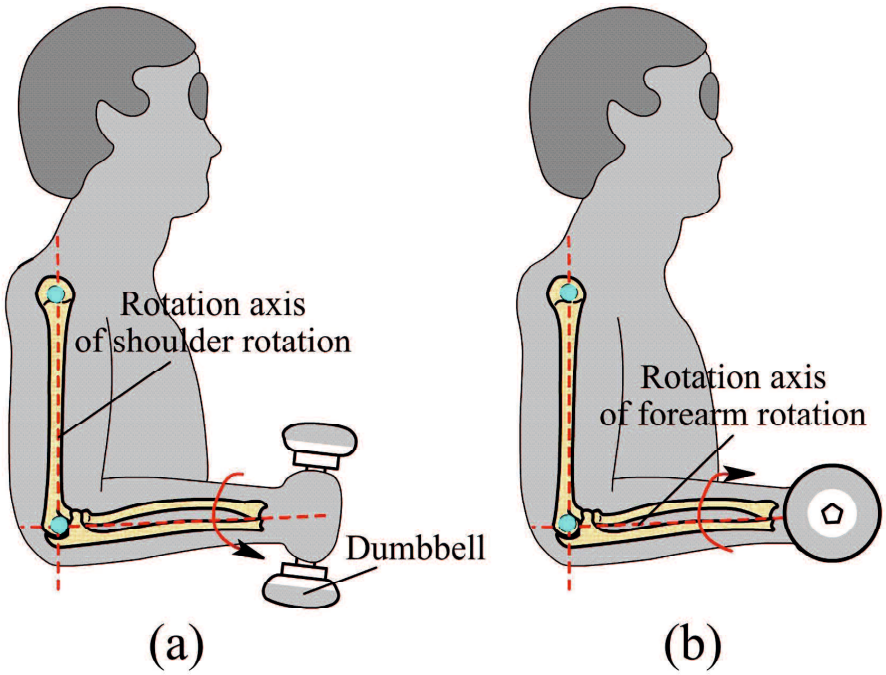

Figure 2.10 The subject is doing bicep curl exercise to lift a dumbbell with his palm: (a) facing left (at neutral position) and (b) facing up (supination angle is 90°).

3.1 Musculoskeletal modeling in AnyBody

The AnyBody (version 7.2, AnyBody Technology, Denmark) is a commercial

software which is designed for constructing complex models of the human body and for determining the environment's influence on the body. The mathematical and mechanical methods of the system were described in detail in [30]. A lot of templates are available in the software and users can built their own model by modifying the template, thus providing users a convenient and efficient method for simulating human movements. In this section, the template of *The Shoulder Arm Model* is used and modified to built a simulation model of people doing biceps curl to lifting a dumbbell. The built model is illustrated in Figure 2.11. The model includes 5 degrees of freedom (DOF) that define the kinematics of the shoulder and elbow joint. At the shoulder joint, the three degrees of freedom are elevation plane, thoracohumeral angle (also referred to as elevation angle), and shoulder rotation. The elbow is defined by elbow flexion and forearm rotation. This muscle model includes major muscles cross the shoulder joint and elbow joint, and the parameters of muscle architecture are based on the preset values in the model. During the simulation, the three degrees of freedom in the shoulder joint are constrained to keep shoulder joint at neutral position and humerus in parallel with y axis of thorax. The pronation or supination angle of forearm rotation is kept at a specific angle and the elbow flexion and extension joint is driven by a force driver. This model is built for the purpose of simulating subject standing straight and doing biceps curl to lifting a dumbbell in his sagittal plane. And an ordinary dumbbell weighted 5 Kg is attached to the subject's hand through the *Palm Joint* on his hand.

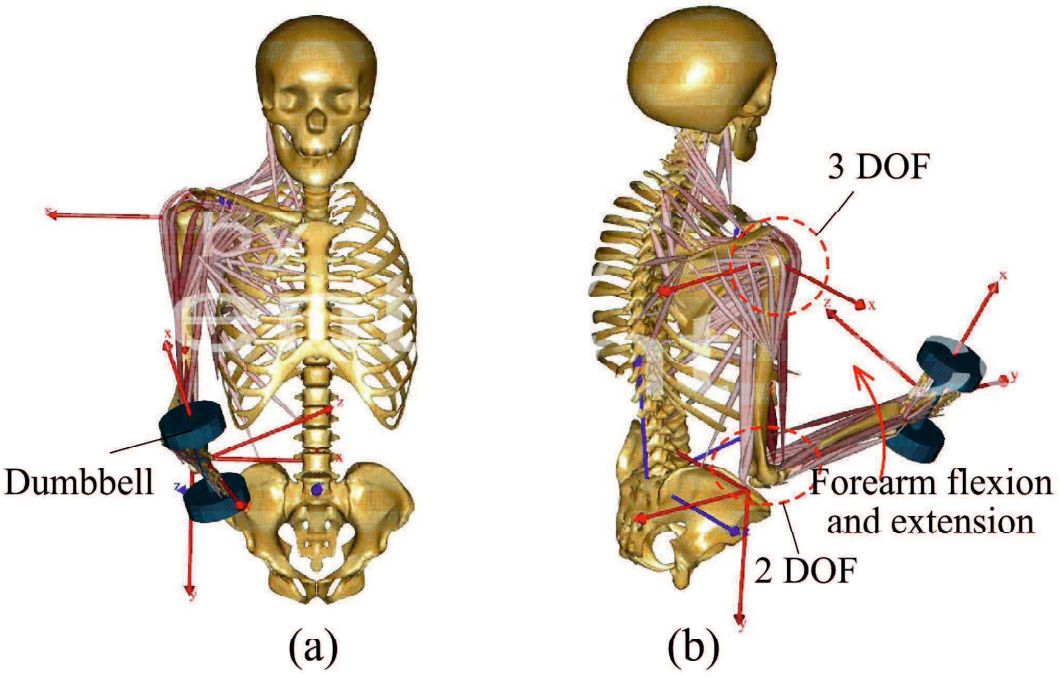

Figure 2.11 The musculoskeletal model established in AnyBody. The subject is standing in straight and doing biceps curl to lifting a dumbbell in his sagittal plane. (a) is the frontal view and (b) is the posteriolateral view.

3.2 Simulation results

After building the musculoskeletal model in AnyBody, a series of simulations were carried out with different pronation and supination angle. As illustrated in Figure 2.4, the force-sharing of MTF across the elbow joint is different when forearm rotation is at different pronation and supination angle, results in the difference in muscle activation patterns. Thus in this section, we want to analysis the difference in muscle activation patterns due to pronation and supination angle when subject is doing biceps curl to lifting a dumbbell. Figure 2.12 vividly expresses the variation range of pronation and supination angle of forearm rotation. In the neutral position, the palm of subject is facing left. When the supination angle reaches 90°, the palm is facing up, and when the pronation angle reaches 90°, the palm is facing down.

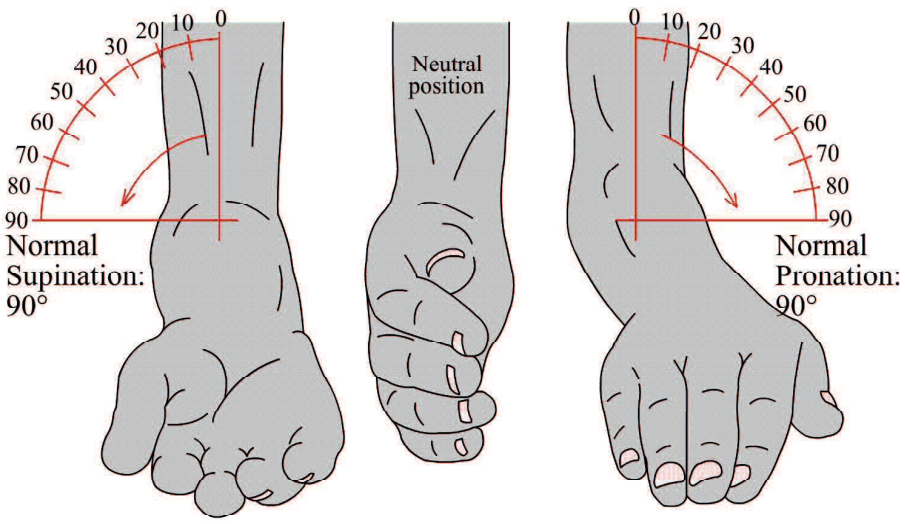

Figure 2.12 Definition of pronation and supination angle of forearm rotation.

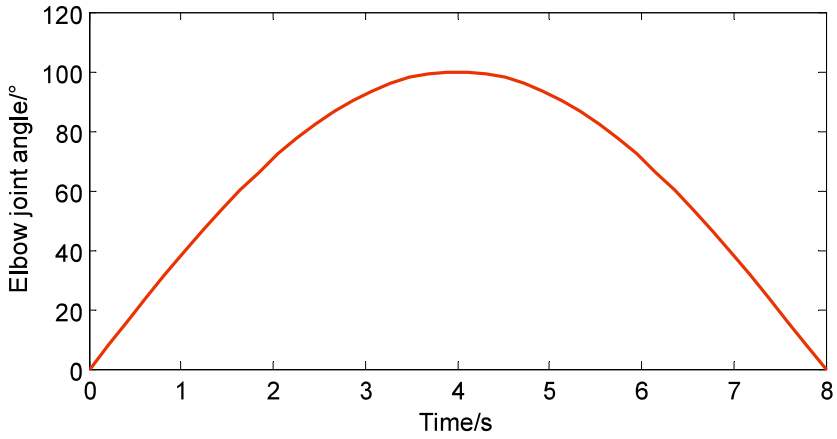

Figure 2.13 Elbow joint angle as a function of time.

We changed the rotation angle of forearm from supination 90° to pronation 90° in the model, and got the muscle length and muscle-tendon force at different pronation and supination angle. As illustrated in Figure 2.13, the elbow joint is driven by a *Force Driver* and the elbow joint angle changes with time like a sinusoid. The elbow joint angle varies from 0° to 100° and the period of the sinusoid is 16s. The flexor muscles are dominated in the flexion of forearm (Table 2.1). The simulation results of muscle length and muscle-tendon force at different pronation and supination angle are illustrated in Figure 2.14 and Figure 2.15. Different from our muscle model described in the previous section, the musculoskeletal model in the AnyBody divide the BRD and BRA muscle into two parts. But as we can see from Figure 2.14 and Figure 2.15 , the muscle length and muscle-tendon force are almost the same during the simulation, so we treat them as one muscle. From

Figure 2.14 we also found that the muscle length of BICl and BICs becomes longer as the forearm rotation angle changes from supination to pronation, with the BRD and BRA change little. And according to Figure 2.15, we can see from the results that the changes in the pronation and supination angle obviously affect the muscle activation patterns. Similar to our simulation results presented in the previous section, the BRA muscle produced the biggest average and maximal force during the simulation. As the forearm angle varies from supination to pronation, the force-sharing of MTF is more and more concentrated on the BRA muscle. This indicates that the different way of lifting dumbbell will results in different training effects on the subject at the muscle level.

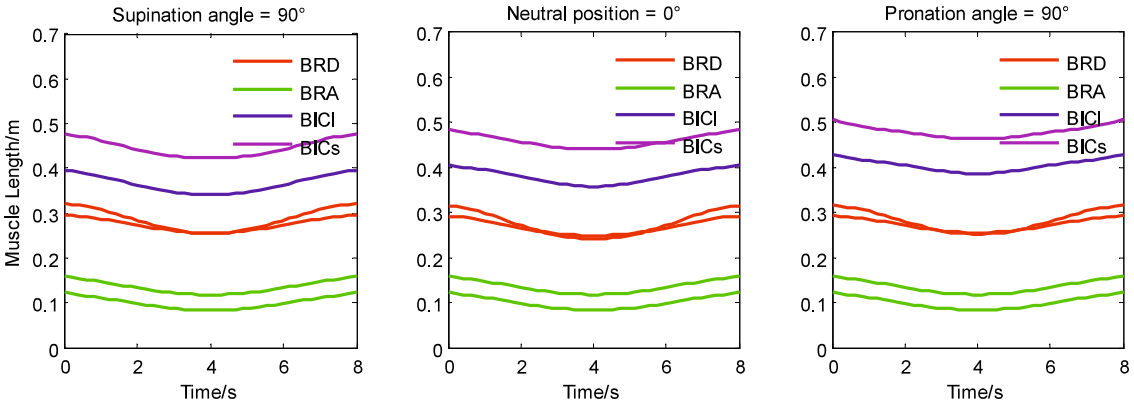

Figure 2.14 Muscle length at different pronation and supination angle.

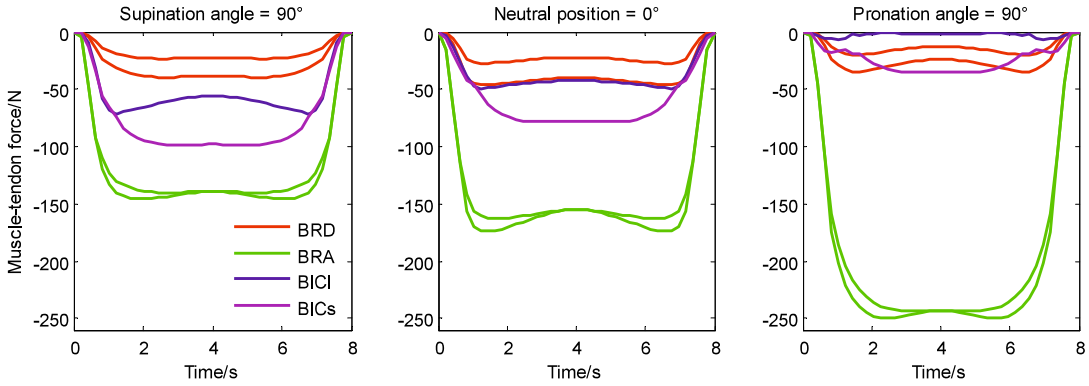

Figure 2.15 Muscle-tendon force at different pronation and supination angle.

3.3 Discussion

The biceps curl to lifting a dumbbell is a simple and common exercise which focuses on development or maintenance of flexor strength of upper extremity. But as illustrated in Figure 2.16, different people may have different ways to life dumbbell. Some people like

to lift the dumbbell with his palm facing up but others prefer facing left or right. The simulation results in previous section have revealed that the rotation angle of forearm affects muscle activation patterns of muscles across the elbow joint. Here we want talk about the rotation-angle-resulted difference in the training effect at the muscle-level.

Figure 2.16 Different ways to lift a dumbbell.

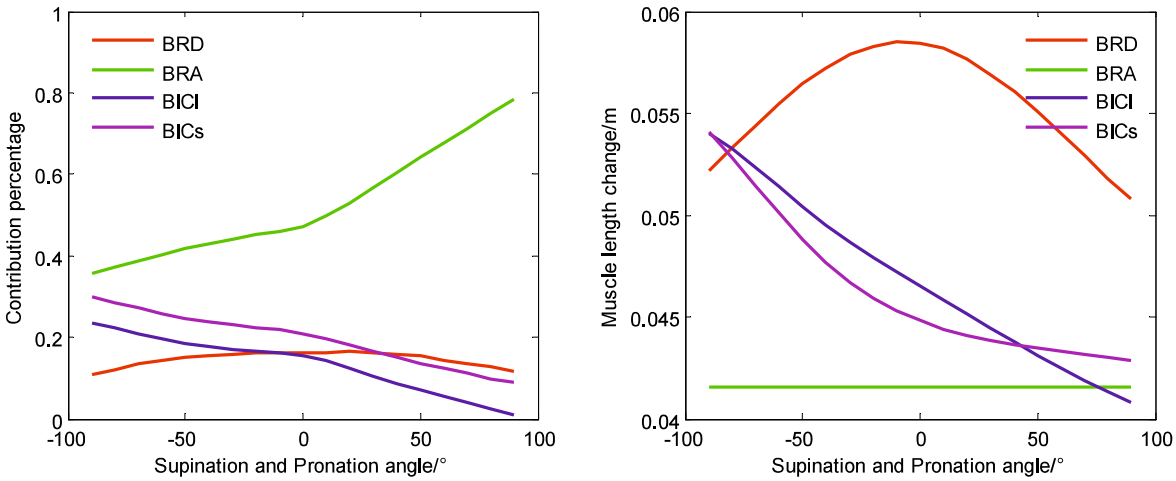

Figure 2.17 Contribution percentage of work and length change of all muscles at different pronation and supination angle.

It is the muscle that helps us moves forward, and the effect of muscle for people is similar to that of an engine for a car. Studies [31] have show that the improvement of muscle strength is a result of mechanical stimuli like work and power. The changes in muscle length will stretch subject's muscles and have the advantages of relieving muscle tightness, improving body flexibility and curing muscle soreness. Therefore, we calculated

the work performed by all muscles and the length change when subject lifts the dumbbell to the maximum angle, and show the results in Figure 2.17. As we have mentioned in previous section that the BRA is the biggest energy provider. The work contribution percentage of flexor muscles is changed with the forearm rotation angle. The contribution percentage is more balanced when subject's palm faces up and the force-sharing of MTF is concentrate on the BRA muscle when the forearm rotation angle changes from supination to pronation. The length change of BRD reaches peak when the forearm is at neutral position. To some extend, the simulation results provides good instructions when subjects doing biceps curl to lift a dumbbell. It is suggested to put your palm faces up if you want get a more balanced force-sharing of muscle force across the elbow joint and the stretching effect on your BRD muscle is best when you forearm is at neutral position. In order to avoid excessive concentration of muscle force, you'd better not put your palm faces down.

4. A simple analytical model for estimating muscular states

In later chapters, we will use the dumbbell lifting exercise to assess the elbow flexor muscle's frailty level of elderly people. To achieve that goal, in this section we present a simple analytical model for estimating muscular states based on the techniques and methods introduced in the previous sections. Generally speaking, the methods used for estimating muscle status described in Section 2 of this Chapter is a method of numerical calculation and it require parameter optimization to solve the redundant problem of muscle force sharing. But because of the intrinsic property of static optimization, the calculation process is time-consuming and the optimized results are closely related to the objective function and constraint conditions. Therefore, to solve the problems mentioned above, we built a simple analytical model by using techniques and methods introduced in Section 2 and Section 3 of this Chapter.

4.1 The analytical model

Before building the analytical model, we need to make some proper assumptions. The

mechanism by which the neuromuscular system controls muscle activation to produce intended movement is very complicated, especially for multi-joint movement. But for single-joint movement like dumbbell lifting, the activation pattern of muscles is mainly related to joint position. Therefore, In this analytical model, we assume that: 1. When lifting a dumbbell, the activation pattern of muscles across the elbow joint is depend on the elbow joint angle, and has nothing to do with the dumbbell weight; 2. When the muscle fiber activation rate of the biggest moment contributor reaches its biggest value (100%), the elbow joint angle reaches its maximum value.

According to Figure 2.1, we can see that it is the elbow flexor muscles that bend the elbow to lift the dumbbell. The elbow flexor muscles include the Brachialis, Brachioradialis, Biceps brachii (long) and Biceps brachii (short) muscle. Since different muscles have different physiological cross-sectional area and moment arm, therefore, their moment contribution to lift the dumbbell is also different. We did simulation of dumbbell lifting by using the AnyBody model established in Section 3 of this Chapter and the simulation results of the moment contribution ratio of each muscle when lifting a dumbbell is illustrated in Figure 2.18. The elbow joint angle varies from 0° to 135° and the period of the sinusoid is 16s. The dumbbell weight is 6Kg in the model. We use the moment contribution ratio as gold standard to determine individual muscle moment contribution ratio.

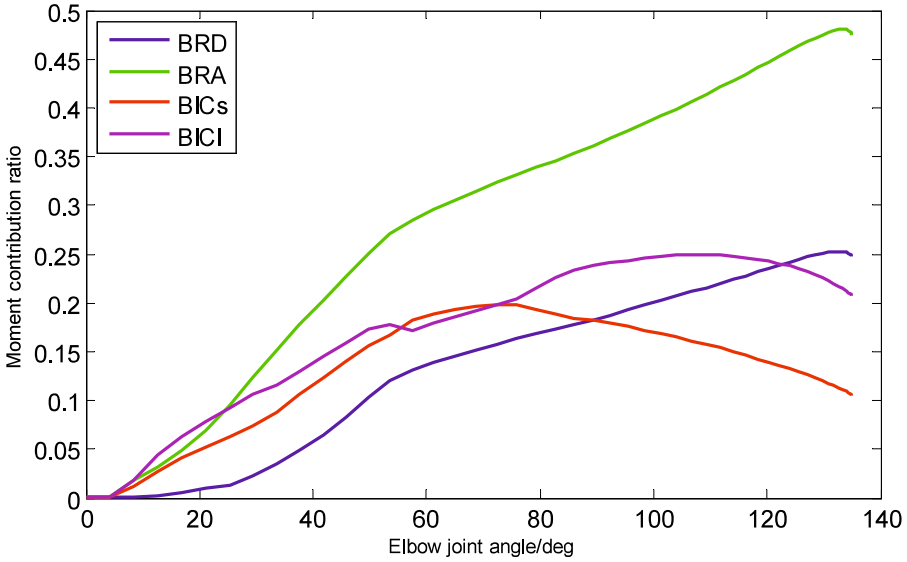

Figure 2.18 Simulation results of moment contribution of each muscle when lifting a dumbbell.

From the simulation results, we can see that the contribution of each muscle is not the same and the ratio is changes with the elbow joint angle. The Brachioradialis (BRD) muscle is the biggest moment contributor. Suppose the moment contribution is only depend on the elbow joint angle, the moment contribution of BRD ($K(\theta)$) can be expressed as:

$$K(\theta) = \Psi_1(\theta) \tag{7}$$

where θ is the elbow joint angle and $\Psi_1(\theta)$ is a polynomial of θ.

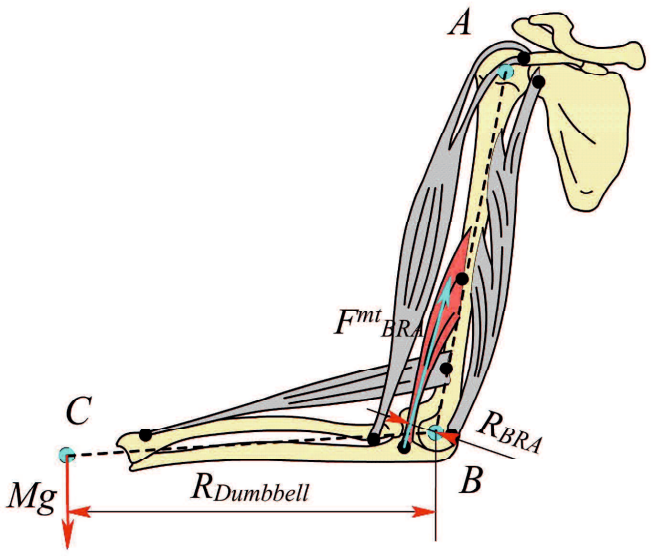

Figure 2.19 Force analysis of muscle across the elbow joint.

Figure 2.19 gives the force analysis of muscle across the elbow joint. The muscle across the elbow joint includes 7 muscles or muscle parts. According to equilibrium equation of force in the theoretical mechanics, the moment of dumbbell is the sum of moment of all muscles across the elbow joint. Which can be expressed as:

$$Mg \cdot R_{Dumbbell} = F^{mt}_{BRA} \cdot R_{BRA} + F^{mt}_{BRD} \cdot R_{BRD} + F^{mt}_{BICs} \cdot R_{BICs} + F^{mt}_{BICl} \cdot R_{BICl} \tag{8}$$

where M is the dumbbell weight and g is the gravitational acceleration. $R_{Dumbbell}$ is the moment arm of dumbbell force. F_A^{mt} is the muscle tendon force of A muscle and R_A is its corresponding muscle moment arm. Since the BRD muscle is the biggest moment

contributor and the moment contribution of BRD is obtained from the simulation of AnyBody, we can write Formula 8 as:

$$K(\theta)\cdot Mg\cdot R_{Dumbbell}=F_{BRA}^{mt}\cdot R_{BRA} \tag{9}$$

From the formulas (3) and (9), we can get a more concise equation for linking external dumbbell force to internal muscle parameters as:

$$K(\theta)\cdot MgL_1\sin(\theta)=\left[f_A(l)f(v)a(t)+f_P(l)\right]F_0^M R_{BRA}^{mt}(\theta)\cos(\varphi) \tag{10}$$

where L_1 is the length of forearm. The meaning of other variables such as l and v are the same with Formula (3). Which can be expressed as:

$$\begin{aligned} l&=\frac{l^{mt}(t)}{l_0^m}\\ v&=\frac{v^{mt}(t)}{v_0^m}\\ v^m(t)&=\frac{dl^m(t)}{dt}\\ l^m(t)&=\Psi_2(\theta)\\ \theta(t)&=\Psi_3(t) \end{aligned} \tag{11}$$

where $\Psi_2(\theta)$ is a polynomial of θ, and $\Psi_3(t)$ is a polynomial of t.

For the BRA muscle, its muscle moment arm is a function of θ which can be expressed as:

$$R_{BRA}^{mt}=7.89e^{-8}\theta^4-4.27e^{-5}\theta^3+4.96e^{-3}\theta^2+0.11\theta+3.2 \tag{12}$$

The muscle length of BRA is:

$$l_{BRA}^{mt}=2.431e^{-7}\theta(t)^4-4.931e^{-5}\theta(t)^3-5.55e^{-4}\theta(t)^2-0.2025\theta(t)+362.2 \tag{13}$$

Furthermore, we can get the muscle fiber velocity as:

$$v_{BRA}^{mt} = \frac{dl_{BRA}^{mt}}{dt} = (9.725e^{-7}\theta(t)^3 - 1.479e^{-5}\theta(t)^2 - 1.11e^{-3}\theta(t) - 0.2025)\omega(t) \quad (14)$$

Therefore, according to Formulas (11) ~ (14), if we know the elbow joint angle as a function of time, we can estimate the internal muscular states simply and easily. In the next section, we will show some simulation results.

4.2 The simulation results

In this section, we will show some simulation results explain how the external parameters and internal muscle parameters will affect the state of activation of the muscle fibers a(t). In later chapters, the a(t) is an important parameter in evaluation of the frailty level. Figure 2.20 is the moment arm of the dumbbell and BRA muscle in the model.

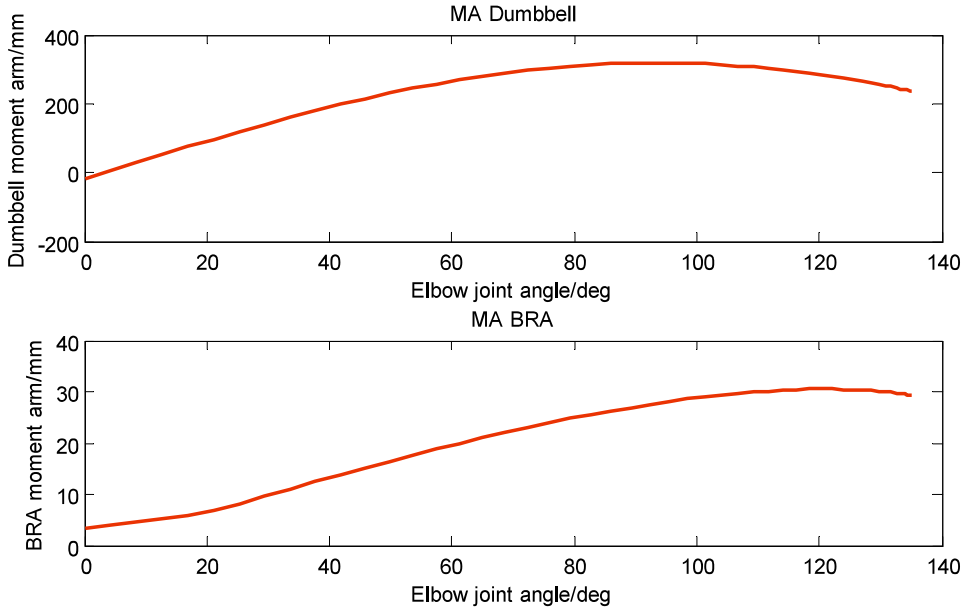

Figure 2.20 The moment arm of the dumbbell and BRA muscle.

4.2.1 Impact of F_0^M on the simulation results

It is widely accepted that the aging will results in a decrease in muscle mass that has a direct impact on the ability to produce force. Here we will investigate the impact of F_0^M on the simulation results. We decrease the value of F_0^M in the model to simulate the decline in

muscle strength of elderly people as they age. Table 2.3 are the different cases of F_0^M in the simulation. In the simulation, the subject is lifting a 6Kg dumbbell from 0° to 120° in 1 second and put it down. The elbow joint angle can be expressed as a function of time:

$$\theta(t) = 120 \cdot \sin\left(\frac{\pi}{2} \cdot t\right) \quad (t = 0 \sim 2s) \tag{15}$$

Correspondingly, the elbow joint angular velocity can be expressed as:

$$\omega(t) = 60\pi \cdot \cos\left(\frac{\pi}{2} \cdot t\right) \quad (t = 0 \sim 2s) \tag{16}$$

Table 2.3 Different cases of F_0^M in the simulation. F_0^M is the peak muscle force.

Case A	F_0^M = 461.76N×100%
Case B	F_0^M = 461.76N×60%
Case C	F_0^M = 461.76N×30%
Case C_0	F_0^M = 461.76N×17%

Figure 2.21 is the change of activation state of the muscle fibers a(t) with different F_0^M. As we can see from the simulation results, the muscle utilization rate increases with the decrease of F_0^M when a subject want lift a dumbbell to the same position.

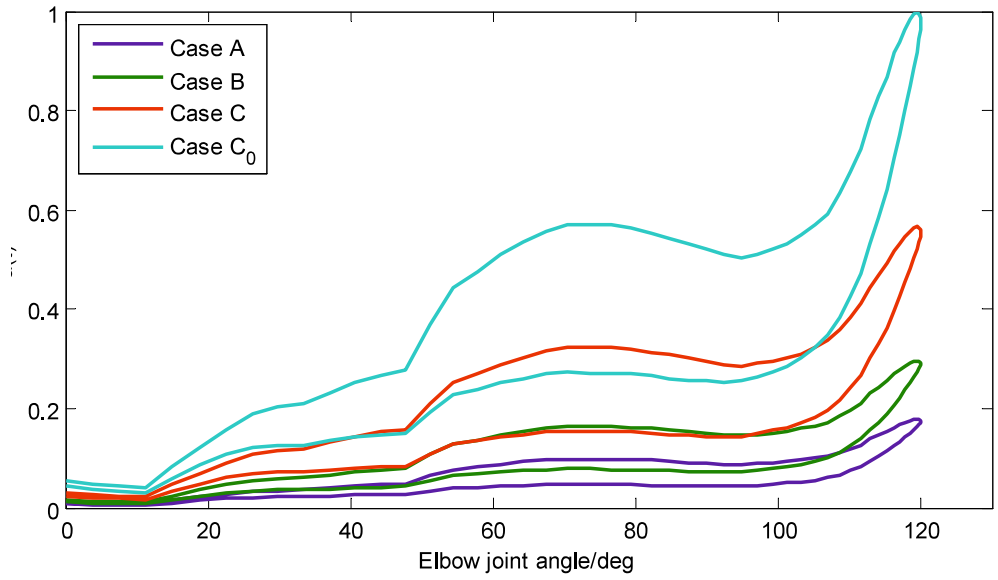

Figure 2.21 The change of activation state of muscle fibers of the BRA muscle a(t) with different F_0^M. When the a(t) is equal to 1, it means that all the fiber are activated.

4.2.2 Impact of elbow joint angular velocity on the simulation results

In this section, we investigate how the elbow joint angular velocity affect activation state of muscle fibers. There are 3 simulation cases with different angular velocity as shown in Table 2.4. The change of elbow joint angle of each simulation case with time is shown in Figure 2.22. In those simulation cases, the subject is lifting a 6Kg dumbbell from 0° to 120° at different speeds. Case D is the most fast and Case F is the slowest. The F_0^M in the model is equals to 461.76N. Figure 2.23 shows the simulation results of the change of a(t) with different angular velocity. From the simulation results, we can see that muscle activation rate during the elbow flexion phase is bigger than that of the elbow extension phase. And the increased angular velocity will results in the increase of muscle fiber activation consumption.

Table 2.4 Different cases with different angular velocity in the simulation.

Case D	$\theta(t) = 120 \cdot \sin(\pi \cdot t) \quad (t = 0 \sim 1s)$
	$\omega(t) = 120\pi \cdot \cos(\pi \cdot t) \quad (t = 0 \sim 1s)$
Case E	$\theta(t) = 120 \cdot \sin\left(\frac{\pi}{2} \cdot t\right) \quad (t = 0 \sim 2s)$
	$\omega(t) = 120\pi \cdot \cos\left(\frac{\pi}{2} \cdot t\right) \quad (t = 0 \sim 2s)$
Case F	$\theta(t) = 120 \cdot \sin\left(\frac{\pi}{4} \cdot t\right) \quad (t = 0 \sim 4s)$
	$\omega(t) = 30\pi \cdot \cos\left(\frac{\pi}{4} \cdot t\right) \quad (t = 0 \sim 4s)$

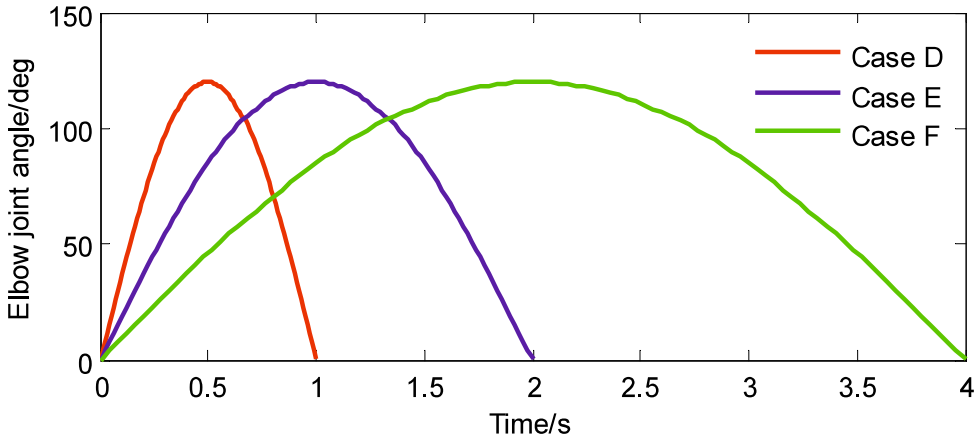

Figure 2.22 The different cases of elbow joint angle changes with time.

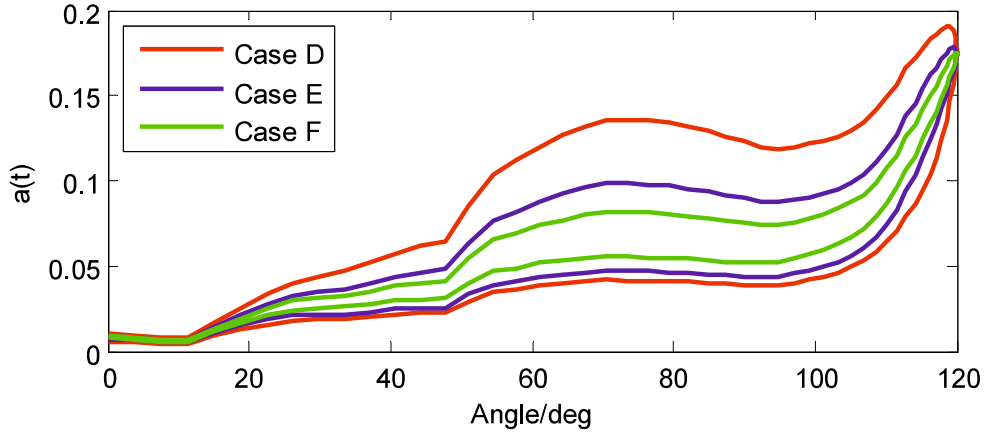

Figure 2.23 The change of activation state of muscle fibers of the BRA muscle a(t) with different angular velocity.

5. Summary

In this section, we presents the concept of using musculoskeletal modeling to estimate muscular states during resistance training and this chapter is mainly on the discussion of the computational aspects musculoskeletal modeling. We take the elbow flexor RT as a simple example and an integrated system was built for this exercise. The design concepts of the system, the measurement and analysis methods were described in detail. Some comparative experiments were carried out to show feasibility and accuracy of this system. Simplicity and low computational costs are two of the biggest advantages of the system. Many results can be displayed to the patient in real-time so that the patient can choose the appropriate training dose based on his feeling or the instruction of physiotherapist. The calculations also demonstrate that musculoskeletal modeling is a considerable method to

vividly show the muscular states during the training. After introducing the computational methods used in musculoskeletal modeling, the exercise of biceps curl to lift a dumbbell was simulated to provide physiotherapists with good instructions to design the training exercise. The simulation results reveal that: 1. If you want get a more balanced force-sharing of muscle force across the elbow joint, please put your palm faces up; 2. The stretching effect on your BRD muscle is best when you forearm is at neutral position; 3. In order to avoid excessive concentration of muscle force, you'd better not put your palm faces down.

In addition, due to the intrinsic property of static optimization, the calculation process is time-consuming and the optimized results are closely related to the objective function and constraint conditions. To solve the problems mentioned above, we built a simple analytical model by using techniques and methods introduced in Section 2 and Section 3 of this Chapter. Simulations were carried out to reveal the impact of F0M and elbow joint angular velocity on the muscle fibers activation state in the case of dumbbell lifting.

6. References

[1] Bamman MM, Clarke MSF, Feeback DL, et al. 1998. Impact of resistance exercise during bed rest on skeletal muscle sarcopenia and myosin isoform distribution[J]. Journal of Applied Physiology. 84:157-163.

[2] Trappe S, Trappe T, Gallagher P, et al. 2004. Human single muscle fibre function with 84 day bed-rest and resistance exercise[J]. The Journal of physiology. 557:501-513.

[3] Ellison, Jennifer Barbee, et al. 2016. "Short-Term Intensive Rehabilitation Induces Recovery of Physical Function After 7 Days of Bed Rest in Older Adults." Journal of acute care physical therapy 7.4: 156-163.

[4] Crewther B, Cronin J, Keogh J. 2005. Possible stimuli for strength and power adaptation[J]. Sports medicine. 35:967-989.

[5] Fielding RA, LeBrasseur NK, Cuoco A, et al. 2002. High-velocity resistance training increases skeletal muscle peak power in older women[J]. Journal of the American Geriatrics Society. 50:655-662.

[6] Reid KF, Fielding RA. 2012. Skeletal muscle power: a critical determinant of physical functioning in older adults[J]. Exercise and sport sciences reviews. 40:4.

[7] Kolditz M, Albin T, Abel D, et al. Evaluation of foot position and orientation as manipulated variables to control external knee adduction moments in leg extension training[J]. Computer methods and programs in biomedicine, 2016.

[8] Suetta C, Andersen JL, Dalgas U, et al. 2008. Resistance training induces qualitative changes in muscle morphology, muscle architecture, and muscle function in elderly postoperative patients[J]. Journal of applied physiology. 105:180-186.

[9] Holzbaur KRS, Murray WM, Delp SL. 2005. A model of the upper extremity for simulating musculoskeletal surgery and analyzing neuromuscular control[J]. Annals of biomedical engineering. 33:829-840.

[10] Dorn TW, Schache AG, Pandy MG. 2012. Muscular strategy shift in human running: dependence of running speed on hip and ankle muscle performance[J]. Journal of Experimental Biology. 215:1944-1956.

[11] Zhong Y, Fu W, Wei S, et al. Joint Torque and Mechanical Power of Lower Extremity and Its Relevance to Hamstring Strain during Sprint Running[J]. Journal of healthcare engineering, 2017.

[12] Neptune RR, McGowan CP, Fiandt JM. 2009. The influence of muscle physiology and advanced technology on sports performance[J]. Annual review of biomedical engineering. 11:81-107.

[13] Niu W, Wang L, Jiang C, et al. Effect of Dropping Height on the Forces of Lower Extremity Joints and Muscles during Landing: A Musculoskeletal Modeling[J]. Journal of healthcare engineering, 2018, 2018.

[14] Mudge S. 2008. A growing web resource of physiotherapy exercises: www.physiotherapyexercises.com[J]. Australian Journal of Physiotherapy. 54:225-226.

[15] Mahrova A, Svagrova K. 2013. Exercise Therapy–Additional Tool for Managing Physical and Psychological Problems on Hemodialysis[M]//Hemodialysis. InTech.

[16] Normandin, Edgar A., et al. "An evaluation of two approaches to exercise conditioning in pulmonary rehabilitation." Chest 121.4 (2002): 1085-1091.

[17] Gigliotti, Francesco, et al. "Arm exercise and hyperinflation in patients with COPD: effect of arm training." Chest 128.3 (2005): 1225-1232.

[18] Garner BA, Pandy MG. 1999. A kinematic model of the upper limb based on the visible human project (vhp) image dataset[J]. Computer methods in biomechanics and biomedical engineering. 2:107-124.

[19] Garner BA, Pandy MG. 2001. Musculoskeletal model of the upper limb based on the visible human male dataset[J]. Computer methods in biomechanics and biomedical engineering. 4:93-126.

[20] Rohen JW, Yokochi C, Lütjen-Drecoll E. 2006. Color atlas of anatomy: a photographic study of the human body[M]. Schattauer Verlag.

[21] Garner BA, Pandy MG. 2000. The obstacle-set method for representing muscle paths in musculoskeletal models[J]. Computer methods in biomechanics and biomedical engineering. 3:1-30.

[22] An KN, Takahashi K, Harrigan TP, et al. 1984. Determination of muscle orientations and moment arms[J]. Journal of biomechanical engineering. 106:280-282.

[23] Erdemir A, McLean S, Herzog W, et al. 2007. Model-based estimation of muscle forces exerted during movements[J]. Clinical biomechanics. 22:131-154.

[24] Crowninshield RD, Brand RA. 1981. A physiologically based criterion of muscle force prediction in locomotion[J]. Journal of biomechanics. 14:793-801.

[25] Ueda J, Ming D, Krishnamoorthy V, et al. 2010. Individual muscle control using an exoskeleton robot for muscle function testing[J]. IEEE Transactions on Neural Systems and Rehabilitation Engineering.18:339-350.

[26] Buchanan TS, Lloyd DG, Manal K, et al. 2004. Neuromusculoskeletal modeling: estimation of muscle forces and joint moments and movements from measurements of neural command[J]. Journal of applied biomechanics. 20:367-395.

[27] Zajac FE. 1989. Muscle and tendon Properties models scaling and application to biomechanics and motor[J]. Critical reviews in biomedical engineering. 17:359-411.

[28] Gordon AM, Huxley AF, Julian F J. The variation in isometric tension with sarcomere length in vertebrate muscle fibres[J]. The Journal of physiology, 1966, 184(1):170-192.

[29] Anderson FC, Pandy MG. 1999. A dynamic optimization solution for vertical jumping in three dimensions[J]. Computer methods in biomechanics and biomedical engineering. 2:201-231.

[30] Damsgaard M, Rasmussen J, Christensen S T, et al. Analysis of musculoskeletal systems in the AnyBody Modeling System[J]. Simulation Modelling Practice and Theory, 2006, 14(8): 1100-1111.

[31] Crewther, Blair, John Cronin, and Justin Keogh. "Possible stimuli for strength and power adaptation: acute metabolic responses." Sports Medicine 36.1 (2006): 65-79.

Chapter 3

Measuring System for Evaluation of Muscle Function

1. Introduction

As we mentioned in Chapter 1, the research scope of this thesis mainly focus on the physical domain of frailty. The muscle strength, motion control ability and exercise tolerance are important aspects of muscle function, and are closely related to the ability to perform activities in daily life. In this section, we introduce the development of a muscle function measurement and evaluation system. Firstly, we need a motion capture system to recognize and record movements of trainee when doing exercise. The resistance force data are also needed to record when trainee is doing resistance training. Later, the data obtained needs to be processed and indexes are needed to quantify the muscle function. Therefore, this section mainly focus on the sensor technology aspect and development of the measurement system. And a repetition segmentation and a muscle action segmentation are also proposed to pre-process the obtained data, for the purpose of presenting indicators for evaluating muscle function in the following chapter. After obtaining the segmented force data, indexes for quantifying muscle fatigue and recovery ability, motion control ability and exercise tolerance were proposed to built the muscle function evaluation system.

2. Review of the motion capture system

A motion capture system (MCS) is needed in the system to recognize and record movements of trainee when doing exercise. Inertial sensors have the advantage of low-cost, low power consumption and small-size which are common options for the development of MCS [1]. An inertial sensor in general consist of a three-axes accelerometer and a

three-axes gyroscope. The inertial sensor can measures the direction of gravity, motion (i.e., translation and rotation) accelerations and turning rates. By the fusion of these information, it is possible to estimate the orientation of a rigid body in the three-dimensional space. Therefore, it may be able to estimate the whole body motions, if the inertial sensor is attached on every body segment of a user. Recently, the inertial sensor was widely adapted to monitor and assess rehabilitation exercises in several well-known research projects [2,3,4,5]. In the research published by Taylor [2], tri-axial accelerometers were used in assessment of exercise quality in the rehabilitation of knee osteoarthritis patients. Similarly, in the research of Chen [3], a system that can identify the type of exercise movement the user performed was developed by using three wearable accelerometers. Accelerometer were used to calculate the inclination angles include the angle of thigh raise, knee flexion, hip external rotation and trunk forward bending. This system was used in the setting of home-based rehabilitation for knee osteoarthritis patients and can provide the physician the ability to tele-monitor the accuracy of rehabilitation the patient performed, and also provide the patient the ability to self-evaluate whether his/her rehabilitation behavior is correct or not. Hou [4] used an inertial sensor to measure subject's elbow joint angle by fusion of acceleration and angular rate using an extended Kalman filter. Other applications of using inertial sensor to measure orientations of body segments include body parts tracking [6,7], measurement of shoulder joint function [8], orthopaedic outcome assessment [9] and so on.

Despite the wide application of inertial sensor in estimation of body segment orientation, there are some shortcomings in the use of inertial sensors. First, the correctness of the angle calculation is largely determined by the alignment of sensor on the body segment and the usage scenario. Incorrect alignment during exercise, incorrect speed of movement and poor quality of movement may have an impact on the efficacy of exercise and may therefore result in a poor outcome. Second, when the angle is calculated by angular velocity integration, the error in the measured angular velocity will result in an increase in the inaccuracy of the estimated orientation, which is a well-known drift effect of the gyroscope [10]. If the system only include one accelerometer or gyroscope, the

long-term or dynamic performance of the system is not good and additional sensors are usually required to improve calculation accuracy [11].

In addition, visual sensors like cameras are another common option for MCS. To the best of our knowledge, the most accurate systems for gait analysis are camera-based systems with reflective markers [12]. These systems acquire spatial movement of many markers positioned on the body, while a software outputs the joint angles and/or other gait parameters. However, these systems need subject wear many markers on the body and require a dedicated laboratory, limited its application in clinical trials. Other non-contact motion capture sensors like Microsoft Kinect [13] had wide application in monitoring and assessment of rehabilitation exercises [14,15]. But the Kinect sensor needs several advanced sensing hardware, like a depth sensor and a color camera, to obtain full-body 3D motion capture [16]. The advanced sensing hardware makes the Kinect an expensive equipment which is unsuitable for common used in the home-based environment. And more importantly, the Microsoft has announced that Kinect has been discontinued in 2017. The cost is an big problem of vision-based monitoring system, but recently, an open framework named OpenPose [17] is built to obtain 2D virtual skeleton joints directly from RGB data and showed good performance and efficiency in situation with multiple people. It only requires RGB data acquired by ordinary cameras, making it an inexpensive choice for monitoring and evaluation of home-based rehabilitation training. But the OpenPose now can only estimate 2D pose and the results are influenced by camera position. This indicates that the OpenPose could serve as a supplementary method to gain additional joint freedom when subject moves.

3. Design of the measuring system

Figure 3.1 gives a visual representation of the design concept of the measuring system. Three types of sensors, include a camera, an accelerometer and gyroscope sensor, and a load cell, are used in the system. We take the biceps curl with a resistance band as an example, as illustrated in the figure, a trainee is standing in front of a screen with his

forearm flexes or extends to stretch a custom-made Thera-Band. A camera is placed on the lateral side of the trainee and the RGB pictures are recorded and sent to the OpenPose to obtain the 2D anatomical key-points of the trainee. The elbow or shoulder joint angle are calculated base on the anatomical key-points. An accelerometer and gyroscope sensor is used to record the acceleration and angular velocity during the training. And when the trainee flexes his forearm in sagittal plane with shoulder joint at neutral position and humerus in parallel with y axis of thorax, the elbow joint angle can be calculated based on the acceleration signal. A load cell is connected with the Thera-Band through a lifting hook and is utilized to record resistance force posed by the Thera-Band. The force signal are recorded and sent to the desktop. A repetition segmentation algorithm is propose to automatically segment the force data into small segments based on muscle actions. The joint angle, acceleration and angular velocity, and training sets are showed to the trainee through a user interface for giving the trainee visual feedback about the training record.

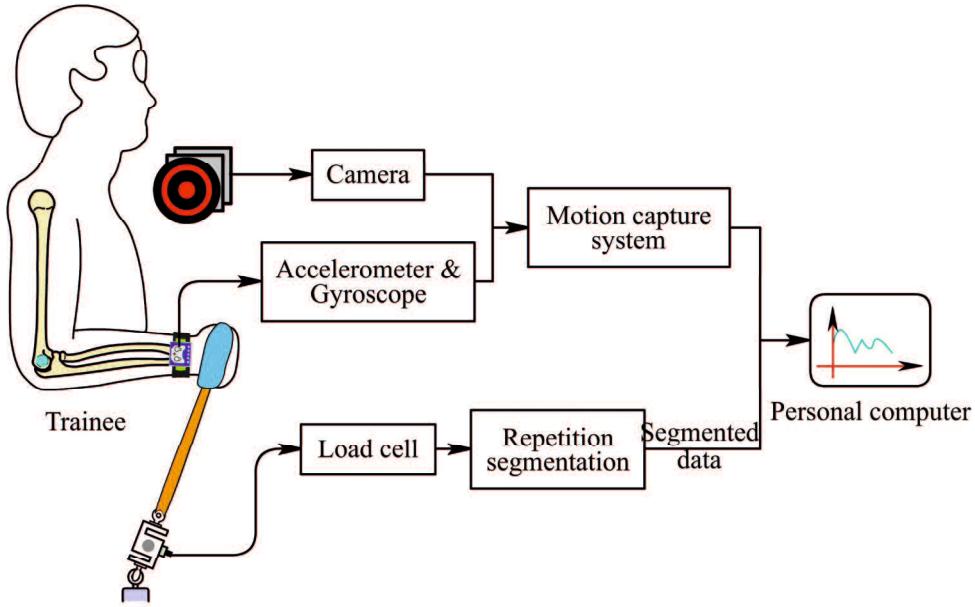

Figure 3.1 Design concept of the measuring system. A motion capture system, which incorporates an accelerometer, a gyroscope and a web camera, is established to recognize the movements of trainee while doing exercise. A custom-made Thera-Band is made to measure the time-varying resistance force during the training. The illustration uses biceps curl with a resistance band as an example. The OpenPose is used as a supplementary method to gain additional joint freedom when subject moves.

3.1 Motion capture system based on inertial and visual sensing

According to the number of joints involved in exercise, upper limb rehabilitation can be divided into multiple joints or single joint exercises. The movement of a single joint (e.g. shoulder lifting and bicep curl) can be recognized by using inertial sensors like accelerometer or gyroscope. However, the gyroscope shows poor performance in long-term measurements of upper limb motion and one accelerometer can usually measure only one degree of freedom. If the inertial sensor is only included in the monitoring system, multiple sensors are required, which makes the system complicated and uncomfortable for the trainee. The OpenPose is an intelligent and efficient method to estimate 2D skeleton joints trough visual sensing. With all of those in consideration, in the motion capture system (as illustrated in Figure 3.2), we use one inertial sensor to measure the angle, angular velocity and acceleration during rehabilitation exercises, and the OpenPose is used as a complementary method to gain additional joint freedom in the movement.

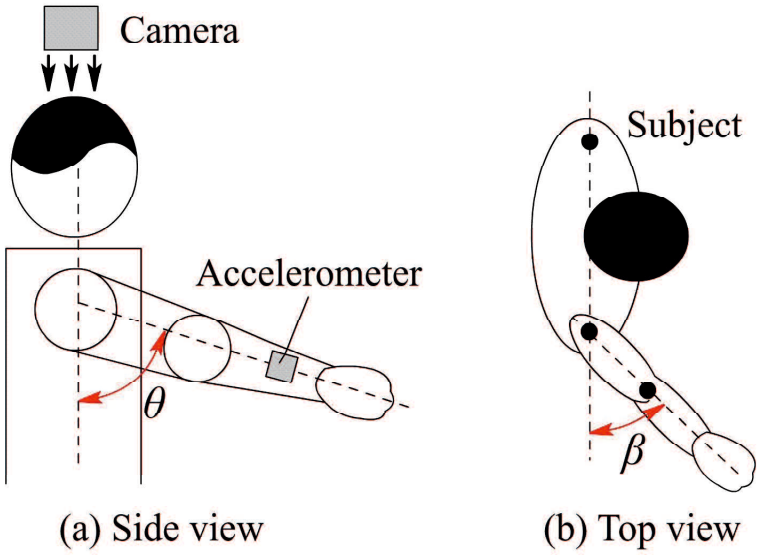

Figure 3.2 Design concept of the motion capture system. In the shoulder lifting exercise, a accelerometer is used to measure shoulder abduction or flexion angle (θ). A camera placed on top of the subject is used to measure the internal/external rotation angle (β) of shoulder.

3.1.1 Estimation of joint angle based on OpenPose

In this section, we will discuss how to use the OpenPose to estimate the human joint angle during the training based on the RGB image obtained from a webcam. Figure 3.3 shows the flow chart of estimation of shoulder joint angle. The OpenPose is firstly used to get the anatomical key-points of body parts in a RGB image recorded from a camera. And

later, the joint angle is calculated by using the vector angle calculation formula.

The OpenPose is a very interesting and recently developed open framework which is freely available on the GitHub [18]. The OpenPose provides Python Application Programming Interface (API) that anyone can download, install and use it in the Python development environment for free non-commercial use. The OpenPose Python API requires python-dev, numpy (for array management), and OpenCV (for image loading) [18,19]. After the installation, the OpenPose can jointly detect human body, hand, facial, and foot keypoints on single pictures. These pictures can be images that already exist or image records from the camera. By calling the body pose estimation function, we can get the anatomical key-points of all persons in the picture. Figure 3.4 and Table 3.1 illustrate a list of key points and their corresponding body parts recognized in the OpenPose. There are 19 key-points in total represent main joints and parts of the human body.

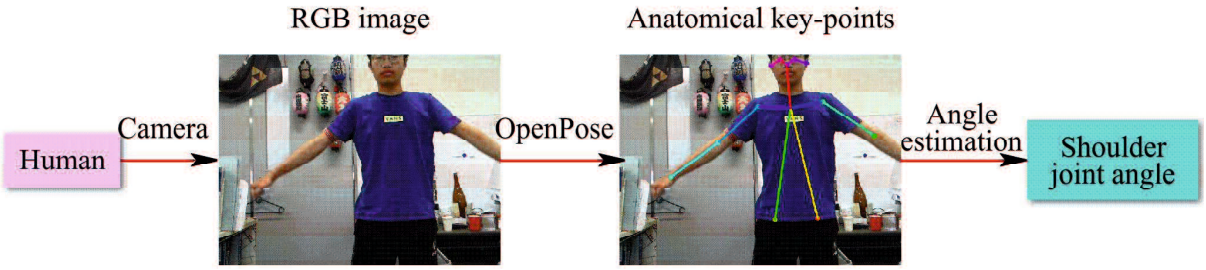

Figure 3.3 The flow chart of calculation of shoulder joint angle.

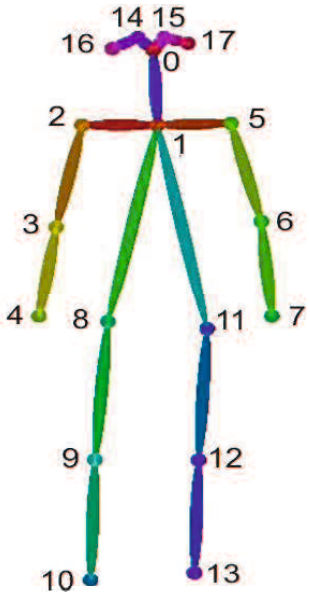

Figure 3.4 The 2D anatomical key-points recognized by the OpenPose. The number is marked near its body part.

Table 3.1 A list of key points and their corresponding body parts.

No.	Body part	No.	Body part	No.	Body part
0	Nose	7	Left Wrist joint	14	Right Eye
1	Neck	8	Right Hip joint	15	Left Eye
2	Right Shoulder joint	9	Left Hip joint	16	Right Ear
3	Right Elbow joint	10	Right Knee joint	17	Left Ear
4	Right Wrist joint	11	Left Knee joint	18	Background
5	Left Shoulder joint	12	Right Ankle joint		
6	Left Elbow joint	13	Left Ankle joint		

The key-points contain the two-dimensional coordinates of each body part in the image coordinate system. Since the image coordinate system are scaled and without a known length or a known coordinate system as a reference, it is impossible to calculate the real length of each body part through the two-dimensional coordinate. However, the shoulder joint angle is not affected by image scaling. Therefore, so we can get the body joint angle base on the anatomical key-points. As illustrated in Figure 3.5, suppose the subject is standing in front of the camera and lifting his arm. The shoulder joint angle can be calculated as the angle between $\boldsymbol{r_1}$ and $\boldsymbol{r_2}$. Which is expressed as:

$$\theta = ar\cos\left(\frac{\boldsymbol{r_1}\cdot\boldsymbol{r_2}}{|\boldsymbol{r_1}|\cdot|\boldsymbol{r_2}|}\right) \tag{2-1}$$

where $|\boldsymbol{A}|$ is the length of vector $\boldsymbol{A}$. $\boldsymbol{r_2}$ is the unit vector along the positive x-axis ([1,0]) and $\boldsymbol{r_1}$ is the vector from P_2 to P_3. Which is expressed as:

$$\boldsymbol{r_1} = P_3(x_3, y_3) - P_2(x_2, y_2) \tag{2-2}$$

where P_2 (x_2,y_2) is the shoulder joint and P_3 (x_3,y_3) is the elbow joint.

We programmatically implemented the algorithm and some experiments were carried out to test the program. The calculation result of the experiment was illustrated in Figure 3.6. In the experiment, a subject was asked to stand in front of a camera and lift his arm for twice. A web camera was used to record the video and the shoulder joint angle of left and right arm were calculated. As we can see from the result, the OpenPose can effectively detect the body parts of subject. However the stability of the detection is not so good,

making the calculation result very uneven. This also indicates that the accuracy of the angular velocity and acceleration which are calculated as the derivation of the obtained angle may not so good. So in addition to the camera, accelerometer and gyroscope sensors are need to obtain the acceleration and angular velocity. A comparison between the angular velocities obtained by the gyroscope and OpenPose will be shown in the next section.

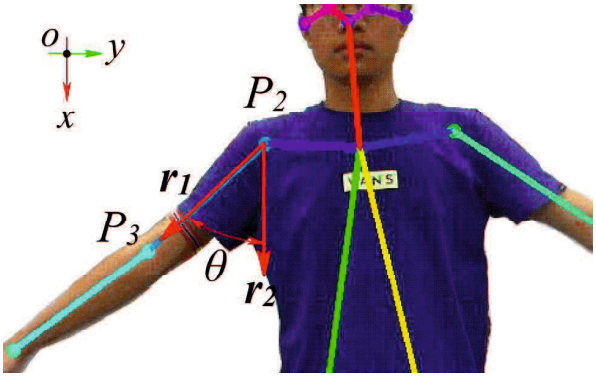

Figure 3.5 The shoulder joint angle θ is calculated as the angle between $\boldsymbol{r_1}$ and $\boldsymbol{r_2}$. P_2 is the shoulder joint and P_3 is the elbow joint.

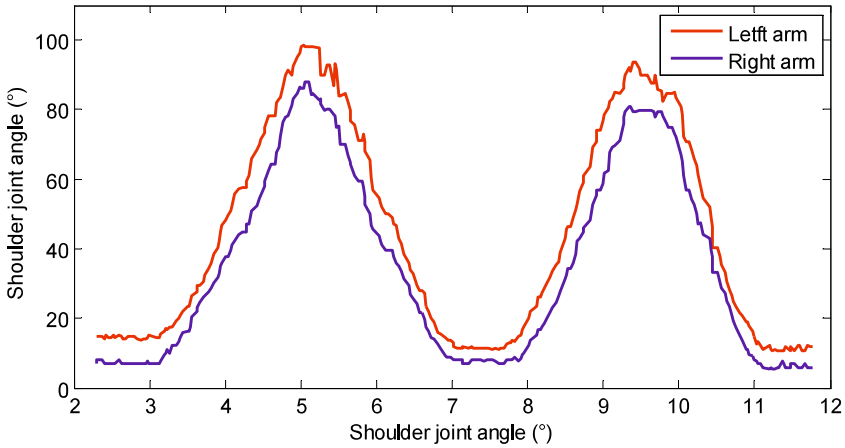

Figure 3.6 The shoulder joint angle calculated by OpenPose.

3.1.2 The 6-DoF inertial measurement unit

In the measuring system, a 6-DoF inertial measurement unit (IMU) which incorporates a three-axis accelerometer (TWE Lite 2525A, size 20×20× 10mm, weight 6.5g) and a three-axis angular rate sensor (L3GD20, size 10×10×2mm) was built to obtain acceleration and angular velocity, and joint angle. A custom-made watchband was designed to attach the sensor on subject's body part through a velcro tape. Figure 3.7 shows the details of the custom-made watchband and the sensor. The LGD20 is a small chip attached to the accelerometer and powered by a 3 volt button battery. Sensor signals were measured

and processed by a wireless transmission module (MONO Wireless, size 62×24×8mm) and sent to the desktop via the COM port for data analysis. Regarding sensors' features, both the accelerometer and gyroscope have many configurable options, including dynamically selectable sensitivities, as well as a choice of output data rates (ODR) for each sensor. In the current IMU, the sensors were configured as follow:

- Gyroscope: one 16-bit word per axis, with a sensitivity of ±2000 degrees per second and ODR of 400 Hz;
- Accelerometer: one 16-bit word per axis, with a sensitivity of ±2 g and ODR of 200 Hz.

When the angular velocity of body segment is not too big, the accelerometer sensor can be used to estimate joint angle. Here we explain how to estimate elbow joint angle when subject is doing bicep curl exercise. Figure 3.8 illustrates the placement and axis direction of the accelerometer sensor. The sensor is comfortably attached to the forearm of subject by a velcro tape and ensures that the z axis of the sensor is parallel to the forearm rotation axis. Because when doing the bicep curl exercise, the forearm is supposed to flexes and extends in the sagittal plane with shoulder joint at neutral position and humerus in parallel with y axis of thorax. So, as illustrated in Figure 3.8, we can obtain the elbow joint angle β by calculating the inclination angle of the accelerometer θ. Which can be expressed as:

$$\beta = 180^{\circ} - \theta \tag{2-3}$$

where θ is the inclination angle which is the angle between vectors of gravity and z axis ($\boldsymbol{R}_z$=[0 0 1]^T) in the sensor coordinate system. That is:

$$\theta = ar\cos\left(\frac{\boldsymbol{G}\cdot\boldsymbol{R}_z}{|\boldsymbol{G}|\cdot|\boldsymbol{R}_z|}\right) \tag{2-4}$$

where $\boldsymbol{G}$ is the vector of gravity. $|\boldsymbol{A}|$ means the normal of vector $\boldsymbol{A}$.

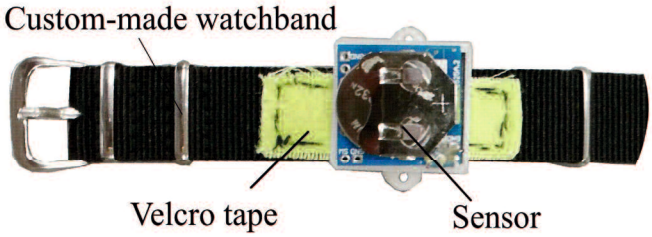

Figure 3.7 Details of the custom-made watchband and the IMU.

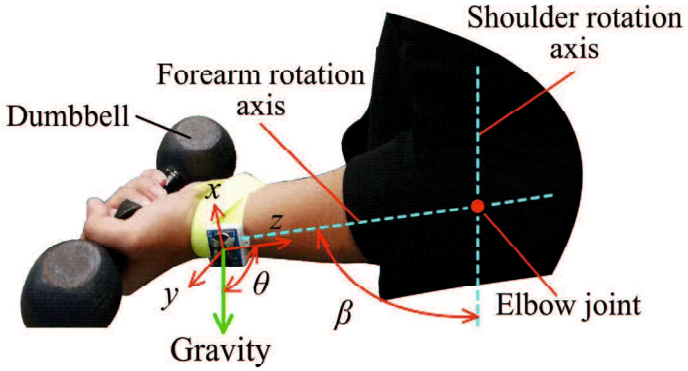

Figure 3.8 Placement and axis direction of the accelerometer sensor.

Similarly, the correctness of the estimation of elbow joint angle using the 6-DoF IMU was tested through an experiment. As shown in Figure 3.9, a female subject is siting on a chair with her shoulder joint at neutral position and humerus in parallel with y axis of thorax. The IMU is attached to her forearm and her forearm flexes and extends in her sagittal plane. The elbow joint angle estimated by using the IMU is compared with that estimated by OpenPose. The compare results is illustrated in Figure 3.10. As we can see from the results, elbow joint angle estimated using the IMU shows a good consistency with that estimated by OpenPose, except when elbow is fully extended. The difference of elbow joint angle when elbow is fully extended is mainly caused by the the famous biomechanical phenomena called carrying angle. The carrying angle of the human elbow refers to the obliquity between the upper arm and the supinated forearm when the elbow is held in extension [20]. The good consistency of the estimated angle between IMU and OpenPose demonstrates that this measuring system can correctly estimate elbow joint angle when forearm flexes or extends in sagittal plane.

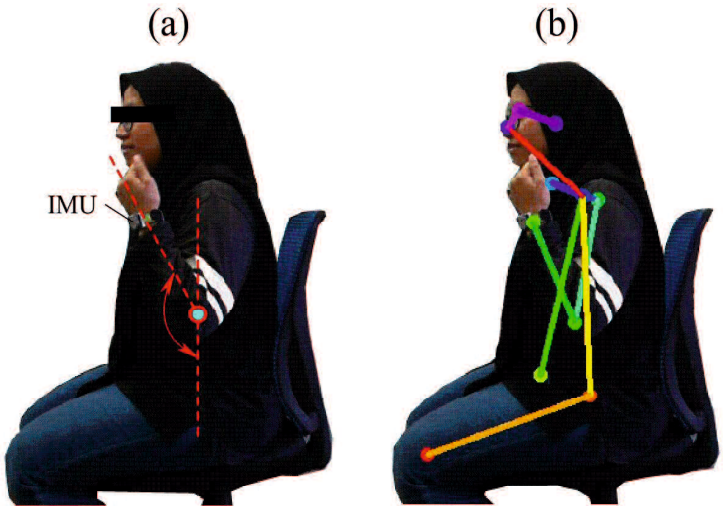

Figure 3.9 (a) The IMU is attached to subject's forearm to estimate elbow joint angle when subject doing bicep curl exercise. (b) The elbow joint angle is estimated by OpenPose as a comparison.

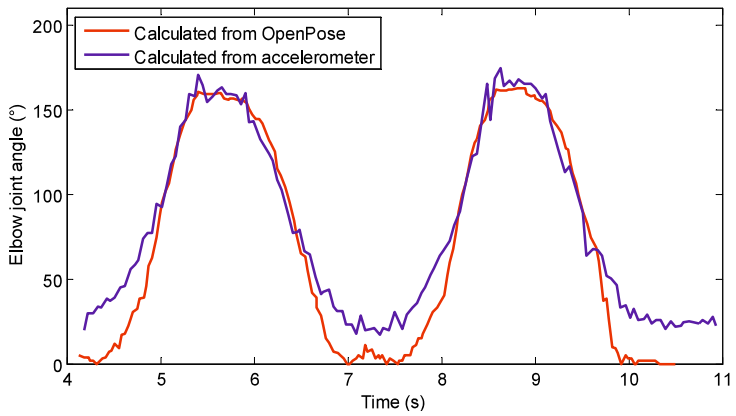

Figure 3.10 Comparison of elbow joint angle calculated by accelerometer and OpenPose.

3.2 The custom-made Thera-Band and Load cell

Accommodating resistance devices such as bands and chains are useful methods to maximize gains in strength and hypertrophy. These devices have significant feature of variable resistance force throughout the range of motion and positive benefit on neuromuscular adaptation [20]. In our system, we use Thera-Band [21] to help subject do resistance training. Since the training load was different among different trainees, three different types of Thera-Band (Green, Red, and Yellow) were constructed and connected to the handle using a carabiner clip. A load cell (SC301A, 100 kg) was used to measure the time-varying resistance. The analog signals were converted into digital signals through an A/D converter (AE-HX711-SIP, 30 Hz). The load cell was calibrated and the scale factor

was calculated before the experiments using calibration weights. Details of the Load cell and the custom-made Thera-Band are illustrated in Figure 3.11. As it can be seen in Figure 3.12, each Thera-Band was tested under uniaxial tensile extension and the force data were recorded in order to obtain its load versus extension curve. Based on the curves, it can be observed that the green band had the highest resistance, while the yellow band had the lowest. In the experiments, different combinations of Thera-Bands were used to set different training loads for the trainees according to their muscle strength.

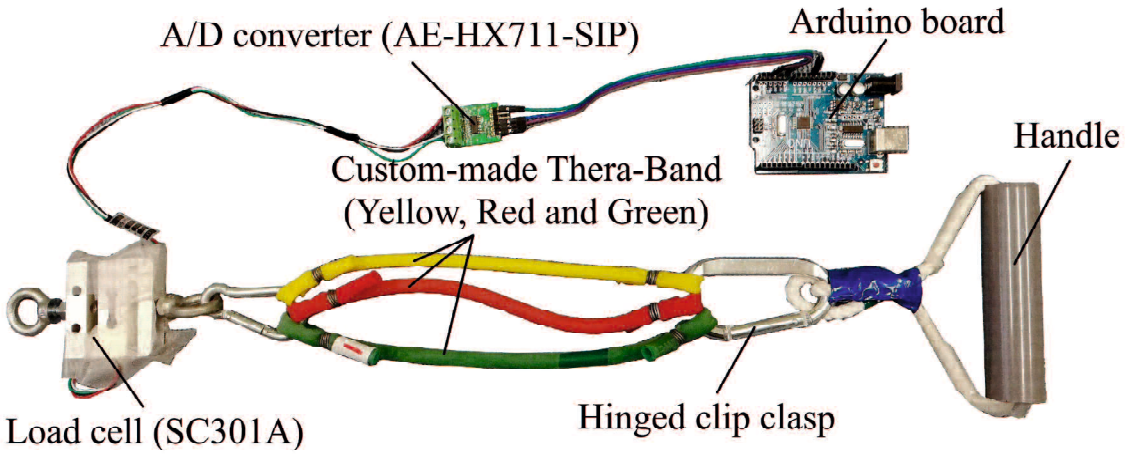

Figure 3.11 Details of the Load cell, custom-made Thera-Band and Arduino board.

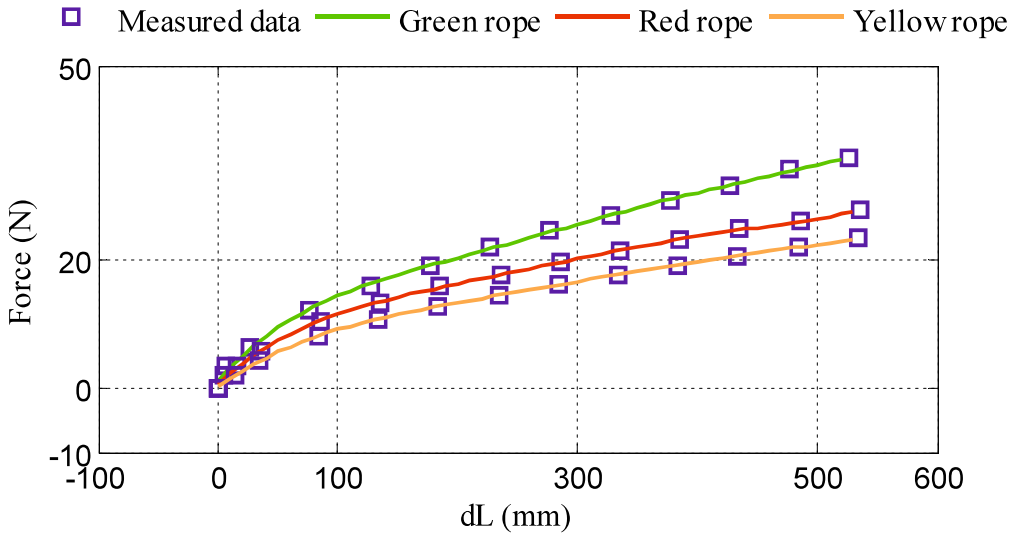

Figure 3.12 Load versus length change curves of the custom-made Thera-Bands.

4. Force data segmentation

For the bicep curl exercise with a custom-made Thera-Band illustrated in Figure 3.13,

the contraction include multiple phases in one repetition. Normally, four contraction phases are included in one repetition, which are concentric (CON), eccentric (ECC), and isometric (ISOM) contraction phase, and plus the rest period, as shown in Figure 3.14. During the CON phase, the subject flex his forearm to resistance against the resistance force produced by the custom-made Thera-Band, and hold the force for a while during the ISOM phase. Later release his forearm in ECC phase. The subject usually need to have a short rest during the Rest phase. During different contraction phase, the role of muscle is different. Thus, we can use the force data during different phase to quantify subject's muscle function. In this section, we propose an force data segmentation algorithm to segment the force data into small segments. The first objective was to propose an algorithm for automatically segmenting the force data into small segments based on muscle actions. The proposed algorithm incorporates repetition segmentation and muscle action segmentation.

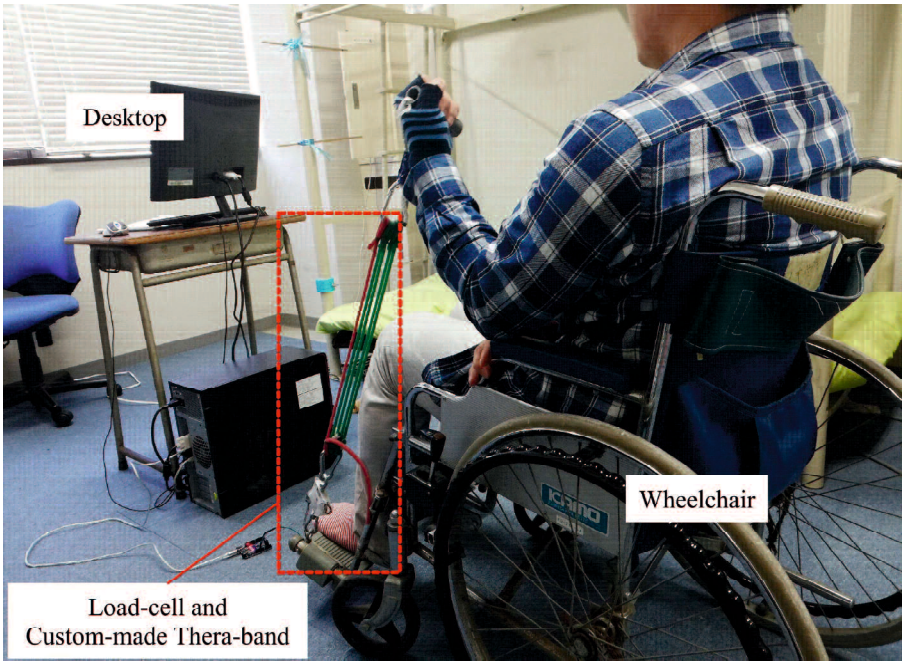

Figure 3.13 Picture shows a subject is performing performing the bicep curl exercise with a custom-made Thera-Band.

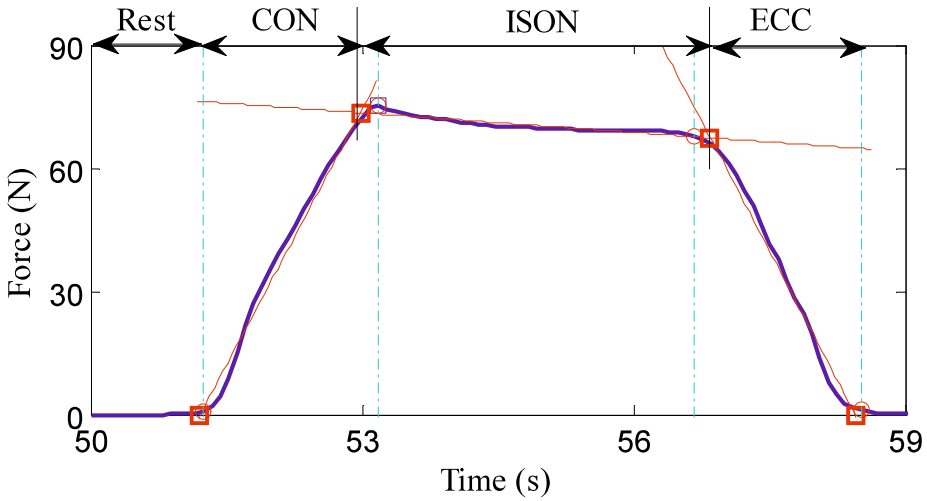

Figure 3.14 Different contraction phases in one repetition. Rest is the rest period. The CON is the concentric phase. The ISOM is the isometric phase and the ECC is the eccentric phase.

4.1 Repetition segmentation

Repetition segmentation is a pre-processing stage, where the force data are divided into individual segments according to the training cycle. Its purpose is to increase the accuracy of muscle action segmentation. Figure 3.15 illustrates a typical plot of resistance data during the bicep curl exercise. As it can be seen from the curve, the force signal exhibits strong periodicity with distinct peaks and troughs. A simple and efficient peak detection method [22] was used to find the minimum value of the trough, which was taken as the segmentation point. In the segmentation process, the mean resistance value was used as the threshold value to divide the force signal into peaks and troughs. This method was implemented with the aid of MATLAB(R2012b) and an example of a segmentation result is illustrated in Figure 3.16.

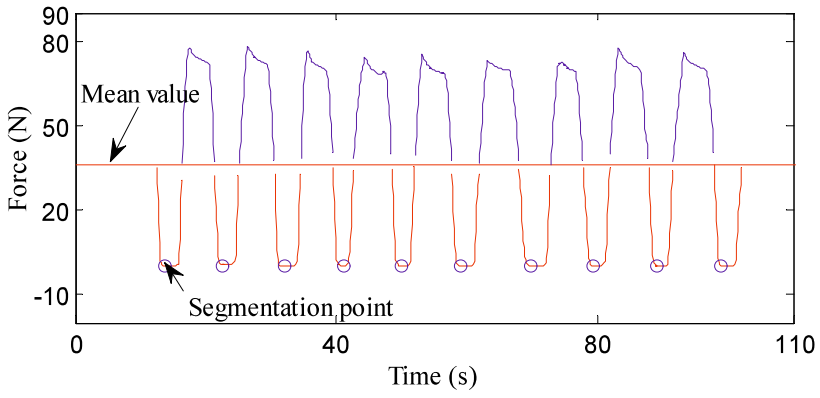

Figure 3.15 Segmentation points locating logic. The minimum value of the trough was chosen as the segmentation point.

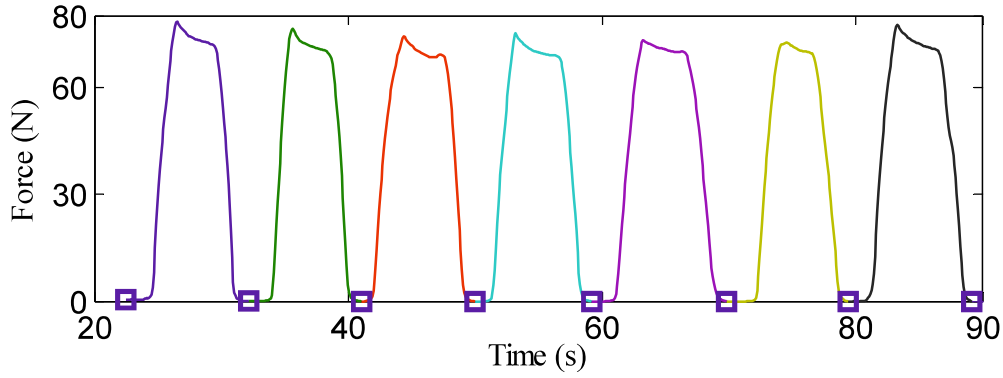

Figure 3.16 Example of a segmentation result. Different training cycles are illustrated in different colors.

4.2 Muscle action segmentation

Different muscle actions play different roles in resistance training, and their effects on muscle strength and power adaptation are also different [23]. The bicep curl exercise is an easy-to-recognize movement, which incorporates all the CON, ISOM, and ECC muscle actions. However, usually there is no clear cut-off point between CON, ISOM, ECC, and rest phases, since training is a complex process that is affected by many subjective factors, such as personal ability, willingness, and fatigue. In this section, a muscle action segmentation algorithm was proposed to approximately divide each biceps curl cycle into four time-windows.

Figure 3.17 gives a visual representation of how the segmentation algorithm operates. The core idea of the segmentation algorithm is based on the difference in force derivatives at the different contraction phases. Raw force data containing one flexion-extension repetition were obtained using the repetition segmentation algorithm proposed in the previous section. Firstly, the first order derivative of force versus time was numerically calculated. Then, from the derivative curve, it was perceived that the maximum and minimum values were the most discriminating features. In CON contraction, the force-derivative increases rapidly at the beginning, reaches a maximum value, and then rapidly decreases to zero. In ISOM contraction, the subject keeps his/her forearm in quasi-static state for a few seconds and the force-derivative does not change much. In ECC

contraction, the subject releases his/her forearm and the force-derivative reaches a minimum value. Consequently, the maximum and minimum values of the force-derivative were considered as important thresholds to segment the force data. The segmentation model can be expressed as:

$$F(t) \in \begin{cases} CON, & (0.1*Max \le dF(t) \le \max) \\ ISOM, & (0.1*Min < dF(t) < 0.1*Max) \\ ECC, & (Min \le dF(t) \le 0.1*Min \end{cases} \quad (1)$$

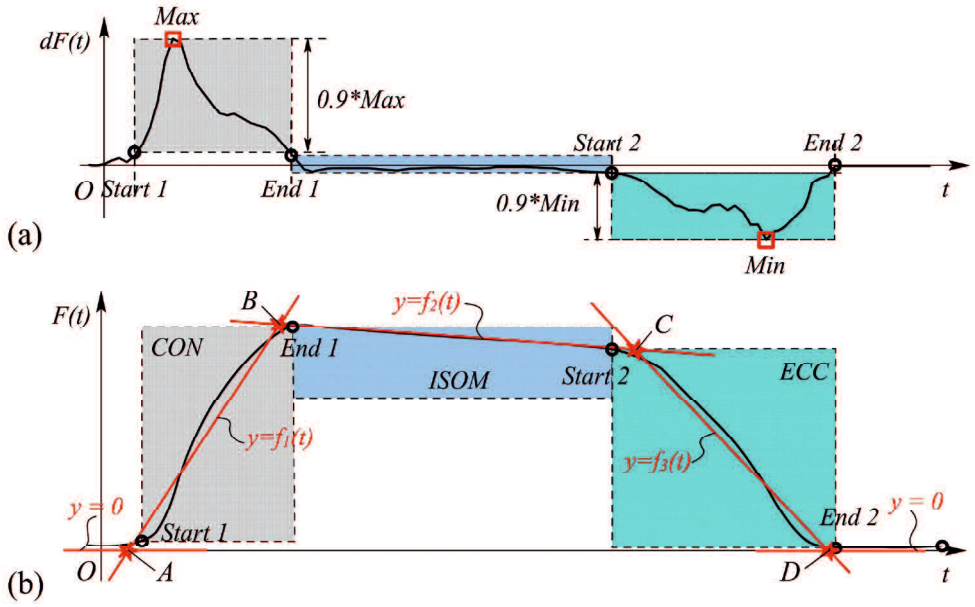

Figure 3.17 Schematic diagram of the segmentation algorithm. (a) The maximum and minimum values of the first order derivative of force versus time were used as thresholds to divide the data into three parts. (b) Trend line intersections were used to segment the arm biceps curl exercise into four contraction phases (CON, ISOM, ECC and rest).

In CON and ECC contraction, data with a derivative greater or less than 10% of the maximum and minimum values were chosen and the trend line was calculated to approximate the change in force during these contraction phases. The trend line is an approximate alternative of the data in the contraction phases. On the one hand, this approximation eliminates some accidental situations in the data, such as fluctuations or slacks. On the other hand, when the forearm flexes or extends, the force tendency is preserved as much as possible. The trend line ($y = fi(t)$, i = 1~3) was calculated using linear regression. The trend line intersections (A~D) and the line of constant function (y = 0) divided the arm biceps curl exercise into the CON, ECC, and ISOM contraction phases and

the rest period.

4.3 Performance of the Segmentation Algorithm

To the best of our knowledge, this is the first study that uses an automated method to segment resistance force data into contraction phase specific segment. Compared to other manual methods, this method exhibited high efficiency. Using a dual-core 3.5 GHz Intel processor laptop, the rating time for one trial takes no more than 5 seconds. Some typical segmentation results are presented in Figure 3.18. As it can be seen, the proposed algorithm can correctly segment the force data into the four contraction phases (CON, ISOM, ECC, and Rest), even when there are some fluctuations or slacks between two contraction phases. In some cases, when the trainee bended his/her arm at the beginning of CON, some failed startups occurred. During those failed startups, the resistance was relatively small and these data do not produce effective TUT. In such cases, the algorithm removed these invalid data and used the trend line to determine the most likely starting point. In other cases, the boundary between two contraction phases was clearly marked by the trend line intersection. The segmentation results were visually checked and it was found that the algorithm successfully segmented all the data.

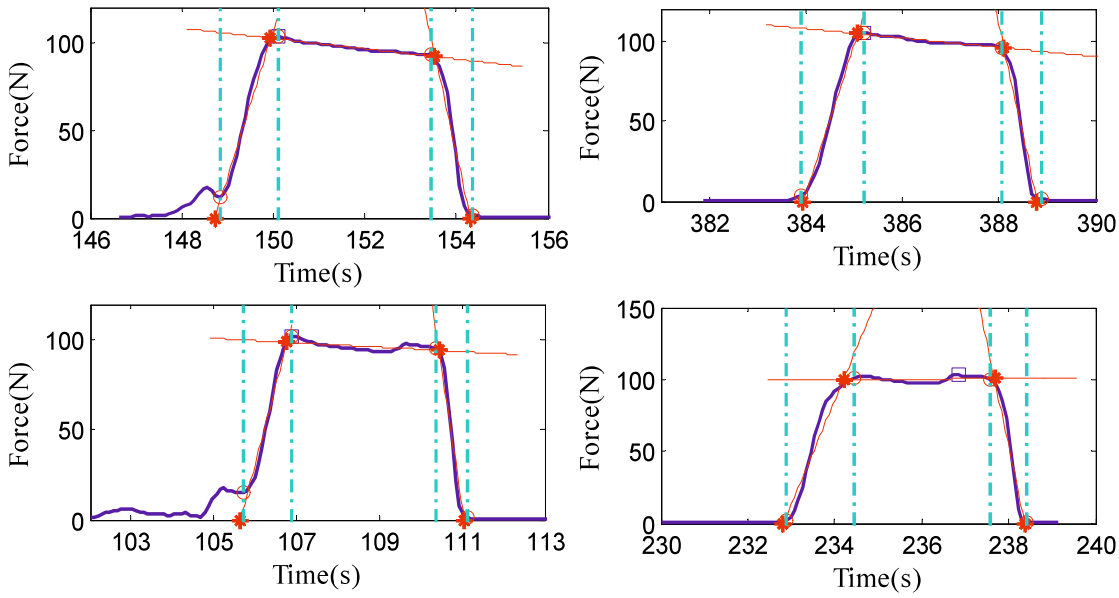

Figure 3.18 Four representative examples of segmentation results. Red asterisks denote intersections and red circles denote segmentation points. The trend lines are denoted by the red lines.

In order to further verify the correctness of the algorithm, two assessors, who were unfamiliar with the experiment, were recruited to manually pick the visually observed cut-off point between two contraction phases, and the TUT was calculated as the gold standard. The TUT comparison is demonstrated in Figure 3.19. As it can be seen, there was a good agreement in TUT between the proposed algorithm and the assessor. The total TUT was exactly the same, however the algorithm's TUT was a little longer than that of the assessors during CON and ECC, while during ISOM, the algorithm's TUT was a little shorter than that of the assessors. In addition, from the comparison results, it can be seen that there was difference also in the rating results between assessors, which means that the rating of the data was subjectively influenced by the assessor. The proposed segmentation algorithm was implemented programmatically, avoiding the subjectivity of the assessors. Therefore, it is an automated and objective method for quantifying the exercise dosage during home-based elbow flexor resistance training.

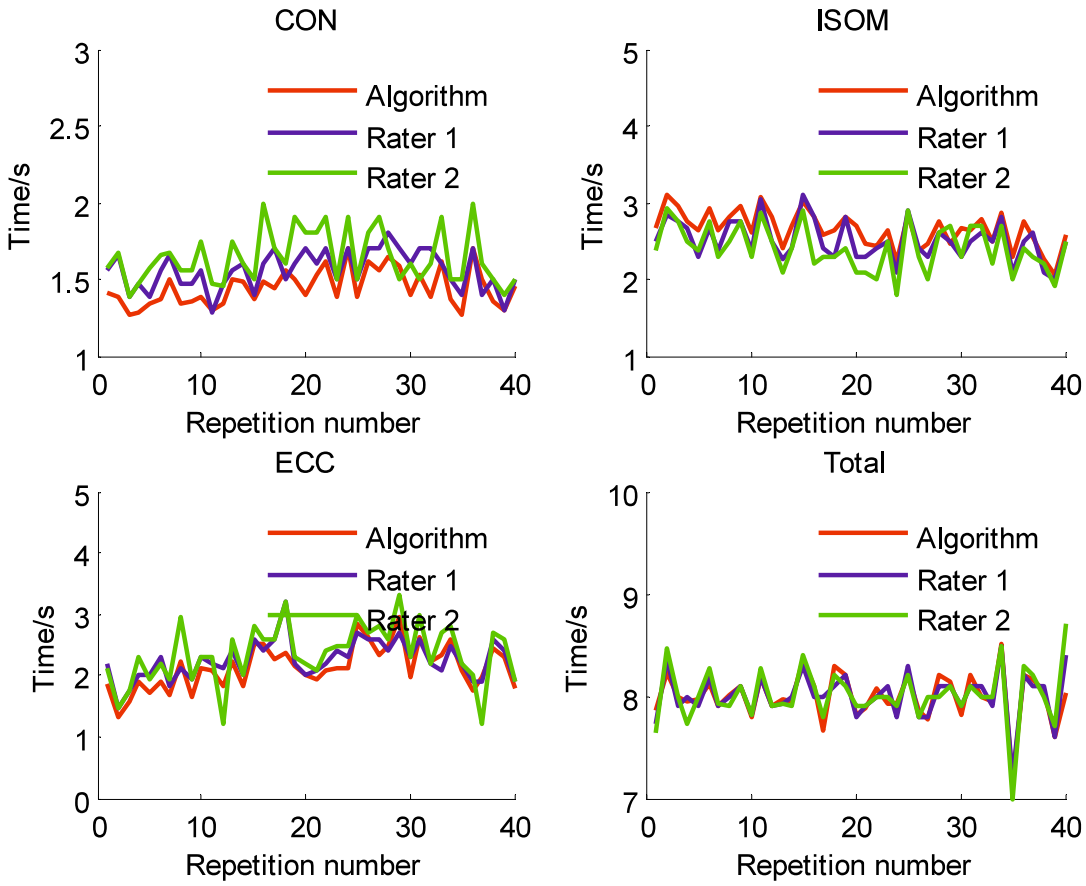

Figure 3.19 TUT comparison for one participant at different phases.

5. Indexes for quantifying muscle function

5.1 Extraction of fatigue and recovery indexes

Exercise is usually accompanied by muscle fatigue. When fatigue occurs, the threshold to trigger action potentials in a motor unit increases, i.e., the motor unit's tendency to fire decreases [24,25]. Since the discharge rate changes, the number of recruited motor units is reduced, resulting in the reduction of muscle force. Here, muscle fatigue was defined as the relative decline in average force ($F_{ave}(i)$) during ISOM contraction and the decreasing slopes (*k1* and *k2*) of $F_{ave}(i)$ were used as index of fatigability. The recovery of $F_{ave}(i)$ after 1-minute rest (1MinRec) was used to quantify subject's ability to recover from fatigue.

Figure 3.20 explains how the decreasing slopes and the recovery of the average force after rest were calculated. The average force during ISOM contraction is expressed as:

$$F_{ave}(i) = \frac{B_i(y) + C_i(y)}{2} \tag{2}$$

where $B_i(y)$ and $C_i(y)$ are the y value of the starting and ending point of ISOM, respectively. The regression slopes *k1* and *k2* were calculated using a regression function. The calculation of 1MinRec is expressed as:

$$1MinRec = \frac{P2(y) - P1(y)}{F0} \times 100\% \tag{3}$$

where *P2(y)* and *P1(y)* are the y value of points $P1$ and *P2*, respectively, and *F0* is the initial force.

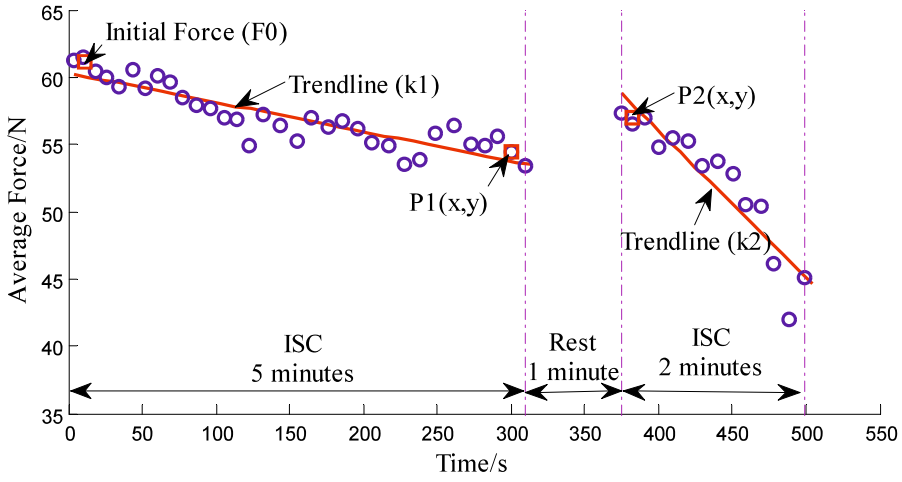

Figure 3.20 Average force distribution and regression trend line of a male subject. Initial force (*F0*) and *P1(x,y)* are the mean value of the first and last three data during the 5-minute ISC. *P2(x,y)* is the mean value of the first three data during the 2-minute ISC.

5.2 Indexes for quantifying muscle motion control ability

The Thera-Band is a typical accommodating resistance device that provides the trainee with adaptive resistance force throughout the range of motion and has good adaptation effect in the neuromuscular system. The shortening and lengthening contractions of muscle are combined effects of motor units and nervous-system system [24]. In the sub-maximal contraction of arm biceps curl with resistance band, firstly, the brain sends down a command (voluntary drive) through the spinal cord and peripheral nerves to muscles, and then the muscle generate a impulse, forcing the forearm to stretch the resistance band. The contraction process includes acceleration and deceleration phases. As illustrated in Figure 3.21, we used the quotient of acceleration and deceleration time (R_1) to quantify muscle motion control ability of subject to voluntarily contract his forearm. Which is expressed as:

$$R_1 = \frac{T_1}{T_2} \tag{4}$$

where T_1 and T_2 are the time windows of acceleration and deceleration during CON contraction. Similarly, the quotient (R_2) during ECC contraction is expressed as:

$$R_2 = \frac{T_3}{T_4} \tag{5}$$

where T_3 and T_4 are the time windows of acceleration and deceleration during ECC contraction.

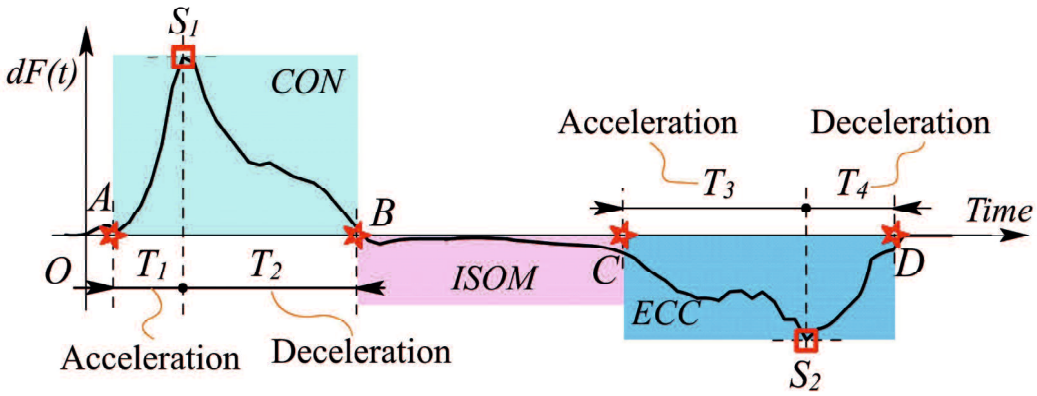

Figure 3.21 Schematic diagram illuminates how to divide the CON and ECC into acceleration and deceleration phases.

5.3 Indexes for quantifying muscle exercise tolerance

As we can see from Figure 3.15, the resistance force during ISOM phase did not remain unchanged during the experiment. The fluctuation in force during ISOM phase reflects the ability of subject's muscle to keep the force at a constant value, or to some extend, reflects subject's exercise tolerance or holding ability. Here, we use the Coefficient of Variation (CV) to quantify the fluctuation in force during ISOM phase. Figure 3.22 is the flow chart of extracting coefficient of variation for quantifying muscle exercise tolerance. With the repetition segmentation and muscle action segmentation algorithm mentioned above, as illustrated in Figure 3.22, we can get the force data of each contraction phase. Since the force data changes over time and we only want to count the distribution of the magnitude of the force throughout the experiment. So we use the phase-plot analysis to get the frequency distribution heat map of force during ISOM phase at the phase space. Figure 3.23 is an example of phase-plot of one trail. We use the force data as the x-axis data and derivative of force versus time, which can be obtained by numerical calculation, as the y-axis data. Finally, as illustrated in Figure 3.24, we count the

frequency of occurrences in the phase space and get the frequency distribution heat map of force and force derivative of time (Figure 3.25).

After getting the frequency distribution heat map, the coefficient of variation is calculated to quantify muscle holding ability. The coefficient of variation (CV) is a statistical measure of the dispersion degree of data points in a data series around the mean. The coefficient of variation represents the ratio of the standard deviation to the mean, and it is a useful statistic for comparing the degree of variation from one data series to another, even if the means are drastically different from one another. The coefficient of variation (CV) is a dimensionless variable and its calculation formula is expressed as:

$$CV = \frac{\sigma}{\mu} \tag{6}$$

where σ is the standard deviation and μ is the mean. We calculated the standard deviation and mean value by using *std2()* and *mean2()* functions in MATLAB. A bigger value of coefficient of variation means a bigger fluctuation in force during ISOM phase.

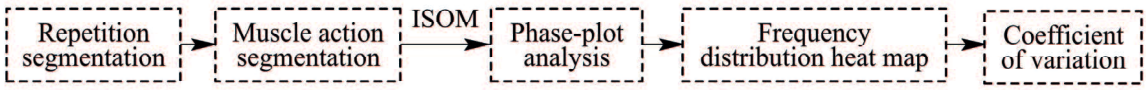

Figure 3.22 Flow chart of extracting coefficient of variation for quantifying muscle exercise tolerance.

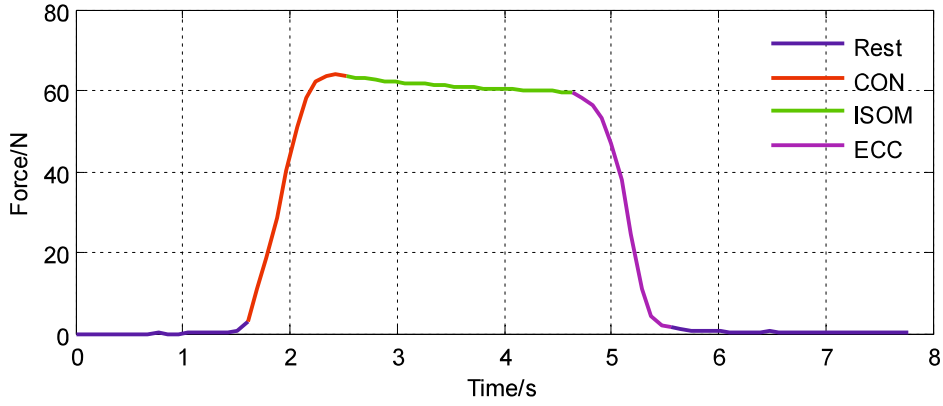

Figure 3.23 Example of segmentation result in one repetition. We use different colors to distinguish different phases.

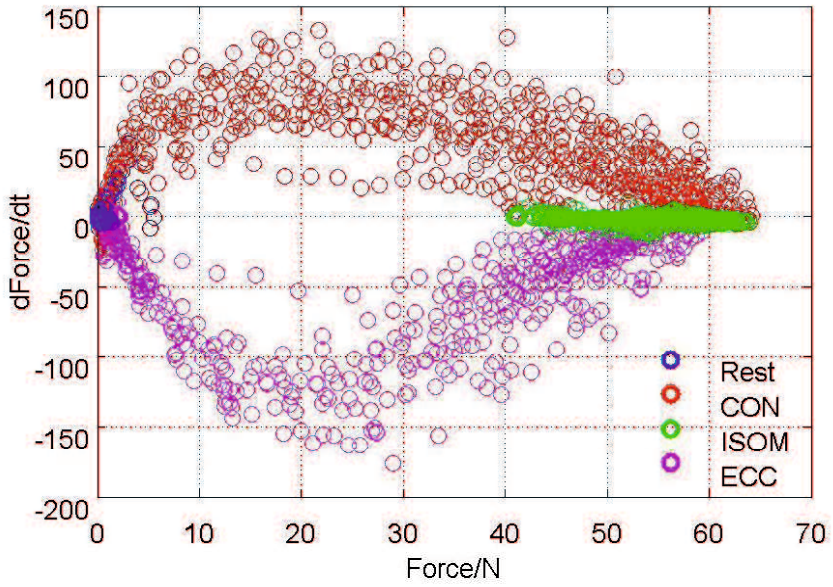

Figure 3.24 Example of phase-plot of one trail. We use different colors to distinguish different phases.

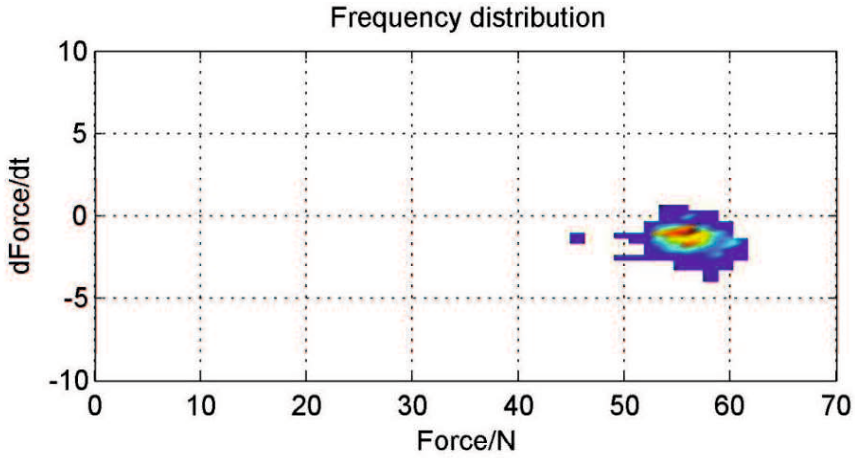

Figure 3.25 Example of frequency distribution heat map of force and force derivative of time during ISOM phase in the phase space. The color represents how many times a data appears at a certain point. Blue represents fewer times and red represents more times.

6. Summary

In this section, we talked about the establishment of a measurement system for muscle function measurement and evaluation. The design concepts and sensor technology are described in detail. The measurement system incorporates an motion capture system and a custom-made Thera-Band. The motion capture system is built based on inertial and visual sensing for recognizing and recording movements of trainee when doing exercise. The

Thera-Band is used to help subject do resistance training and the resistance force is recorded through a load cell. In addition, a repetition segmentation and a muscle action segmentation algorithm are proposed to obtain force segments during different contraction phases and the performance of the segmentation algorithm was evaluated. Since during different contraction phase, the role of muscle is different. The force data during different phase can be utilized to quantify subject's muscle function. At last, after obtaining the segmented force data, indexes for quantifying muscle fatigue and recovery ability, motion control ability and exercise tolerance were proposed to built a muscle function evaluation system.

7. References

[1] Jung P G, Oh S, Lim G, et al. A mobile motion capture system based on inertial sensors and smart shoes[J]. Journal of Dynamic Systems, Measurement, and Control, 2014, 136(1): 011002.

[2] Taylor P E, Almeida G J M, Kanade T, et al. Classifying human motion quality for knee osteoarthritis using accelerometers[C]//2010 Annual international conference of the IEEE engineering in medicine and biology. IEEE, 2010: 339-343.

[3] Chen K H, Chen P C, Liu K C, et al. Wearable sensor-based rehabilitation exercise assessment for knee osteoarthritis[J]. Sensors, 2015, 15(2): 4193-4211.

[4] Hou J, Sun Y, Sun L, et al. A pilot study of individual muscle force prediction during elbow flexion and extension in the neurorehabilitation field[J]. Sensors, 2016, 16(12): 2018.

[5] Foxlin E M, Harrington M, Altshuler Y. Miniature six-DOF inertial system for tracking HMDs[C]//Helmet-and Head-Mounted Displays III. International Society for Optics and Photonics, 1998, 3362: 214-228.

[6] Foxlin E. Inertial head-tracker fusion by a complementary separatebias Kalman filter[C]//Proc. VRAIS. 185-194.

[7] Körver R J P, Senden R, Heyligers I C, et al. Objective outcome evaluation using inertial sensors in subacromial impingement syndrome: a five-year follow-up study[J]. Physiological measurement, 2014, 35(4): 677.

[8] Bolink S, Grimm B, Heyligers I C. Patient-reported outcome measures versus inertial performance-based outcome measures: A prospective study in patients undergoing primary total knee arthroplasty[J]. The Knee, 2015, 22(6): 618-623.

[9] Bouvier B, Duprey S, Claudon L, et al. Upper limb kinematics using inertial and magnetic sensors: Comparison of sensor-to-segment calibrations[J]. Sensors, 2015, 15(8): 18813-18833.

[10] Luinge H J, Veltink P H. Measuring orientation of human body segments using miniature gyroscopes and accelerometers[J]. Medical and Biological Engineering and computing, 2005, 43(2): 273-282.

[11] Racic V, Pavic A, Brownjohn J M W. Experimental identification and analytical modelling of human walking forces: Literature review[J]. Journal of Sound and Vibration, 2009, 326(1-2): 1-49.

[12] Han J, Shao L, Xu D, et al. Enhanced computer vision with microsoft kinect sensor: A review[J]. IEEE transactions on cybernetics, 2013, 43(5): 1318-1334.

[13] Otten P, Kim J, Son S. A framework to automate assessment of upper-limb motor function impairment: A feasibility study[J]. Sensors, 2015, 15(8): 20097-20114.

[14] Olesh E V, Yakovenko S, Gritsenko V. Automated assessment of upper extremity movement impairment due to stroke[J]. PloS one, 2014, 9(8): e104487.

[15] Zhang Z. Microsoft kinect sensor and its effect[J]. IEEE multimedia, 2012, 19(2): 4-10.

[16] Cao Z, Simon T, Wei S E, et al. Realtime multi-person 2d pose estimation using part affinity fields[C]//Proceedings of the IEEE Conference on Computer Vision and Pattern Recognition. 2017: 7291-7299.

[17] Cao Z, Hidalgo G, Simon T, et al. OpenPose: realtime multi-person 2D pose estimation using Part Affinity Fields[J]. arXiv preprint arXiv:1812.08008, 2018.

[18] https://github.com/CMU-Perceptual-Computing-Lab/openpose

[19] Arandjelović, Ognjen. "A mathematical model of neuromuscular adaptation to resistance training and its application in a computer simulation of accommodating loads." European journal of applied physiology 110.3 (2010): 523-538.

[20] Van Roy P, Baeyens J P, Fauvart D, et al. Arthro-kinematics of the elbow: study of the carrying angle[J]. Ergonomics, 2005, 48(11-14): 1645-1656.

[21] https://www.theraband.com/

[22] Bird, Stephen P., Kyle M. Tarpenning, and Frank E. Marino. "Designing resistance training programmes to enhance muscular fitness." Sports medicine 35.10 (2005): 841-851.

[23] Liu, Jing Z., Robert W. Brown, and Guang H. Yue. "A dynamical model of muscle activation, fatigue, and recovery." Biophysical journal 82.5 (2002): 2344-2359.

[24] Enoka, Roger M., and Andrew J. Fuglevand. "Motor unit physiology: some unresolved issues." Muscle & nerve 24.1 (2001): 4-17.

Chapter 4

Assessment of Physical Frailty based on Muscle Function

1. Introduction

Exercise intervention has physiological effects on the brain, endocrine system, immune system, and skeletal muscle [1,2] and has received much attention recently. Many studies have revealed that exercise interventions, particularly those involving strength and balance training, can be successful at improving muscle strength and therefore, improve muscle function abilities in long-term care residents [3,4,5]. Strength training is acknowledged as a means of preventing or delaying frailty and loss of function [6], recommended by national health organizations, such as the American College of Sports Medicine (ACSM) and the American Heart Association [7,8,9]. But an important issue that arises is how to choose the appropriate training volume according to his frailty state. Assessment of subject's frailty state is necessary before designing exercise intervention for frailty people. We already mentioned in Chapter 1 that the research scope of this thesis mainly focus on the physical domain of frailty. Physical frailty affects patients' oral function, mobility function and upper limb function, and ultimately lead to a decline in quality of daily life.

Actually, one of the biggest causes of frail is muscle weakness [1]. In our daily lives, it is our muscle system that drives us to complete the complex movements. The muscle strength, motion control ability and exercise tolerance are important aspects of muscle function and are closely related to the ability to perform activities in daily life [1,2]. Considerable evidence suggests that the ability to perform a physical task is determined by a threshold level of muscular strength and endurance [10,11]. Individuals lacking the requisite muscular strength may not be able to perform various activities of daily living that are important determinants of independence. The muscle strength decides the ability of

a people to restrain loads. The motion control ability decides the ability of a people to control muscles to perform complex movements and the exercise tolerance decides how long the movement can lasts.For example, as illustrated in Figure 4.1, when an elderly people is using his mobile phone, his elbow flexor muscle helps him keep his forearm at a stable position and helps him click on different locations on the screen. That means the exercise tolerance (keep at a stable position) and motion control ability (touch different locations on the screen) are important muscle function when using the mobile phone. The strength of hand muscle determines the magnitude of hand gripping strength.

Figure 4.1 Elderly people using mobile phone. The elbow flexor muscle is highlighted in pink.

In addition, the upper-limbs play an important role in the process of walking and affect elderly people's mobile ability. For example, when the elderly people are walking with a cane (shows in Figure 4.2), the upper-limbs need to bear part of the body weight and maintain their body balance. Even the muscle strength of lower limbs are very weak, the elderly people can still walk a certain distance with the help from their upper limbs. Therefore, it is necessary to evaluate the upper-limb function when evaluating elderly people's mobile ability.

Besides, since different people have different body types and different ages, the established frailty screening criteria need consider the impact of age and body shape on the screening criteria. Figure 4.3 describes the flow chart of how to assess subject's frailty level. The input demographic data, like age, body weight and limb length, are used to set the experimental conditions and build up the simulation muscle model. The muscle model is used to establish the evaluation criteria of normal people. Experiments are carried out to get the experimental value. The frailty evaluation criteria is built to compare the experimental value and normal criteria value to get the frailty level. Normally, there are four steps needed in the evaluation of the frailty level, which are: A. How to set the experimental conditions; B. How to conduct the experiment and obtain experimental value of elderly people; C. How to establish the criteria of normal people; D. How to establish the frailty evaluation criteria. In next section, we will explain these four steps in detail by using the maximum dumbbell lifting experiment.

Figure 4.2 An elderly man walks with the help of a Cane. Both the elbow flexor and extensor muscles were recruited to bear part of the body weight. The extensor show a higher activation status than the flexor muscles. The elbow flexor muscle strength is utilized to keep the elbow joint stable.

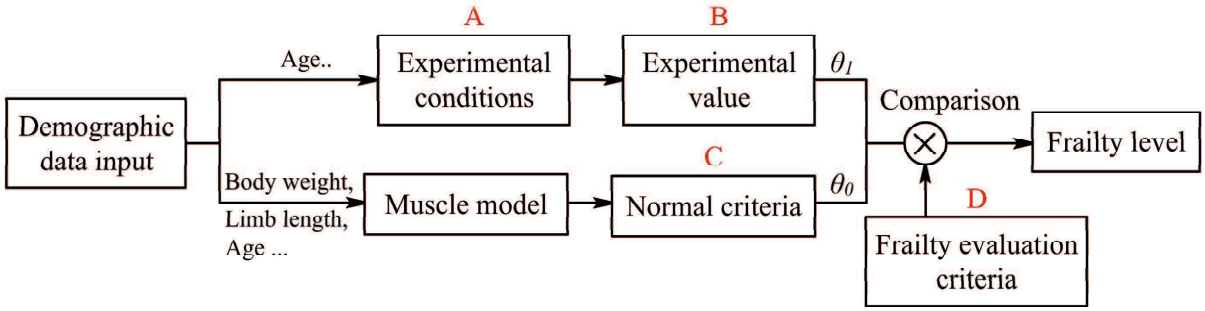

Figure 4.3 A flow chart explaining the frailty level assessment process.

2. Assessing frailty level based on elbow flexor muscle strength

In this section, we introduce a novel and simple method used to assess frailty level of elderly people based on elbow flexor muscle strength. During the evaluation process, the subject just need to perform the maximum dumbbell lifting experiment and the maximum angle he can lift is measured and compared with normal criteria value to get the frailty level of his/her elbow flexor muscle. The core idea of this method is that for a suitable dumbbell weight, thee maximum angle that people of different ages and weights can lift is different. Therefore, we can use the ratio of elderly people to normal healthy people to describe the relative frailty level of elderly people (As illustrated in Figure 4.4). To achieve that, one important issue is to get the criteria value of maximum angle that the normal healthy people can lift. However, to the best of the author's knowledge, there are no researches on the maximum angle a healthy subject can lift especially for the elderly people. However, we can find data on the relationship between age and muscle area [12] and the relationship between muscle area and maximum muscle strength [13]. Besides, we have shown in Chapter 2 that for a give dumbbell, the maximum angle a subject can lift is closely related to the maximum muscle strength. Consequently, we can calculate the normal criteria value for normal healthy subject by using the analytical muscle model and data on the relationship between age and muscle, and the relationship between muscle area and maximum muscle strength. The evaluation process involves multiple steps and this section will explain those steps in detail.

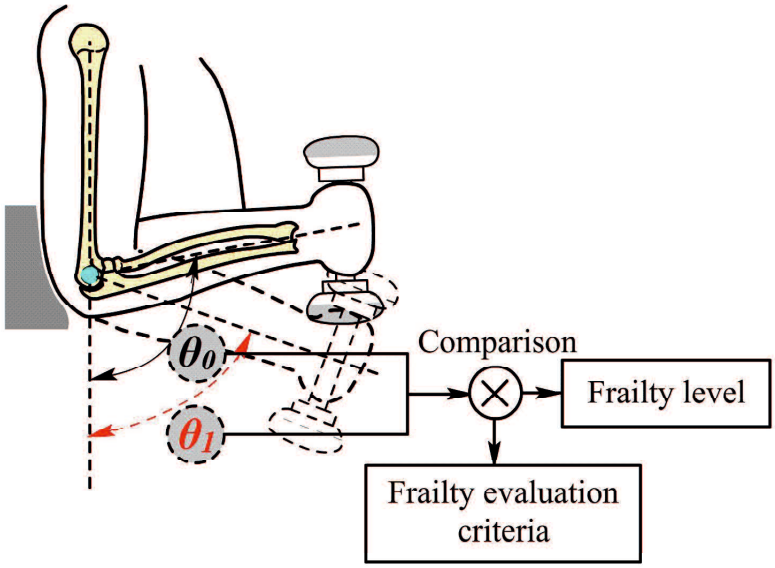

Figure 4.4 Core idea of the assessing method. θ_0 is the maximum angle of normal healthy people and θ_1 is the measured angle of elderly people. The θ_0 is used as an control criterion of normal people.

2.1 Setting the experimental conditions

As we mentioned in the previous chapter, the muscle strength changes with age. Therefore, before doing the experiment, we need choose the suitable dumbbell weight according to subject's actual ability. Here, we explain how to select the suitable dumbbell weight based on the age entered, which means that the dumbbell weight is depends solely on patient's age. Since the elbow flexor muscles are recruited to bear part of the body weight when elderly subjects walking with a cane, we choose the suitable dumbbell weight by referring how much weight the cane needed to bear during the walking. Toshio Soma [14] and his colleagues did electromyography (EMG) analysis of shoulder joint muscles in standing with ambulatory aids. As illustrated in Figure 4.5, they use the EMG signal to analysis the activity of all muscles across the shoulder joint. The EMG signal of the Biceps brachii, Triceps brachii, Brachioradialis deltoid, Pectoralis major and the Latissimus dorsi muscles were recorded when a subject is standing with the help of a cane, and the results of the Biceps brachii and Triceps brachii were shown in Figure 4.6. The partial weight borne by the cane were also recorded by using a force plate, and the results of 5 seconds were illustrated in Figure 4.7.

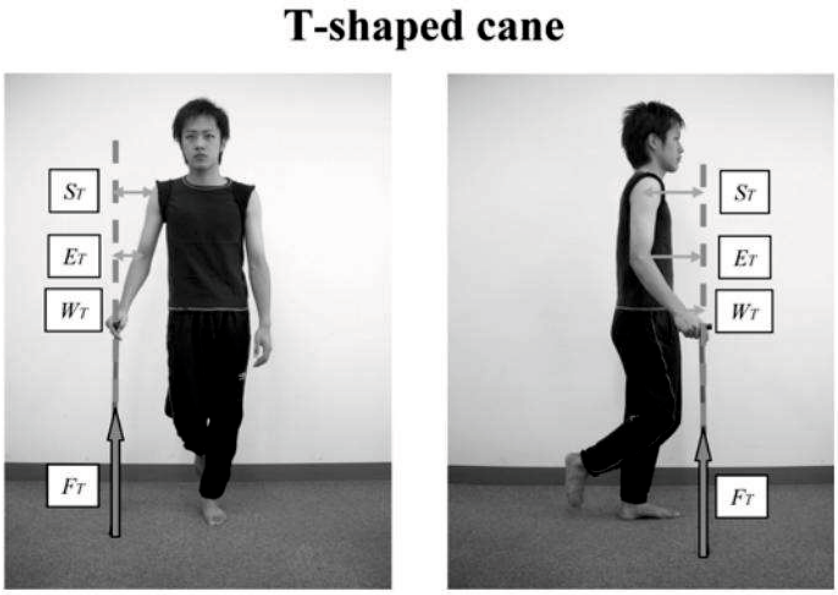

Figure 4.5 A subject is standing with the help of a T-shaped cane. The EMG activity of all muscles across the shoulder joint and the floor reaction force FT were measured in the experiments. Picture obtained and modified from Reference [14].

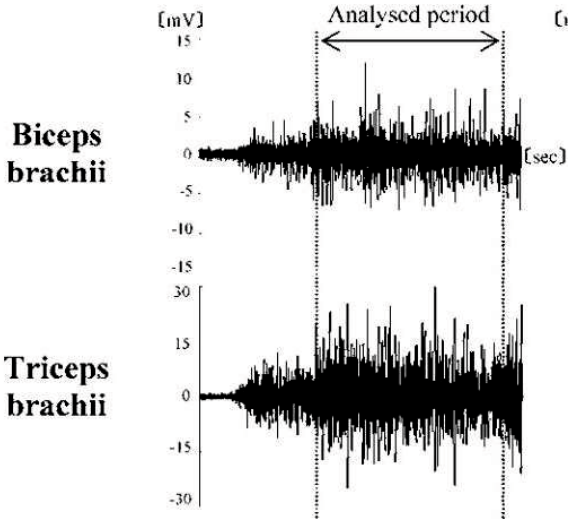

Figure 4.6 EMG activity of the Biceps brachii and Triceps brachii muscle when a subject standing with the help of a T-shaped cane. Picture obtained and modified from Reference [14].

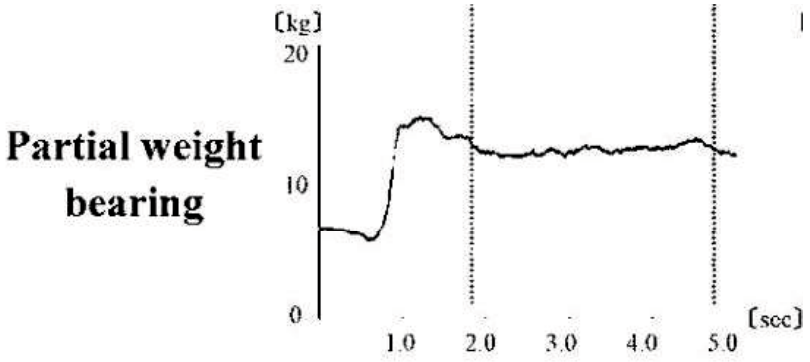

Figure 4.7 Partial weight borne by the cane. The data from 0~1 s is the deadweight of the cane and the data from 2~5 s is the stable partial weight born by the cane. Picture obtained and modified from Reference [14].

From the EMG results illustrated in Figure 4.6, we can see that both the elbow flexor and extensor muscles were activated to bear part of the body weight. However, the activation ratio between elbow flexor and extensor is different, which means that their contribution is different during the walking. From the results, we can see that the amplitude of EMG activity of extensor muscles is approximately three times that of flexor muscles. In addition, the data of the partial weight borne by the cane reveals that pure weight born by the cane is about 8 Kg (13 Kg-5 Kg). Consequently, the body weight born by the flexor muscles is estimated to be 8/3 Kg. However, the 8/3 Kg is the usual weight but in the maximum dumbbell lifting exercise, the dumbbell weight need be a little bigger. Moreover, the muscle strength changes with age. Figure 4.8 is the relationship between age and muscle area. From the data, we can see that the muscle area reaches its maximum at the age of 25 and after that continuously declines with age. Therefore, we refer to the trend of this curve and suppose the suitable dumbbell weight for people at the age of 90 to 100 years is about 3Kg, the suitable dumbbell weight for different ages is shown in Table 4.1.

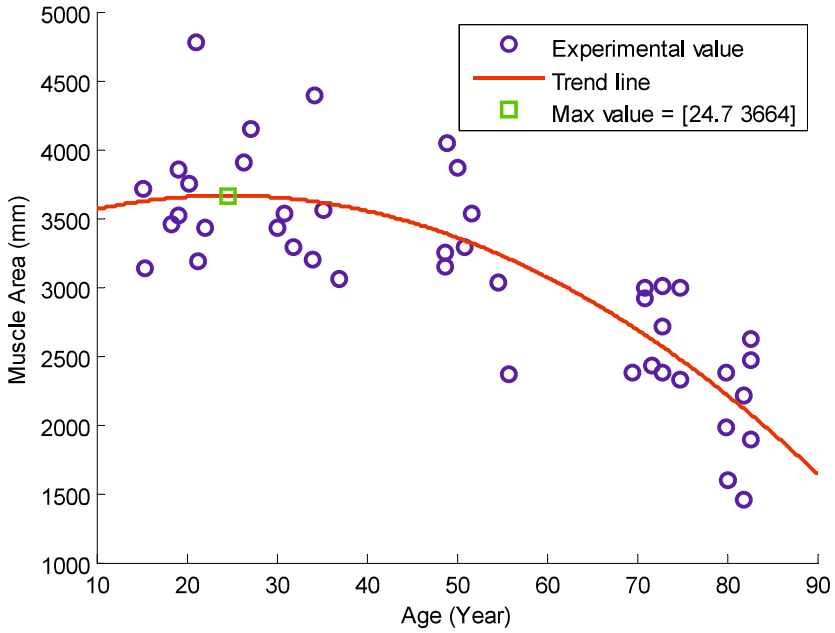

Figure 4.8 Relationship between age and muscle area. Data obtained from Reference [12].

Table 4.1 The suitable dumbbell weight for different ages.

Age/years	10~20	20~30	30~50	50~70	70~90	90~100
Dumbbell weight/Kg	9	10	9	7	5	3

2.2 Conduct the experiment and obtain experimental value

During the experiment, the subject need perform the maximum dumbbell lifting exercise. Each subject need perform the experiment for three times and the average is used as the final result. We use the accelerometer sensor described in Chapter 3 to estimate the elbow joint angle. Placement and axis direction of the accelerometer sensor were shown in Figure 4.9. The accelerometer sensor was attached to the lateral side of his forearm and sensor signals were measured and processed by a wireless transmission module and sent to the desktop. Because when doing the bicep curl exercise, the forearm is supposed to flexes and extends in the sagittal plane with shoulder joint at neutral position and humerus in parallel with y axis of thorax. So, as illustrated in Figure 4, we can obtain the elbow joint angle β by calculating the inclination angle of the accelerometer θ [15]. Which can be expressed as:

$$\beta = 180^{\circ} - \theta \tag{1}$$

where θ is the inclination angle which is the angle between vectors of Gravity and z axis ($\boldsymbol{R}_z$=[0 0 1]^T) in the sensor coordinate system. That is:

$$\theta = ar\cos\left(\frac{\boldsymbol{G}\times\boldsymbol{R}_z}{|\boldsymbol{G}||R_z|}\right) \tag{2}$$

where $|\boldsymbol{A}|$ means the normal of vector $\boldsymbol{A}$.

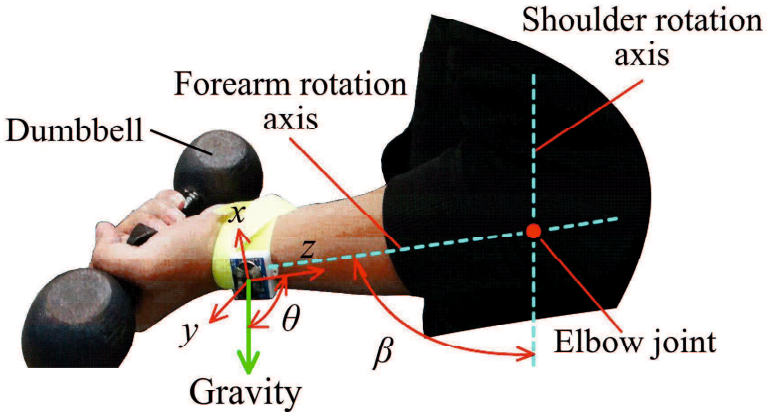

Figure 4.9 Placement and axis direction of the accelerometer sensor.

2.3 Establishment of the criteria of normal people

In this section, we talk about how to calculate the criteria value of normal subject. Figure 4.10 is the flowchart of estimating the maximum angle the subject can lift. According to the simulation results in Chapter 2, if we know the subject's maximum isometric muscle fiber force F_0^M and the dumbbell weight, we can calculate the maximum angle the subject can lift based on the muscle model. As stated in the previous section, the weight of the dumbbell can be determined by the age entered. Besides, we need to know the maximum muscle strength F_0^M according to the age and body weight entered. Many researches reveal that the maximum muscle strength is related to subject's age and body weight [12,13,15]. Figure 4.8 is the relationship between age and muscle area. Ikai and his colleagues measured the muscle strength and muscle area of 245 healthy human subjects, and they found that there is a linear relationship between muscle strength and muscle area, as illustrated in Figure 4.11. Therefore, based on the relationship between age and muscle area (Figure 4.8), and the relationship between muscle strength and muscle area (Figure 4.11), we can get the relationship between age and muscle strength as illustrated in Figure 4.12. Besides, the muscle strength is also affected by the body weight. Maughan and his colleagues [16] found there is a weak linear relationship between muscle strength and body weight. Their results were shown in Figure 4.13. Take the BRA muscle as an example, we can get the curves of muscle strength changes with the age and body weight. That means if we know the subject's age and body weight, we can calculate the maximum force of a certain muscle of him.

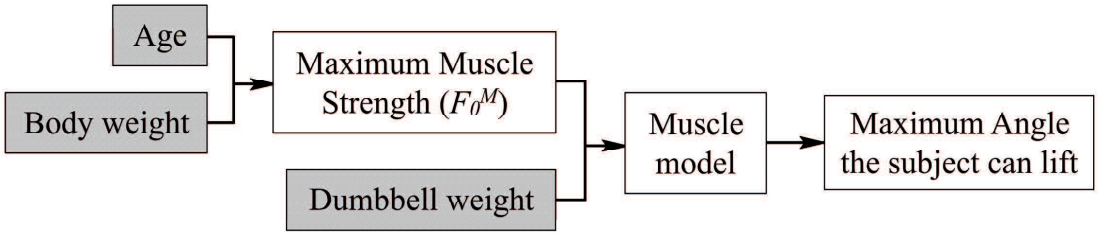

Figure 4.10 Flowchart of estimating the maximum angle the subject can lift.

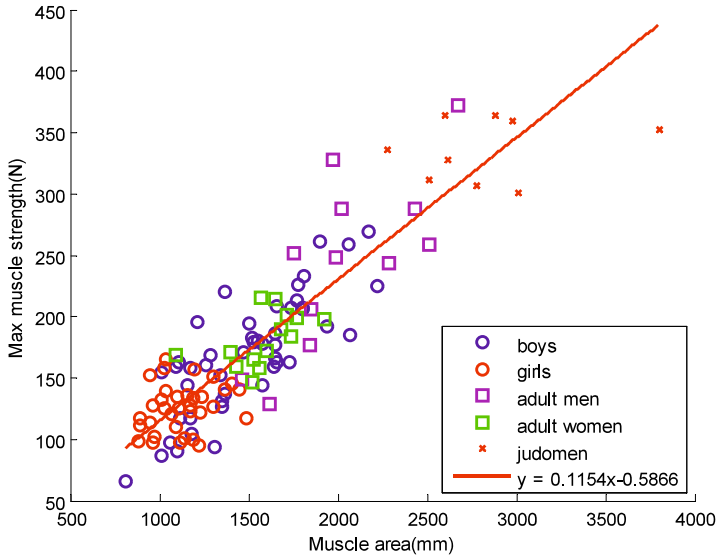

Figure 4.11 The linear relationship between muscle strength and muscle area.

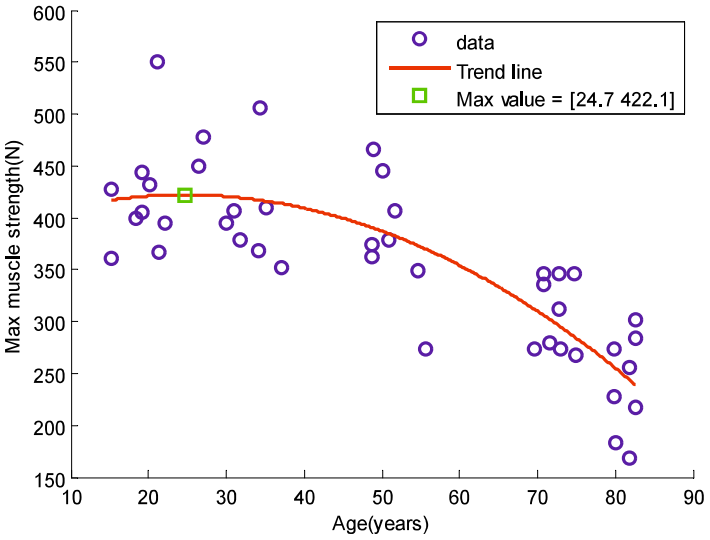

Figure 4.12 Relationship between age and muscle strength.

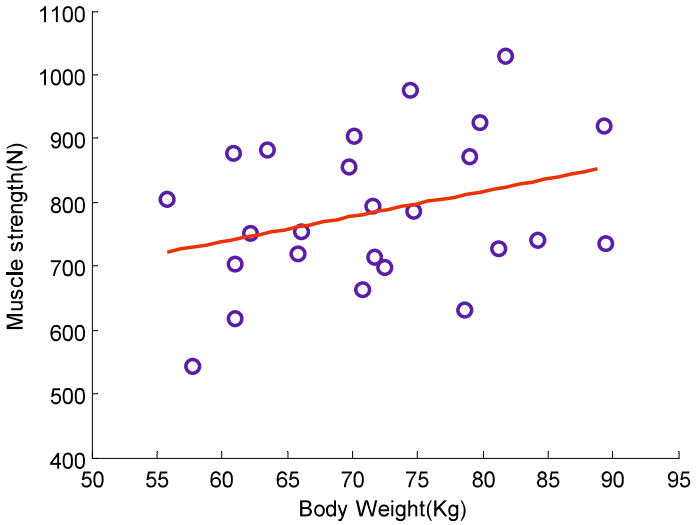

Figure 4.13 Relationship between body weight and muscle strength.

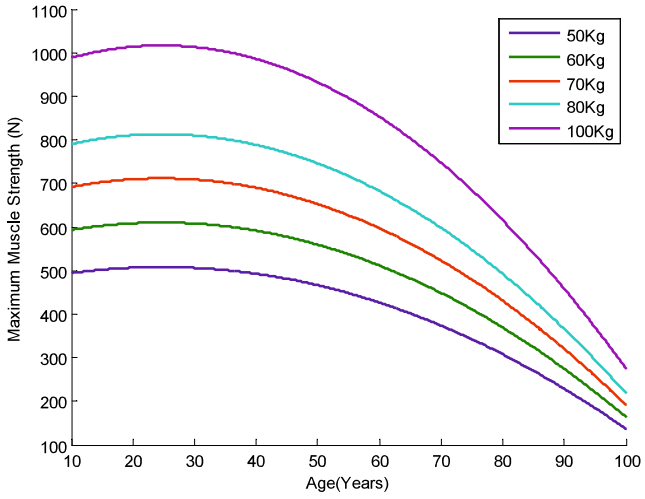

Figure 4.14 Effect of body weight on the relationship between age and F_0^M. Take the BRA muscle as an example.

After getting subject's F_0^M and the dumbbell weight, we can eventually calculate the maximum angle he can lift by using the muscle model. However, as illustrated in Figure 4.14, we need the elbow joint angle as input to calculate the maximum muscle force F_0^M in the muscle model. But there is a one-to-one relationship between θ and F_0^M. So by using special numerical calculation methods, it is possible to calculate the maximum angle based on the input F_0^M. If the reader want to know more details about the analytical muscle model, please refer to Chapter 2.

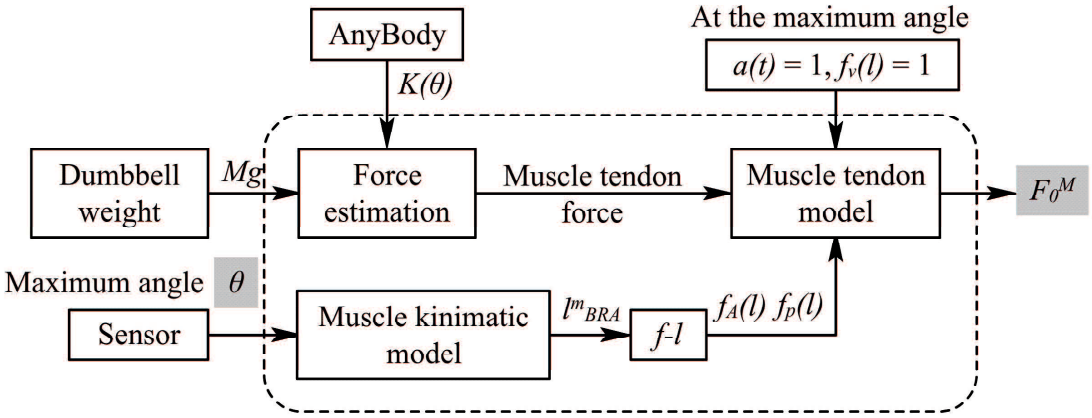

Figure 4.14 Flowchart explains how to calculate the maximum muscle force under the circumstances that a specific dumbbell (M) can only be lifted to a certain maximum angle (θ).

Here we also show some simulation results reveal how the body weight, age and dumbbell weight affect the maximum angle a subject can lift in a comprehensive way.

Figure 4.15 is the effect of body weight on the and maximum angle the subject can lift with a specific dumbbell weight. Figure 4.16 is the effect of dumbbell weight on the and maximum angle the subject can lift if we know his body weight.

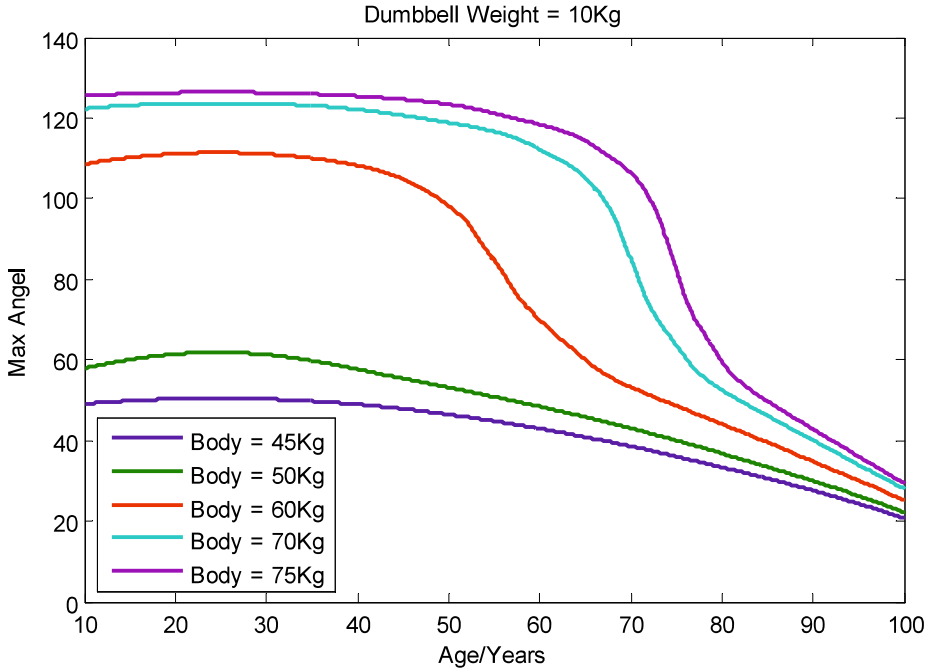

Figure 4.15 Effect of body weight on the and Maximum angle the subject can lift with a specific dumbbell weight. The dumbbell weight is 10Kg.

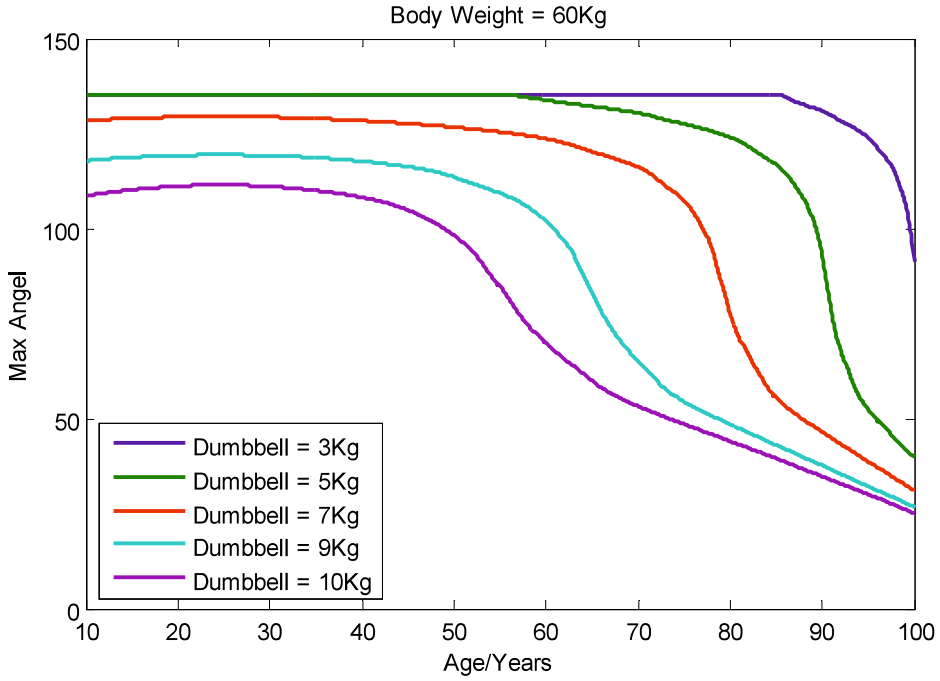

Figure 4.16 Effect of dumbbell weight on the and Maximum angle the subject can lift if we know his body weight. The body weight of the subject is 60Kg.

2.4 Establishing the frailty evaluation criteria

After getting the measured maximum angle θ_1 and the calculated maximum angle θ_0, we still need a frailty evaluation criteria to assess subject's frailty level. The Frailty state can be expressed as Formula 3. Table 4.2 is a simple frailty evaluation criteria to screen frailty level.

$$\text{Frailty state} = \frac{\theta_1}{\theta_0} \times 100\% \tag{3}$$

Table 4.2 A simple frailty evaluation criteria to screen frailty level.

$0 \le \theta_1/\theta_0 \le 0.4$	$0.4 < \theta_1/\theta_0 \le 0.8$	$0.8 < \theta_1/\theta_0 \le 1.2$	$1.2 \le \theta_1/\theta_0$
Frailty	Pre-frail	Normal	Strong

3. Indicators for evaluating motion control ability and exercise tolerance

In this section, the bicep curl exercise with a custom-made Thera-Band was performed by subjects to assess their muscle function. The bicep curl exercise focuses on development or maintenance of flexor strength of upper extremity and it is simple and applicable for many circumstances like hospital, rehabilitation center and home. In the exercise, the subject need to flex his forearm to resistance against the resistance force produced by the custom-made Thera-Band. It is the elbow flexor muscle that drives the forearm to a certain angle that the force data during the flexing stage can be used to quantify flexor muscle's motion control ability. After the resistance force reaches a maximum value, the subject need hold the value for a while. The force data segments in the holding phase can be used to quantify subject's exercise tolerance. Usually, one repetition incorporates four contraction phases, which are concentric (CON), eccentric (ECC), isometric (ISOM) contraction phase and the Rest phase. During the CON phase, the subject flex his forearm to resistance against the resistance force produced by the custom-made Thera-Band, and hold the force for a while during the ISOM phase. And later, subject release his forearm in the ECC phase. The subject usually need to have a short rest during the Rest phase.

3.1 Concepts and big picture

Figure 4.17 illustrates the concepts and flow chart of the system. Firstly, the force data segmentation algorithm described in Chapter 3 was used to automatically segment force data into small segments based on muscle actions. Then, after obtaining the segmented force data, indexes for quantifying muscle function proposed in Chapter 3 were used to quantify motion control ability and exercise tolerance of elbow flexor muscle.

As illustrated in Figure 4.17, the subject sits on a wheelchair while performing the bicep curl exercise against resistance produced by a custom-made Thera-Band. A load cell is connected with the Thera-Band to measure the resistance. Analog signals corresponding to the resistance were sampled and digitized by an analog-to-digital (A/D) converter and the data were sent to a desktop computer through an Arduino board. A graphical user interface (GUI) was built for monitoring the training process, and the force signals were acquired and saved for further analysis and post-processing. A peak detection method was firstly used to find signal valleys, in order to divide the force data into small segments (Fi(t)), and then calculate the number of repetitions. In each segment, the first order derivative of force versus time was numerically calculated, and the maximum and minimum values were taken as the discriminating feature to segment the training cycle into the CON, ECC, and ISOM contraction phases. The force data segments in CON phase are used to quantify subject's motion control ability and force data segments in ISOM phase are used to quantify subject's exercise tolerance.

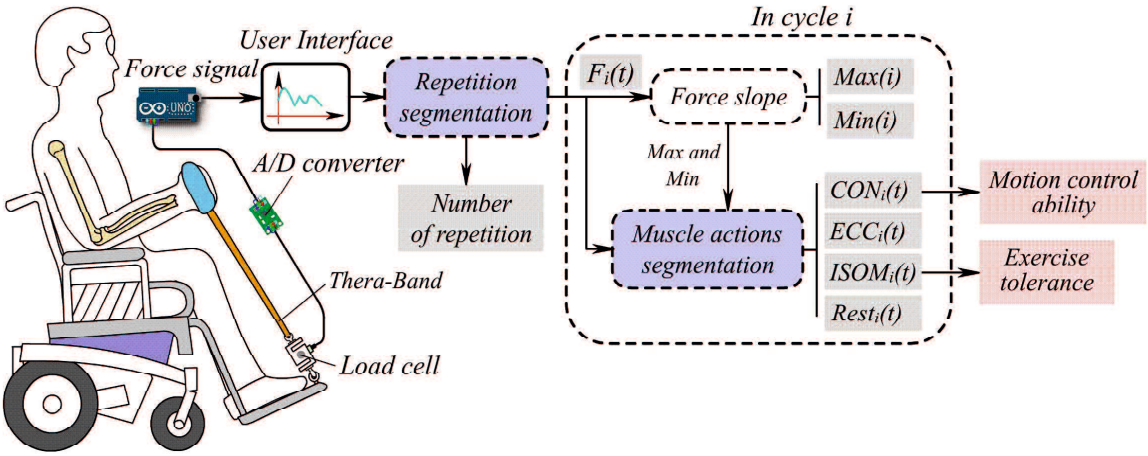

Figure 4.17 Concepts and big picture of the system. $F_i(t)$ is the resistance in repetition *i*. *Max(i)* and *Min(i)* are the maximum and minimum force slope values. CON, ECC, and ISOM are concentric, eccentric, and isometric contraction, respectively. $Rest_i$ is the force data in the Rest phase.

3.2 The measuring system

Figure 4.18 shows the experiment set-up. A standard wheelchair is utilized to help the subject sit in a stable position and to help him/her lean the left or right arm against the armrest of the wheelchair. The subject flexes his/her forearm in the sagittal plane against the resistance produced by the custom-made Thera-Band. In resistance training, the subject pulls the handle which is connected to the Thera-Band. The Thera-Band is attached to the load cell, which is anchored to the footplate of the wheelchair by a lifting hook. As mentioned above, a load cell (SC301A, 100 kg) was used to measure the time-varying resistance. The analog signals were converted to digital signals through an A/D converter (AE-HX711-SIP, 30 Hz). The load cell was calibrated and the scale factor was calculated before the experiments using calibration weights. A personal computer (PC) was used to acquire, display, save, and process the force data through a serial COM port. Figure 4.19 shows the GUI designed with the aid of MATLAB to help users supervise the training process and is also used as a real-time signal display and storage. Users can type initial setups of the experiment into the system through the GUI. The resistance force and elbow joint angle are displayed in the GUI in real-time. For the convenience of the operator monitor the training process, a musculoskeletal model is also included in the system and the subject can interact with it in real-time. Since the training load was different among different trainees, three different types of Thera-Band (Green, Red, and Yellow) were constructed and connected to the handle using a carabiner clip. More details about the measuring system is described in Chapter 3.

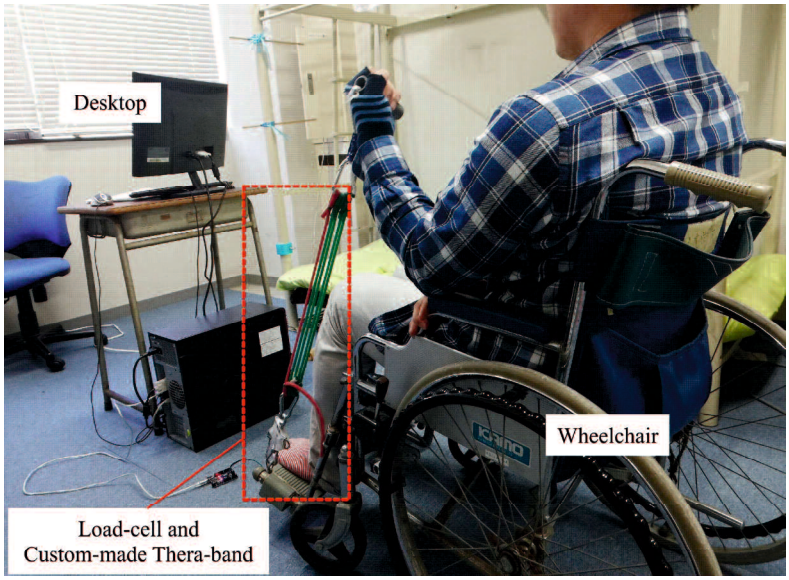

Figure 4.18 Details about the experiment set-up.

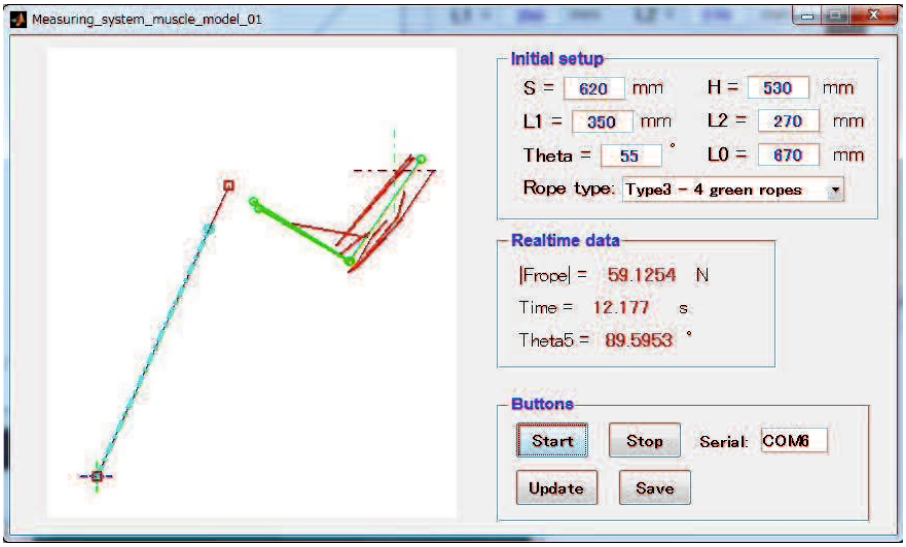

Figure 4.19 GUI built for receiving and saving the force data.

3.3 Experimental procedure

Six healthy subjects (3 male and 3 female, age 27.3 ± 4.2, weight 60.3 ± 11.7 Kg, height 171 ± 9.7 cm) volunteered to participate in this pilot experiment. All subjects were familiarized with the research procedures and gave their informed consent. All subjects reported no known neurological, musculoskeletal, or orthopedic disorders. Figure 4.20 gives a visual representation of the procedure followed in the fatigue and recovery protocol. The protocol has been carefully designed to incorporate four parts: one-repetition maximum (1RM) test, 5-minute intermittent submaximal contraction (ISC), 1-minute rest, and 2-minute ISC. The 1RM test is performed to assess subject's flexor muscle strength

and the obtained value is the basis for selecting the combination of elastic bands. Three sets of contractions were performed, and the average force was taken as the final 1RM. In the 1RM test, the number of bands was empirically increased to reach the maximum load the subject can pull while flexing his/her forearm throughout the full range of motion (elbow joint angle more than 150°). During the 5-minute ISC, the number of elastic bands was chosen to ensure that the initial average force was 40~60% that of 1RM. ISC is an intermittent and dynamic voluntary contraction process with many repetitions. During each repetition, the subject flexes his/her forearm to a maximum angle (CON contraction), maintains the angle for about 3 seconds (ISOM contraction), and then returns to a relaxed state (ECC contraction). A short rest was allowed between each repetition and the rest time was usually no more than 4 seconds. During the 1-minute rest, the subject was encouraged to stand up from the wheelchair and swing his/her arm to recover from the fatigued state. The 1-minute rest and 2-minute ISC were performed in succession after the 5-minute ISC. The subjects performed the exercises with both hands and were given ample rest between experiments. All subjects were right-handed. A training session was conducted in order to get the subjects familiar with the experimental procedure before the formal experiment. A metronome was used to help subjects maintain a pace while performing each repetition phase. The subjects should find the contraction beat by themselves.

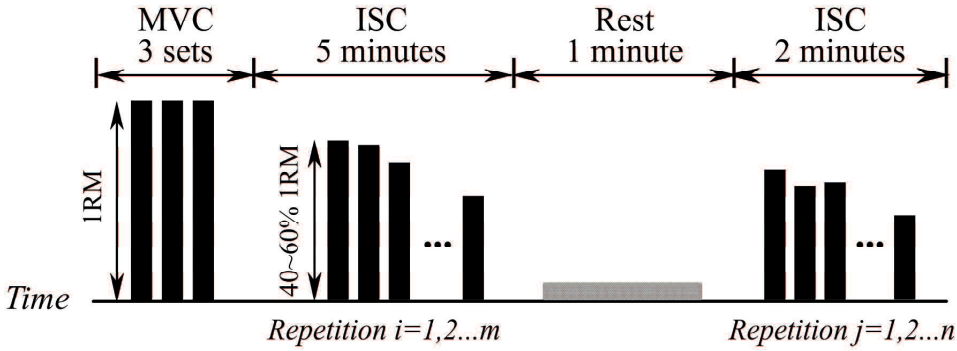

Figure 4.20 Schematic of the experimental procedure. 1RM is the one-repetition maximum test, MVC is the maximum voluntary contraction, and ISC is the intermittent submaximal contraction. Each black bar represents 1 repetition, which incorporates the CON, ISOM, and ECC contractions.

3.4 Experimental results

Figure 4.21 shows a typical force-time curve of a male subject. As dynamic

contraction progressed, the maximum force the subject could reach reduced gradually and was restored to a certain extent after the 1-minute break. When the participants got tired, there were some fluctuations in force during ISOM contraction. Demographic data of the study participants and other details about the experiment, such as the initial force, are presented in Table 4.1. As described in the previous section, the combination of Thera-Bands was chosen based on subject's muscle strength. By looking at Table 4.1, it can be noticed that the female subjects had lower 1RM force than the male subjects. The left hand of the subjects was weaker than the right hand, which is consistent with the actual situation. Based on their performance in the experiment, it was noted that S02 was the weakest one and S06 was the strongest (served in the army). The repetition numbers before rest (m) and after rest (n) were calculated and are given in Table 4.1.

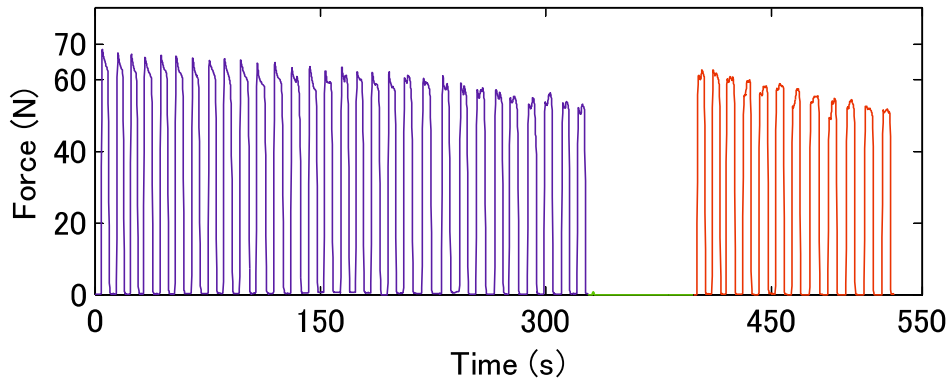

Figure 4.21 Representative data of a male subject. The blue curve represents data during the 5-minute ISC and red curve represents data during the 2-minute ISC.

Table 4.1 Demographic data of the study participants and experiment details. The 2R means subject used 2 Red Thera-bands in exercise.

Subject No.		Age (Year)	Weight (Kg)	Hand	1RM (N)	Initial F_{ave} (N)	Combination of Thera-Bands	Repetitions	
								m	n
Female	S01	34	50	Left	87.8	45.1	2 R	40	17
				Right	91.6	58.4	1 G + 1 R	37	20
	S02	24	57	Left	67.1	42.0	1 R +1 Y	39	18
				Right	59.5	44.7	1 R +1 Y	41	16
	S03	27	48	Left	108.6	43.0	1 G + 1 R	49	19
				Right	111.2	47.2	1 G + 1 R	45	23
Male	S04	28	65	Left	152.5	82.5	3 R + 1 Y	41	16
				Right	163.2	91.3	3 R + 1 Y	40	17
	S05	22	62	Left	132.2	65.3	2 R + 1 Y	30	12
				Right	140.8	73.4	3 R	32	10
	S06	29	80	Left	193.6	112.8	4 G +1 R	37	17
				Right	189.6	120.6	4 G +1 R	35	19

3.4.1 Distribution of R_1 and R_2

As mentioned in Chapter 4, the quotients of T_1 and T_2, T_3 and T_4 were used to quantify the motion control ability of participant's elbow flexor muscles, gaining insight into the control strategy of subject's neuromuscular system in shortening or lengthening the muscles to resist external resistance. The time-varying R_1 and R_2 before and after rest for all participants were calculated and shown in Figure 4.22 a,b.

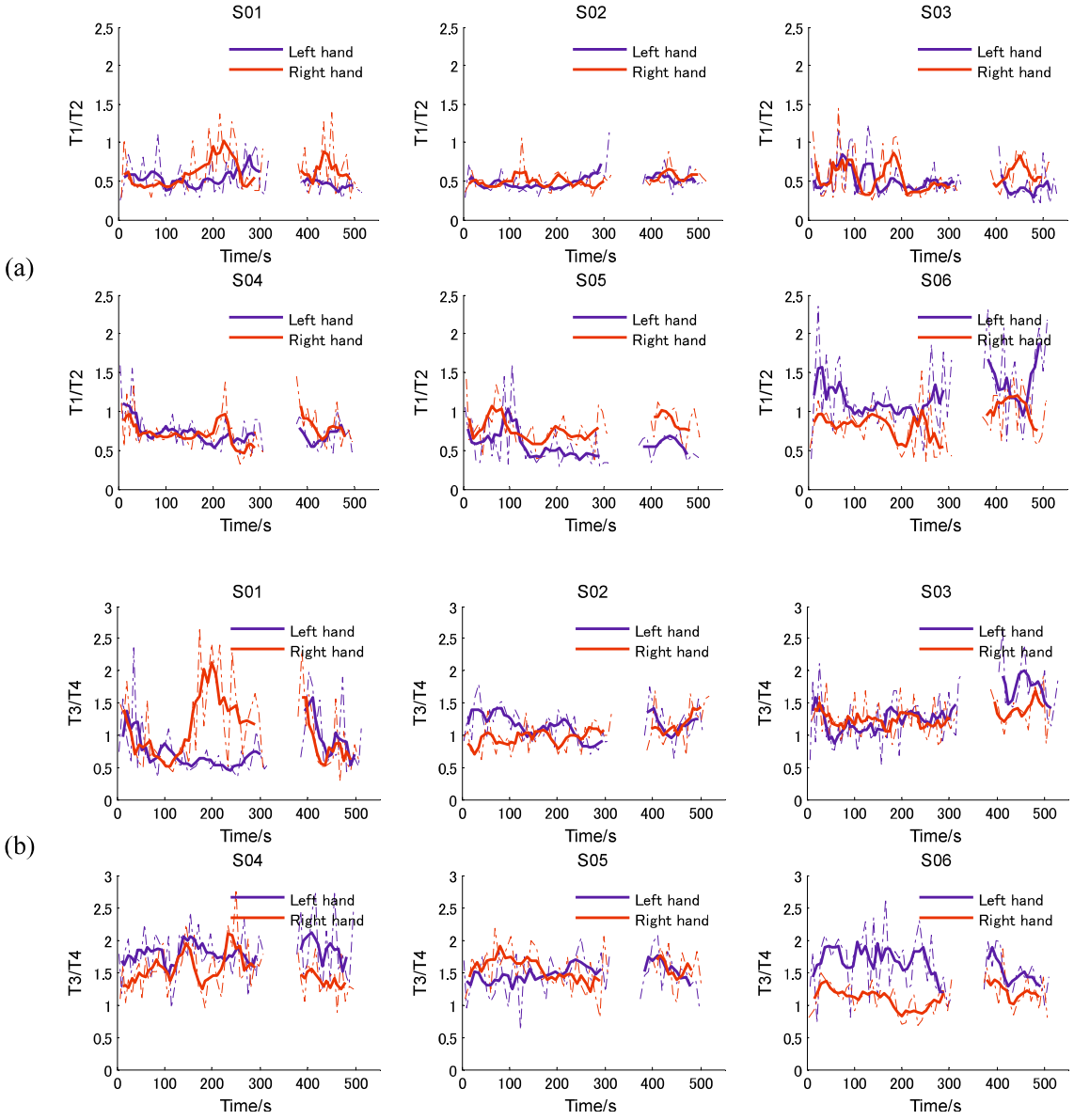

Figure 4.22 Variations in (a) R_1 and (b) R_2 before and after rest for all participants. The dotted line is the raw data and moving average was performed to highlight the data trends.

As we can see from Figure 4.22a, different from the decreasing slope and peak velocity, the R_1 and R_2 change with time but are not continuously decreasing or increasing. In CON contraction, female subjects usually have R_1 values smaller than male subjects (the

mean and standard deviation of female subjects were 0.529 ± 0.0411, compared with 0.790 ± 0.182 for male subjects). As mentioned above, S06 is the strongest participant whose R_1 usually bigger than others (the average of R_1 in left hand is 1.133 and the right hand is 0.787), which reminded us that the R_1 may related to subject's muscle strength. For female subjects, duration of the acceleration phase lasts less than the deceleration phase and the R_1 value fluctuates around 0.5. In contrast, during ECC contraction, duration of the acceleration phase lasts longer than the deceleration phase. The female subject's R_2 value fluctuates around 1, and the male subject's R_2 value fluctuates around 1.5. Moreover, there was no significant difference between R_1 and R_2 before and after 1 minute rest.

3.4.2 Phase-plot analysis of force and force derivative

We use the phase-plot analysis to count the distribution of the magnitude of the force throughout the experiment in the phase space, regardless of time. With the repetition segmentation and muscle action segmentation algorithm mentioned in previous chapters, we firstly get the force data of each contraction phase and the force derivative versus time were calculated through numerical calculation. And later, the force data were used as x-axis data and the derivative of force versus time were used as y-axis data to get the phase diagram in Figure 4.23 and Figure 4.24.

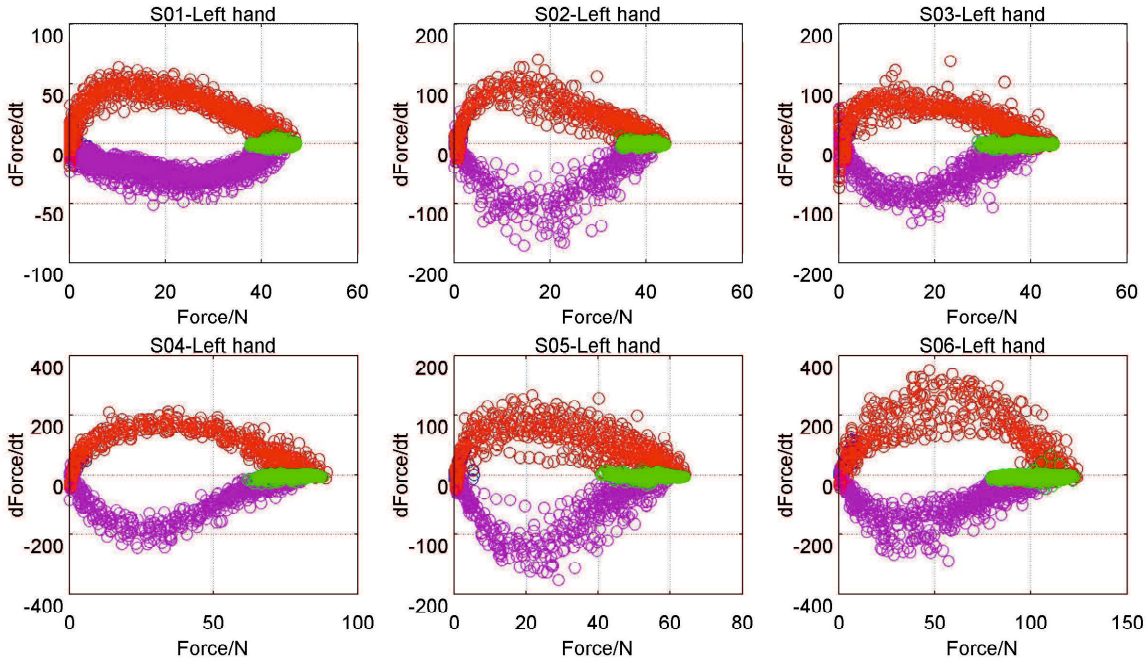

Figure 4.23 Phase diagram of left hand for all subjects. In the figures, blue circles represent data in rest period, red circles represent data in CON phase, green circles represent data in ISOM phase and pink circles represent data in ECC phase.

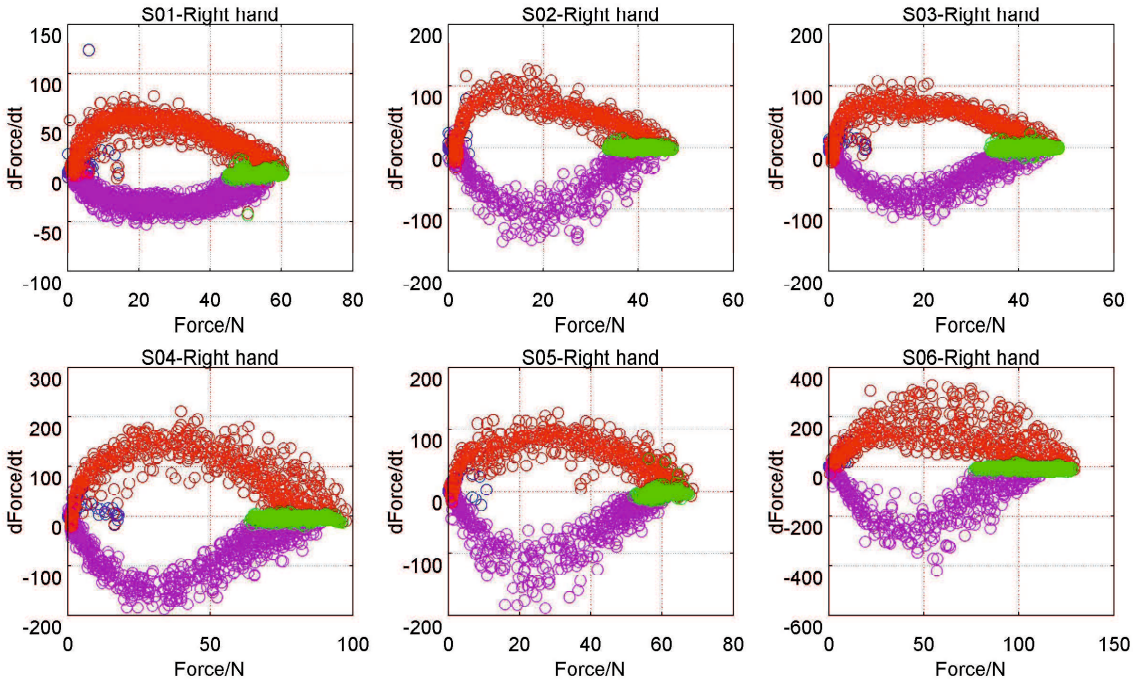

Figure 4.24 Phase diagram of right hand for all subjects. In the figures, blue circles represent data in rest period, red circles represent data in CON phase, green circles represent data in ISOM phase and pink circles represent data in ECC phase.

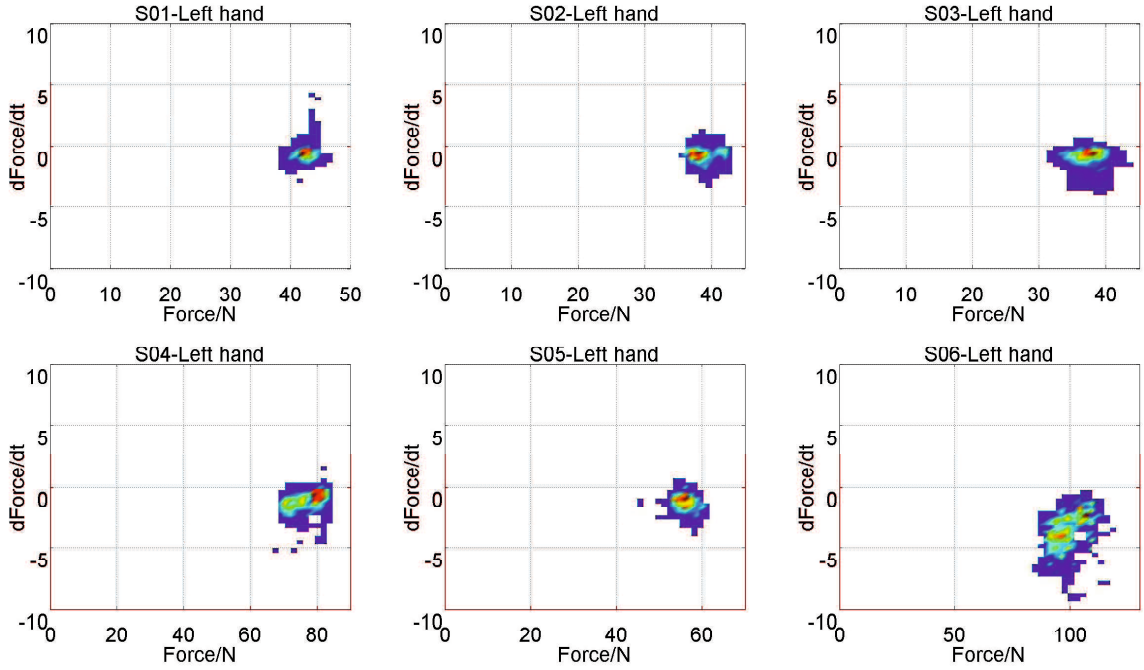

Figure 4.25 Heat map of the frequency distribution of left hand during ISOM phase for all subjects. The color represents how many times a data appears at a certain point. Blue represents fewer times and red represents more times.

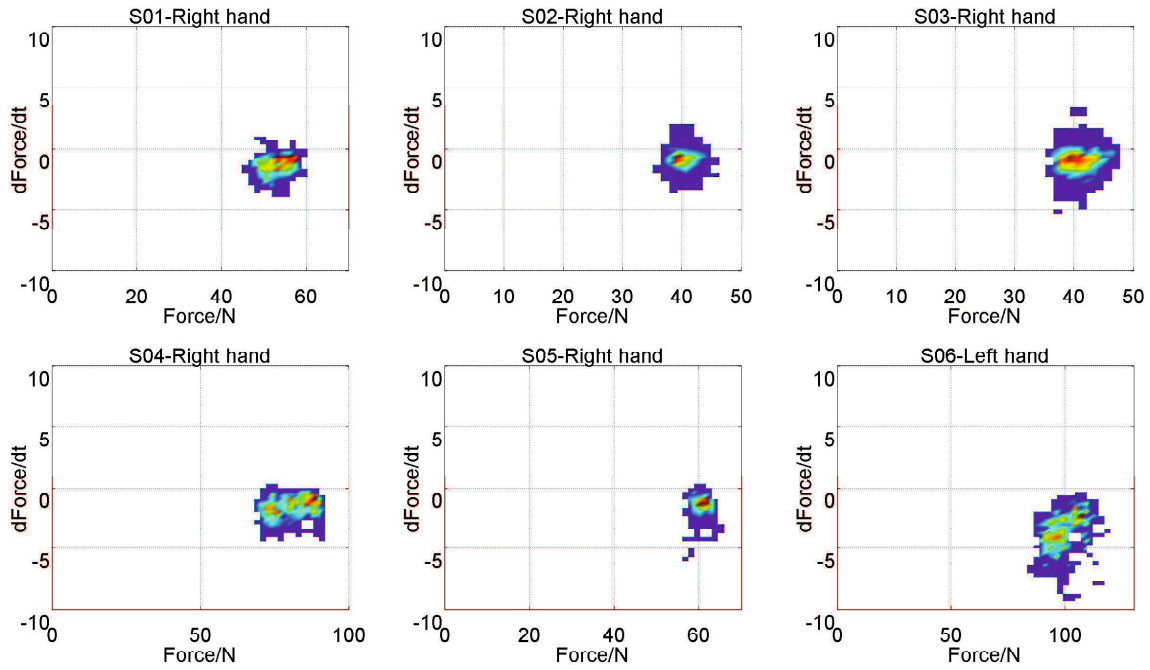

Figure 4.26 Heat map of the frequency distribution of right hand during ISOM phase for all subjects. The color represents how many times a data appears at a certain point. Blue represents fewer times and red represents more times.

As can be seen from the phase diagram, the curve shape during CON and ECC phase is different for different subject. The shape of the curve is affected by the time when the force derivative reach its maximum. That means that the the quotients of T_1 and T_2, T_3 and T_4 are related to the curve shape. Here, we want to analysis the fluctuation in force during ISOM phase. Therefore, for the data in ISOM phase, we count the number of occurrences at a certain point and get the heat map of the frequency distribution of left hand during ISOM phase for all subjects in Figure 4.25 and Figure 4.26. As we can see from the frequency distribution diagram, the heat map of female subject is more concentrated than male subject. Indicate that the coefficient of variation of female subject is bigger than male subject.

3.5 Assessment of elbow flexor function

In the previous sections, the measurement system was described and a segmentation algorithm that automatically segments the biceps curl cycle into small parts based on muscle actions was proposed. A pilot experiment with 6 subjects was conducted and the

distribution of R1 and R2, phase-plot analysis of force and force derivative were presented. In this section, we want to use the frequency distribution of R1 to assess motion control ability and the coefficient of variation to assess exercise tolerance.

3.5.1 Assessing motion control ability based on frequency distribution of R1

In this section, we show the prospect of using the frequency distribution of R1 to assess subjects' motion control ability. Similar to using grip strength to assess upper limb function, the 1RM value in the experiment is related to flexor muscle strength. That means, to some extend, the 1RM value reflects the weak or strong level of the subject. Firstly, we want to show the linear relationship between average value of R1 and 1RM. And later, the frequency distribution of R1 were divided into three parts to show differences in motion control ability between each other.

In concentric phase of bicep curl with a resistance band, the brain sends down a command through the spinal cord and peripheral nerves to muscles. When the command arrives at the motor unit and it is strong enough, it triggers an action potential, which in turn activates motor units of flexor muscles. Force is generated by contraction of muscle fibers and the forearm starts to flex. The resistance force from the resistance band increases with the increases of elbow joint angle. When the resistance force reaches a certain value, the forearm stops accelerating. The time ratio between acceleration and deceleration indicates the dynamic contraction effort of participant's elbow flexor muscles. A large time ratio means a longer accelerating phase, which also means a bigger contraction command from the brain. Moreover, a positive linear relationship was found between R1 and 1RM (Figure 4.27). All of those inspired us use the time ratio between acceleration and deceleration to assess subject's contraction effort during the concentric phase. In Figure 4.27, we noticed that different from the decreasing slope and peak velocity, the value of R1 change with time but are not continuously decreasing or increasing. The R1 of female subjects fluctuate around 0.5 and the R1 of male subjects usually start from 1. As illustrated in Figure 4.28, we use the frequency distribution of R1 to analysis subject's

contraction effort and the *x* axis is divided into three parts (Part 1: 0<T1/T2<0.5, Part 2: 0.5<T1/T2<1 and Part 3: 1<T1/T2). The proportion of each region for all subjects are illustrated in Figure 4.29. As we can see, S06 has a much bigger area of part 3 and a much smaller area of part 1 than other subjects, which means S06 showed a stronger contraction effort during the experiment. This is consistent with the fact that S06 is the strongest participant. All of those indicate that the frequency distribution of R1 could be used as an important variable to quantify subject's motion control ability.

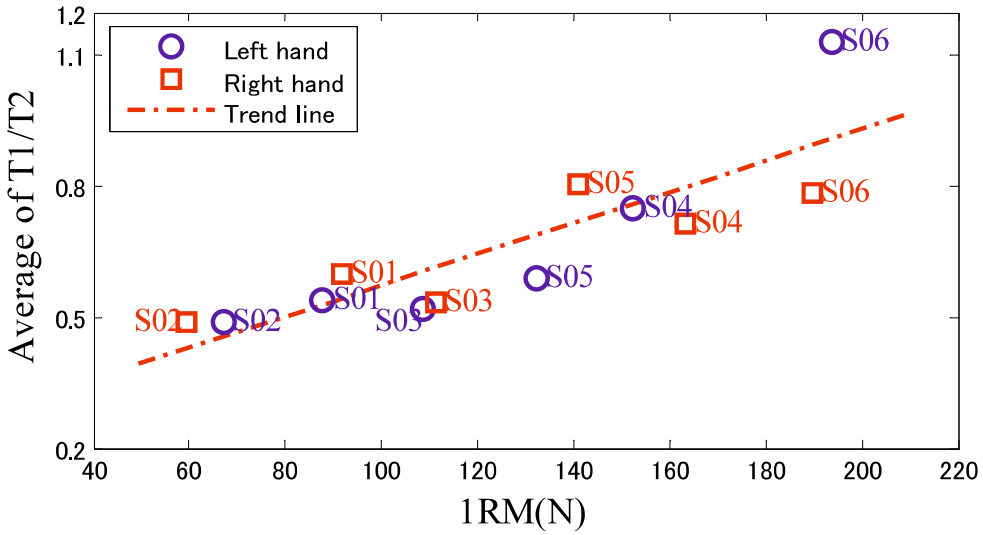

Figure 4.27 Linear relationship between average of R1 and 1RM ($y = 0.0035x + 0.22$). The subject's label is marked near each data point.

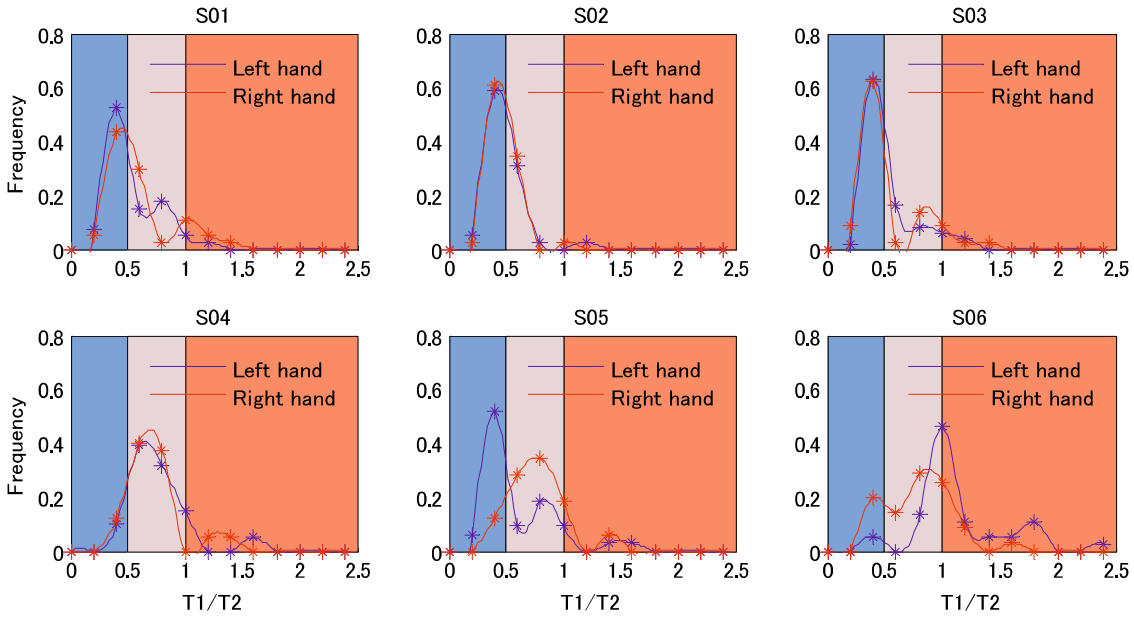

Figure 4.28 Frequency distribution of R1 for all subjects.

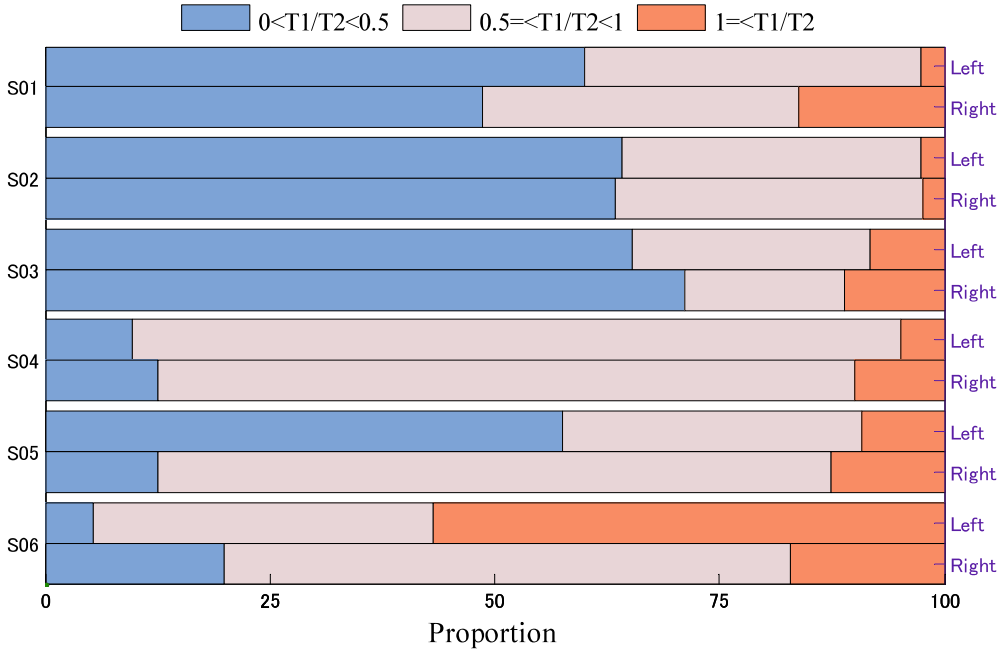

Figure 4.29 Bar charts illustrates the proportion of each region for all subjects.

3.5.2 Assessing exercise tolerance based on coefficient of variation

According to Figure 4.25 and Figure 4.26, we noticed the heat map of female subject is more concentrated than male subject, which indicates that the coefficient of variation of female subject is bigger than male subject. A bigger value of coefficient of variation means a relative bigger fluctuation in force during ISOM phase. A big fluctuation in force means that the subject is unable to maintain a constant resistance force during the ISOM phase, which means that his elbow flexor has lower exercise tolerance. After calculating the coefficient of variation of all subjects, correlation analysis was performed and a negative linear relationship was find between coefficient of variation and 1RM. As illustrated in Figure 4.30, a strong subject with bigger 1RM value has a smaller coefficient of variation, which means that their relative fluctuation in force during the ISOM phase is smaller. All of those shows the prospect of using the coefficient of variation to assess subjects' exercise tolerance of elbow flexor muscles.

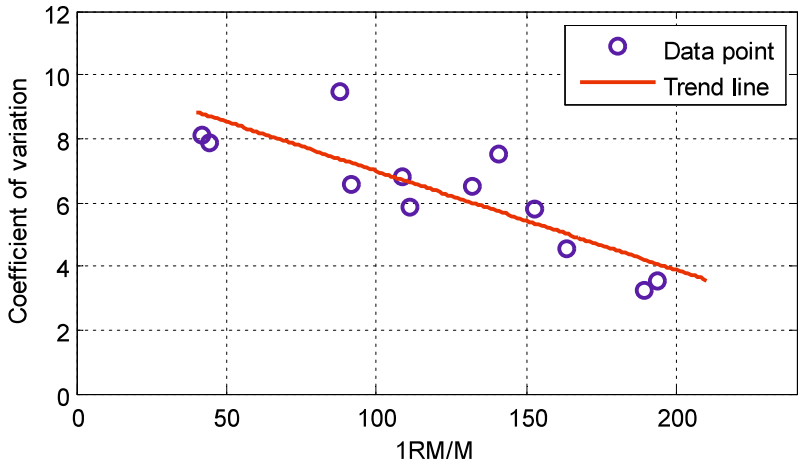

Figure 4.30 Linear relationship between coefficient of variation and 1RM.

4. Summary

In this section, we introduce a novel and simple method used to assess frailty level of elderly people based on elbow flexor muscle strength. During the evaluation process, the subject just need to perform the maximum dumbbell lifting experiment and the maximum angle he can lift is measured and compared with normal criteria value to get the frailty level of his/her elbow flexor muscle. The core idea of this method is that for a suitable dumbbell weight, thee maximum angle that people of different ages and weights can lift is different. Therefore, we can use the ratio of elderly people to normal healthy people to describe the relative frailty level of elderly people.

Besides, we introduce some indicators for evaluating motion control ability and exercise tolerance. An automated method was presented for segmenting resistance data into contraction phase-specific segments during elbow flexor resistance training, for the purpose of establishing an automatic monitoring system for home-based resistance training. The principle of the algorithm was described in detail, and experiments were performed to evaluate the performance of the method. The good agreement in TUT measurements between the proposed algorithm and the assessors indicated that the proposed algorithm can correctly segment the contraction into contraction phase-specific parts, thus providing clinicians and researchers with an automated and objective method for quantifying

home-based elbow flexor resistance training. The objective and automated nature of the segmentation algorithm has the advantage of eliminating the subjective influence of the assessor and improving the rating efficiency.

5. References

[1] Singh M A F, Ding W, Manfredi T J, et al. Insulin-like growth factor I in skeletal muscle after weight-lifting exercise in frail elders[J]. American Journal of Physiology-Endocrinology And Metabolism, 1999, 277(1): E135-E143.

[2] van Praag H. Exercise and the brain: something to chew on[J]. Trends in neurosciences, 2009, 32(5): 283-290.

[4] Barber S E, Clegg A P, Young J B. Is there a role for physical activity in preventing cognitive decline in people with mild cognitive impairment?[J]. Age and ageing, 2011, 41(1): 5-8.

[5] Gleeson M, McFarlin B, Flynn M. Exercise and Toll-like receptors[J]. Exerc Immunol Rev, 2006, 12(1): 34-53.

[6] Handschin C, Spiegelman B M. The role of exercise and PGC1α in inflammation and chronic disease[J]. Nature, 2008, 454(7203): 463.

[7] Rathleff C R, Bandholm T, Spaich E G, et al. Unsupervised progressive elastic band exercises for frail geriatric inpatients objectively monitored by new exercise-integrated technology—a feasibility trial with an embedded qualitative study[J]. Pilot and feasibility studies, 2017, 3(1): 56.

[8] Pollock, Michael L., et al. "The recommended quantity and quality of exercise for developing and maintaining cardiorespiratory and muscular fitness, and flexibility in healthy adults." Medicine and science in sports and exercise 30.6 (1998): 975-991.

[9] Cavanagh P, Evans J, Fiatarone M, et al. Exercise and physical activity for older adults[J]. Med Sci Sports Exerc, 1998, 30(6): 1-29.

[10] Fukagawa, Naomi K., et al. "The relationship of strength to function in the older adult." The Journals of Gerontology Series A: Biological Sciences and Medical Sciences 50.Special_Issue (1995): 55-59.

[11] Buchner, David M., et al. "Effects of physical activity on health status in older adults II: Intervention studies." Annual review of public health 13.1 (1992): 469-488.

[12] Lexell, Jan, Charles C. Taylor, and Michael Sjöström. "What is the cause of the ageing atrophy?: Total number, size and proportion of different fiber types studied in whole vastus lateralis muscle from 15-to 83-year-old men." Journal of the neurological sciences 84.2-3 (1988): 275-294.

[13] Ikai, Michio, and Tetsuo Fukunaga. "Calculation of muscle strength per unit cross-sectional area of human muscle by means of ultrasonic measurement." Internationale Zeitschrift für Angewandte Physiologie Einschliesslich Arbeitsphysiologie 26.1 (1968): 26-32.

[14] Soma, Toshio, et al. "Electromyography analysis of shoulder joint muscles in standing with three ambulatory aids." Journal of Physical Therapy Science 19.2 (2007): 117-123.

[15] Mathie, Merryn J., et al. "Accelerometry: providing an integrated, practical method for long-term, ambulatory monitoring of human movement." Physiological measurement 25.2 (2004): R1.

[16] Maughan, R. J., Jennifer S. Watson, and J. Weir. "Strength and cross ‐ sectional area of human skeletal muscle." The Journal of physiology 338.1 (1983): 37-49.

Chapter 5

Application of the System for Muscle Rehabilitation

1. Introduction

After assessment of frailty, intervention is needed in the treatment of frailty. As we have mentioned in Chapter 1, the exercise intervention is the most common used or, to some extend, the most effective way to release the frailty symptom. Strength training is acknowledged as a means of preventing or delaying frailty and loss of function [1], recommended by national health organizations, such as the American College of Sports Medicine (ACSM) and the American Heart Association [2,3]. The ACSM's position stand [3] on exercise for older adults recommends that exercise prescription for frail people is more beneficial than any other intervention (e.g. caloric and protein support, vitamin D, and reduction of polypharmacy), and that the contradictions to exercise for this population are the same as those used with younger and healthier people.

Accommodating resistance devices such as bands and chains are useful methods to maximize gains in strength and hypertrophy, and these methods are frequently remanded to frail elderly hospitalized patients [1,4]. The population in need of physical rehabilitation is constantly increasing, however the situation is that most people, especially those frail elderly adults [5,6], lack of easy access to public rehabilitation centers, as a result of financial or physical constraints or limited therapist availability [5,7]. Even though the increase in the number of rehabilitation therapists has outpaced the population growth in recent years [8], there is still a shortage of trained rehabilitation service providers in aging societies. After the physiotherapist provides the patient with initial instructions on how to perform the exercise, trainees need to complete the entire training program on their own. However, without the supervision of a therapist, one of the biggest challenges of home-based resistance training is that the therapist may not know if the patient has

performed the exercise as prescribed. Therefore, an exercise monitoring system is necessary and useful for home-based trainees in order to quantify the exercise dosage, and most importantly, to improve their adherence to the training program.

Moreover, exercise is usually accompanied by muscle fatigue. The fatigue and the recovery rate reflect the metabolic capacity of the patient, providing the physiotherapist with an intuitive perception of the subject's exercise capacity. Numerous methods have been proposed to monitor muscular fatigue associated with exercise [9,10] and surface electromyography (sEMG) is the most common one [9,11,12,13]. The regression slope of the linear regression of median frequency has been used as an important muscle fatigue index [12]. Recently, some fatigue-recovery protocols were deliberately designed to study the fatigability and the recovery ability of knee extensor muscle under intermittent, isometric, or dynamic maximal voluntary contractions in old adults [14,15,16]. Knee extension torque and power were measured using a dynamometer and the fatigability and recovery ability were expressed as reductions and increases in torque, velocity, and power.

Monitoring and assessing a subject's response to exercise allows the physiotherapist to have an intuitive perception about his exercise capacity, which plays a significant role in designing appropriate exercise programs and choosing individualized training doses. This section is the application of our system in the field of rehabilitation. Firstly, we use the musculoskeletal model established in Chapter 2 to estimate muscular states during elbow flexor resistance training for bedridden patient. Later, the

2. Estimating muscular states during elbow flexor resistance training for bedridden patient

Frail people are characterized by low physical activities. Bedridden patients have the characteristics of low physical activities. The prolonged bedridden behavior of elderly people will exacerbates skeletal muscle wasting and consequently results in the declining of physical function [17,18]. The decreased physical function increases patient's

dependence on bed rest, which in turn exacerbates the patient's condition. In order to reverses this exacerbation, appropriate and effective exercises are required during patient's bed rest [19]. Here, by using the musculoskeletal modeling method described above, we estimate the muscular states during elbow flexor resistance training for bedridden patient. The simulation results revealed the contribution of each muscle in the flexing process. The design concepts of the system, measurements and analysis methods will be introduced in detail.

2.1 Measurements and analysis methods

2.1.1 Design concepts of the system

Figure 5.1 illustrates the design concepts of the system. For simplicity of the system, we only use one load cell to measure the time-varying resistance force during the training. The measured resistance force is an external variable and its resulting power and work doesn't contain details of stimuli experienced by muscles. Therefore, we established an elbow-joint angle estimation model (EJAEM), a musculoskeletal model (MSM) and a muscle-tendon model (MTM) (described and established in Chapter 2) to estimate muscular states during the training. The EJAEM serves as an analytical description of the experimental setup and it enables real-time interaction between patient and MSM. The MSM is a three-dimensional model of the upper extremity, including major muscles make up the elbow flexor and extensor, and was built base on public data [20, 21]. MSM provides kinematics and kinetics required in optimization of MTF and estimation of muscular states. The MTM was established to estimate the active and passive muscle fiber force for the reason that the optimized MTF is resultant force of active and passive muscle fiber force, and the power of active muscle fiber force is meaningful for evaluation of muscles.

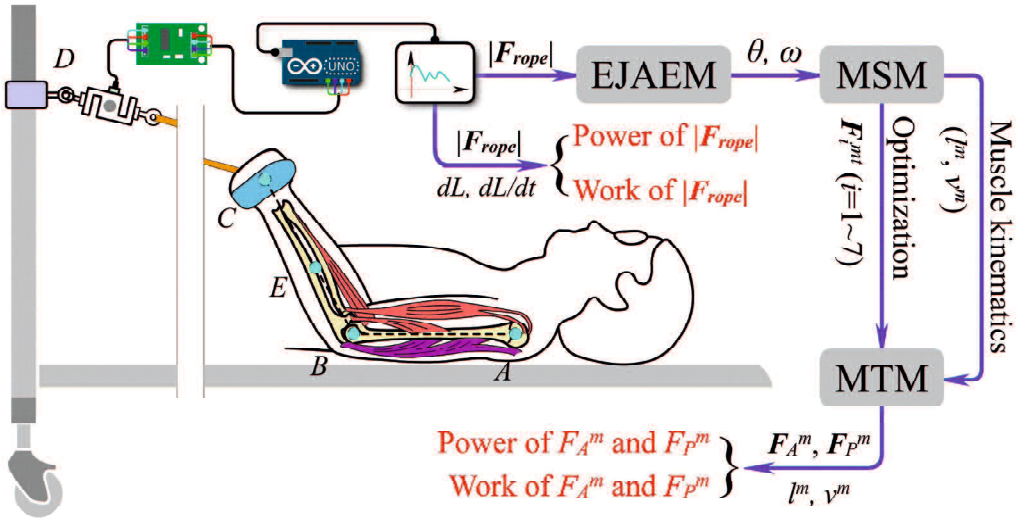

Figure 5.1 Design concepts of the system and data flow in estimation. θ is the elbow joint angle and ω is the angle velocity. |Frope| is resistance force. dL and dL/dt is length change and change rate of the Thera-Band. FAm and FPm is active and passive muscle fiber force. lm and vm is muscle fiber length and velocity. Fimt is the optimized MTF. |Frope| represents mechanical stimuli measured at the body-level and the FAm, FPm, lm and vm represent mechanical stimuli estimated at the muscle-level.

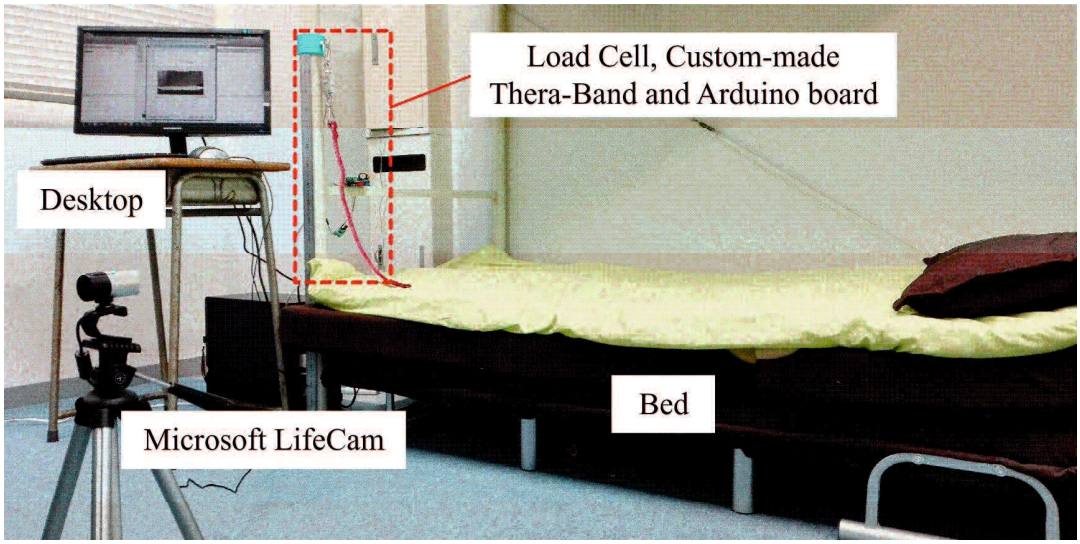

Figure 5.2 Layout of the experimental setup.

Figure 5.2 shows layout of the experimental setup. In the training, patient is positioned in bed in supine with his forearm flexing or extending to oppose resistance force produced by a custom-made Thera-Band. The Thera-Band is connecting with a load cell which is anchored to bed by a lifting hook and utilized to record resistance force posed by Thera-Band. Force data is converted to digital signal by an A/D converter and sent to desktop using Arduino board. The web camera is utilized to record video of the forearm movement and the recorded video was used to calculate real elbow joint angle for test of

the measuring system.

2.1.2 The elbow-joint angle estimation model

The EJAEM plays an essential role in kinematic and kinetic analysis of forearm movement. Figure 5.3 illustrates the physical model used to estimate elbow joint angle and it includes the coordinates and geometrical parameters about the training setup. In the model, L, L_1 and L_2 denote length of Thera-Band, forearm and upper arm. S_1, S_2 represents x-coordinate of elbow and shoulder joint. A, B, C and E denotes position of shoulder, elbow, hand and center of gravity. One end of the load cell is connecting with the bed at point D by using a lifting hook and other end connecting with Thera-Band. θ denotes the elbow joint angle.

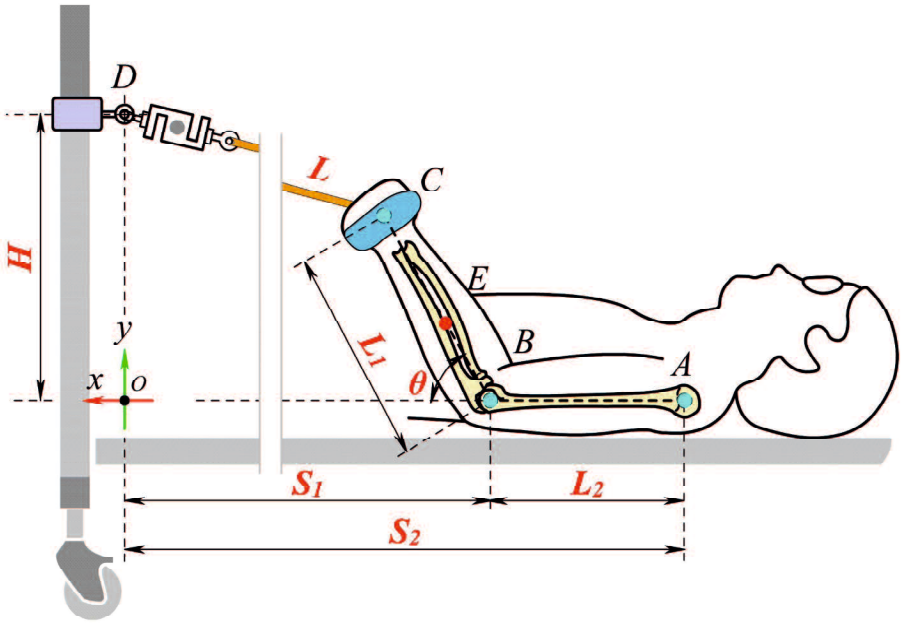

Figure 5.3 Physical model used to estimate elbow joint angle and the geometric parameters and coordinates of the experimental setup. The model is a simplified two-dimensional model in sagittal plane.

As we can see from the physical model, with specific H, S_1, S_2, L_1 and L_2, θ is closely related to current length of Thera-Band L. That implies if we know L, we can predicate elbow joint angle through some simple geometric calculation. As shown in Figure 5.4, we stretched Thera-Band to a series of lengths and recorded the force data to obtain its load-versus-length-change curve.

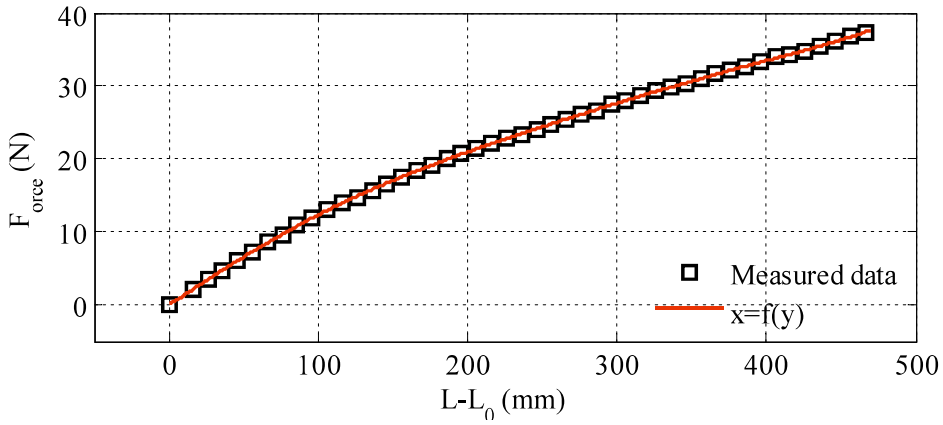

Figure 5.4 Load-versus-length-change curve of the custom-made Thera-Band. L_0 is the initial length of Thera-Band.

Figure 5.4 shows a strong one-to-one relationship between force and length. We use a polynomial equation to approximate the nonlinear relationship between load and length as:

$$L = \Psi_1(|\boldsymbol{F}_{rope}|) \tag{7}$$

where $\Psi_1(x)$ is the polynomial equation of x and its expression is different for different custom-made Thera-Band. $|\boldsymbol{F}_{rope}|$ is the force data recorded from load cell and it is the norm of $\boldsymbol{F}_{rope}$.

According to the physical model, L is a trigonometric function of θ and its mathematical expression can be expressed as:

$$(H - L_1 \sin\theta)^2 + (S_1 - L_1 \cos\theta)^2 = L^2 \tag{8}$$

Because Thera-Band has an initial length L_0 and resistance force is 0 when Thera-Band length is less than L_0, so that the elbow joint angle estimated by EJAEM is never less than the initial angle θ_0. According to (7) and (8), and combine with the recorded $|\boldsymbol{F}_{rope}|$ we eventually get θ as a function of time:

$$\theta(t) = \Psi_2(|\boldsymbol{F}_{rope}|) = \Psi_3(t) \tag{9}$$

Furthermore, we can get the angular velocity ω as:

$$\omega(t) = \frac{d\theta(t)}{dt} = \frac{\Psi_3(t+dt) - \Psi_3(t)}{dt} \tag{10}$$

2.2 Results

2.2.1 Evaluation of the measuring system

Contrastive experiments were carried out to test correctness of the measuring system in estimating elbow joint angle. In experiment, a subject was asked to perform two sets of concentric and eccentric contractions in flexor resistance training (The experiment was conducted with the subject's understanding and consent). Initial configurations of training set-up were measured using rulers and typed into the model (S_1=1080mm, S_2=1384mm, L_1=270mm, L_2=304mm, L_0=870mm, H=230mm). We recorded the video and measured the real elbow joint angle by using protractor and compared it with that estimated in EJAEM. As we can see from results illustrated in Figure 5.5, elbow joint angle estimated in EJAEM shows a good consistency with that measured from video except when angle is less than initial angle θ_0. This is because when $|\boldsymbol{F}_{rope}|$ is zero we set rope length at its initial length in program. Calibration was performed to eliminate the time-delay caused by software and hardware. The good consistency between measured and estimated result demonstrates that this measuring system can correctly estimate elbow joint angle when forearm flexes or extends in sagittal plane.

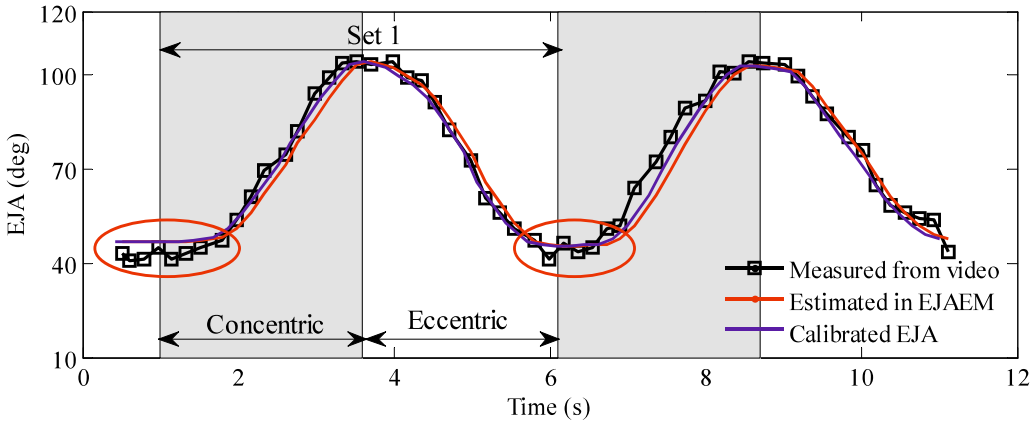

Figure 5.5 Comparison of elbow joint angle measured from video and that estimated in EJAEM.

2.2.2 Evaluation of the musculoskeletal model

The MSM provided by Garner [20, 21] is a detailed three-dimensional model of the human upper-limb. But the EJAEM in this paper is a simplified two-dimensional model in sagittal plane. Therefore, we projected muscles into the sagittal plane, calculated muscle length and moment arm, and compared them with results provided by Garner [22], Lemay [23] and Garner [21] as an evaluation of the MSM. Their results were obtained by using anatomical or experimental data. As illustrate in Figure 5.6 and Figure 5.7, muscle length and moment arm were calculated as a function of elbow joint angle with shoulder joint at neutral position, humerus in parallel with y axis of thorax and elbow joint angle varied from 0° to 150°. We use polynomial coefficients of muscle length and moment arm provided by Pigeon and Lemay, which were approximated by using anatomical or model data, and point data of moment arm illustrated in Garner [21]. Lemay only provides length changes of muscle length so we use the constant portion of muscle length provided by Pigeon [22]. The muscle length and moment arm estimated in this model demonstrate a substantial agreement with that provided in their documents, especially the moment arm compared with Garner. Data used in this model originate from Garner but we use different method in calculating moment arm. Garner calculated the moment arm by computing the derivative of muscle length with respect to joint angle [21]. Good coherence of muscle length and moment arm demonstrates that the established MSM captures important mechanical features of muscles across elbow joint and is adequate to serve as a generic model to analyse muscle kinematics in the case of elbow flexing or extending.

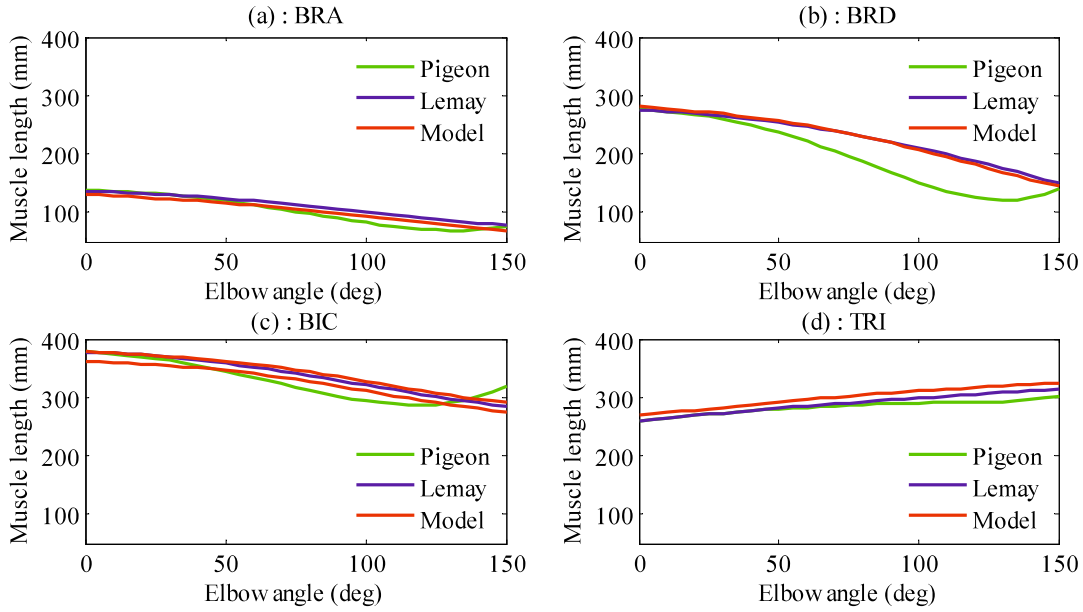

Figure 5.6 Comparison of muscle length as a function of elbow joint angle.

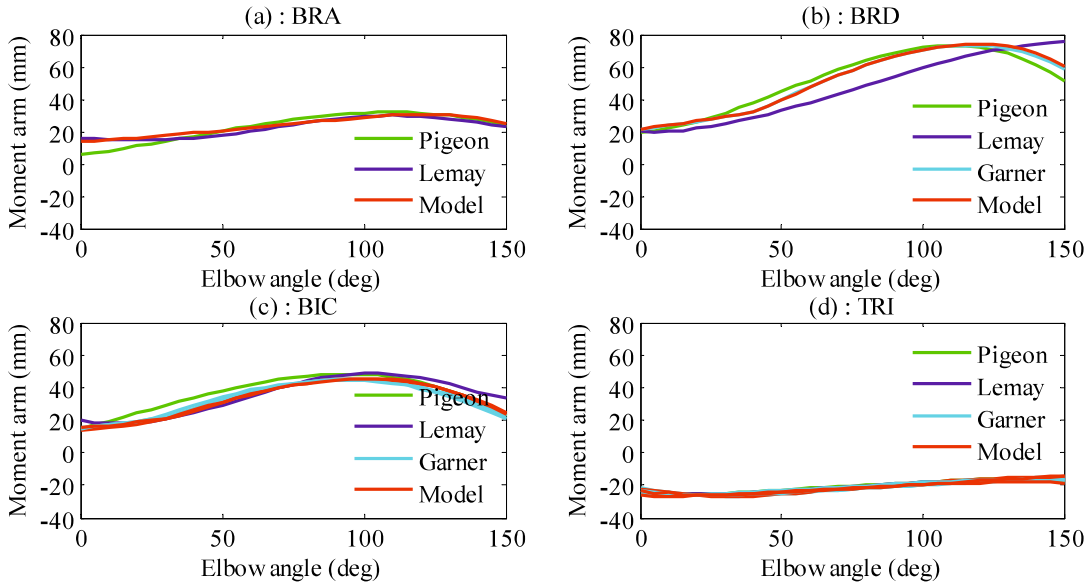

Figure 5.7 Comparison of moment arm as a function of elbow joint angle. Positive values indicate flexion moment arm, negative values indicate extension moment arm. 0° means elbow is fully extended.

2.2.3 Muscular states and mechanical stimuli during flexor resistance training

The muscular state refers to mechanical variables such as the muscle-tendon length changes and the muscle fiber velocity. Mechanical stimuli such as power and work are derivative of those mechanical variables. One set of concentric and eccentric contraction was performed by a healthy subject in flexor resistance training and data were utilized to show body-level and muscle-level stimuli in Figure 5.8 and Figure 5.9, and in Table 5.1. ω,

dL_{rope} and v^m were derivative of θ, rope length and fiber length versus time respectively; power was the product of force and velocity; work was the accumulation of product of force and displacement over each time step; flexor and extensor power was calculated as sum of power of flexor and extensor. Table 5.1 shows work and displacement, as well as the average force of resistance force and muscles. Work is accumulation of the product of muscle fiber force and displacement over each time step. Length change is accumulation of small displacement over each time step and average force is mean value of force.

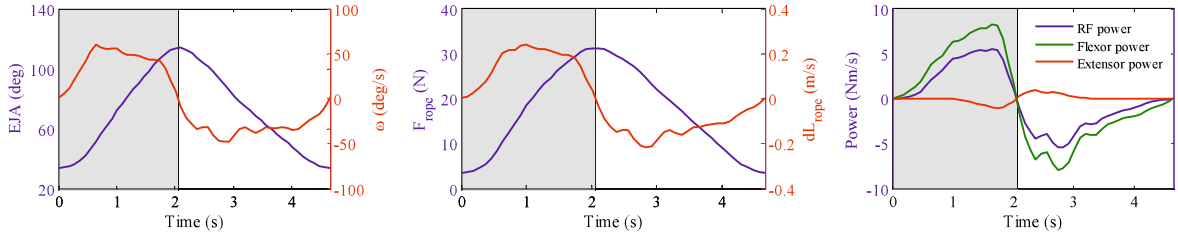

Figure 5.8 The elbow joint angle (EJA), angular velocity (ω), resistance force ($|\boldsymbol{F}_{rope}|$), length change rate (dL_{rope}), power of resistance force, power of flexor and extensor in the training.

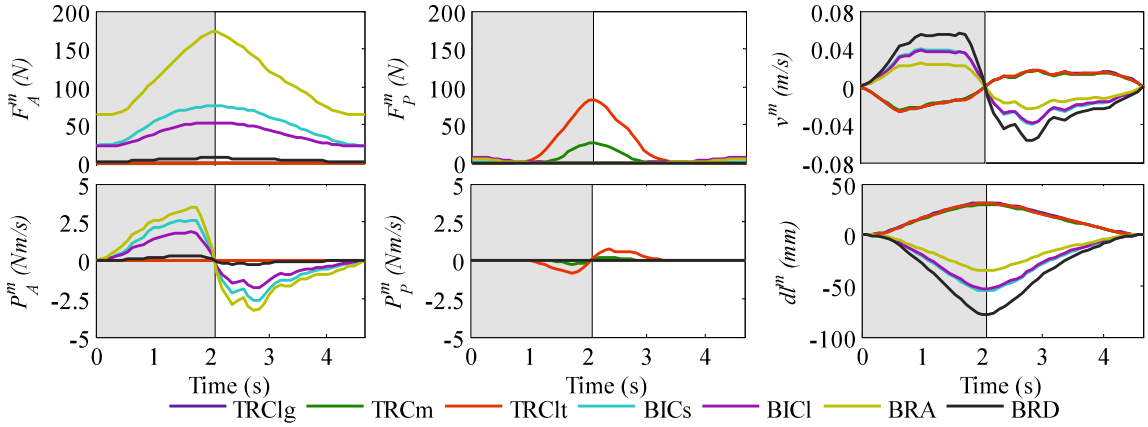

Figure 5.9 The active ($F_A{}^m$) and passive ($F_P{}^m$) muscle fiber force, muscle fiber velocity (v^m), power of active ($P_A{}^m$) and passive ($P_P{}^m$) muscle fiber force, length changes of muscle fiber in the training.

Table 5.1 Work, maximal change in length, average and maximal force of resistance force and muscles. We set direction of elongation along rope or muscle path as the positive direction of force and length change.

	$\lvert\boldsymbol{F}_{rope}\rvert$	Extensor			Flexor			
		TRClg	TRCm	TRClt	BICs	BICl	BRA	BRD
Work (N*m)	-6.24	0	-0.105	-0.502	3.06	2.02	4.03	0.308
Maximal change (mm)	316.04	31.61	30.13	31.34	-55.08	-52.99	-34.89	-78.10
Average force (N)	-17.34	0	-4.98	-20.19	-49.58	-36.62	-109.12	-3.43
Maximal force (N)	-31.27	0	-26.21	-82.76	-74.13	-52.42	-171.93	-5.94

The calculated results show important characteristics about the mechanical stimuli during flexor resistance training. In concentric contraction, resistance force reaches its

maximum within two seconds and the maximal angular velocity is about 50 deg/s. Most of the muscle-level stimuli show a good consistency with the body-level stimuli. For example, near maximal elbow joint angle, the resistance force, active and passive muscle fiber force and length change of muscle fiber reach their maximum or minimum at the same time and their curves show a good consistency. But because of the differences in muscle architecture, the muscle fiber velocity shows a significant difference between flexor and extensor, and the curves of muscle fiber velocity are different from the curve of angular velocity. The resistance force power can be considered as the combined effect of flexor and extensor power. Passive muscle fiber force, which appears when fiber length exceeds its optimal fiber length, affects active muscle fiber force of other muscles. BRA was the biggest energy provider and produced the biggest average and maximal force; this is probably because BRA possesses the biggest PCSA among flexor.

3. Monitoring subjects' fatigue state

3.1 Elbow flexor fatigue and recovery profiles

The average force during ISOM contraction was calculated using the aforementioned algorithm. The force data distributions and the resulted trend lines for all participants are shown in Figure 5.10. For the purpose of comparison, all force data were normalized to the initial value. The decreasing slopes of the average force before and after rest in female and male subjects were analyzed and the statistical result is given in Table 3.3. Table 3.4 reports the statistics of average force recovery in left and right hand after 1-minute rest.

It can be observed in Figure 5.10, that, just as stated in many references that all definitions of fatigue necessitate a decline in force or power, the average force during ISOM contraction decreased continuously. Due to the difference in the initial force, the average force of the right hand decreased faster than the average force of the left hand. It seems that the initial force is related to the decreasing slope of the average force. The Student's t test revealed that there was no significant difference in the decreasing slope

between left and right hands (p = 0.2 and p = 0.14, respectively, Table 3.3). The average force restored to a certain extent after the 1-minute rest, however it decreased much faster than before the 1-minute rest. This was probably because the 1-minute rest does not prevent the development of central fatigue. An inspection of the slopes revealed that the average force of the male subjects decreased faster than that of the female subjects (Table 3.3). Hunter attributed the sex difference in the fatigability of arm muscles to the difference in absolute force. In addition, there was a significant difference in 1MinRec between left and right hands (p = 0.03, Table 3.3), and the recovery ability of the right hand was greater than that of the left hand (Table 3.4).

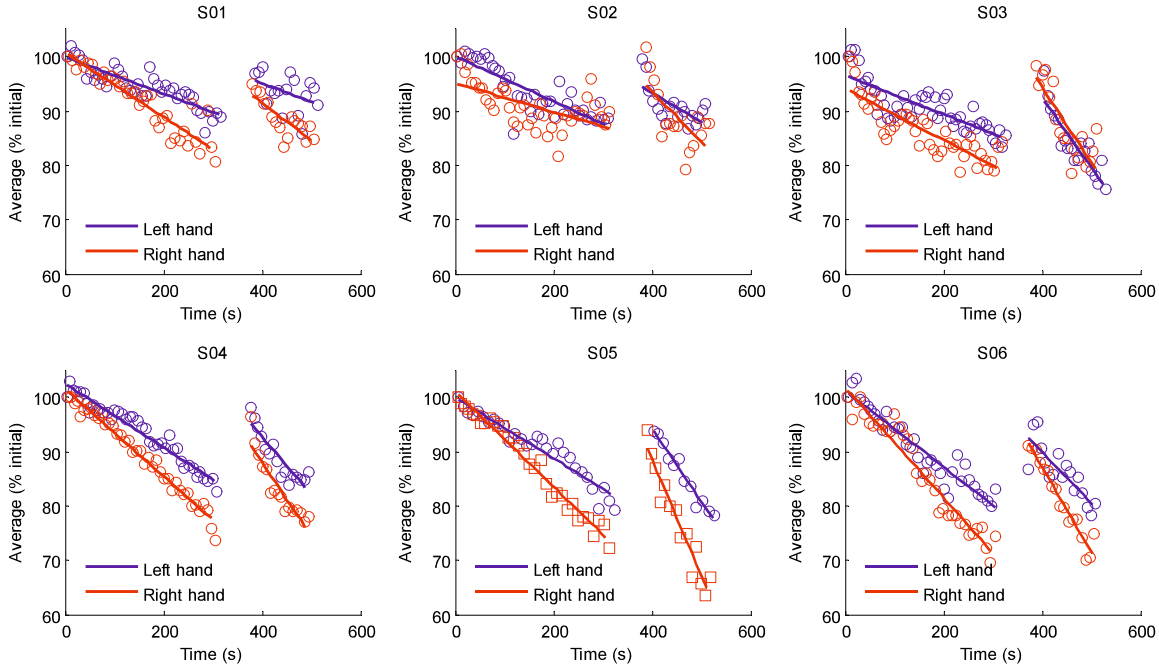

Figure 5.10 Normalized average force distribution and trend lines for all participants.

Table 3.3 Statistics of the decreasing slopes of the average force before and after rest. The smaller the slope, the faster the average force drops. The Student t test was performed to examine the decreasing slope difference between left and right hands. Data is expressed as mean ± standard deviation*. p>0.05**.

	Decreasing slope of average force	
	Before rest (*k1*)	After rest (*k2*)
Female	-0.0407 ± 0.0115*	-0.0860 ± 0.0416*
Male	-0.0758 ± 0.0176*	-0.140 ± 0.0425*
Overall	-0.0582 ± 0.0231*	-0.113 ± 0.0492*
T-test	p = 0.2**	p = 0.14**

Table 3.4 Statistics of 1MinRec in the left and right hand. Data are expressed as mean ± standard deviation; Student test was performed to examine the 1MinRec difference between left and right hands. p<0.05*.

	1MinRec (%Initial)

Left hand	9.968 ± 1.889
Right hand	13.738 ± 3.149
Overall	11.853 ± 3.163
T-test	$p = 0.03$*

3.2 Main parameters affecting subject's fatigue and recovery

According to the experiment data, the average force during ISOM contraction continued to decrease and recovered to some extend after the 1-minute rest. The decrease in average force can be a consequence of central fatigue or muscle fatigue. In the previous section, the decreasing slopes and average force recovery were used to quantify the subject's fatigue and recovery response to exercise. Considering that too high fatigue rates may lead to training-related musculoskeletal diseases or muscle damage, the main parameters that affect subject's fatigue and recovery response should be determined. This would be useful for physiotherapists to choose the suitable training variables when designing resistance training programs. It is easy to imagine that a stronger person will be less prone to fatigue and more likely to recover from fatigue. Thus, a linear relationship between 1RM and decreasing slope, as well as between 1RM and 1MinRec, is assumed.

Although the difference in TUT affects acute fatigue response, the CON, ECC, and rest time in the experiment was not limited and the proportions of TUT varied greatly between subjects. Thus, currently, the variables of interest are the age, weight, 1RM, and initial force. Firstly, linear regression analyses were performed to determine the linear correlation between the above parameters. The analysis results demonstrated a strong linear correlation between 1RM and initial force ($r = 0.93$, $p = 8.96e\text{-}6$). The explanation for the linear correlation is that the combination of bands was chosen according to the subject's 1RM. Many studies have clearly demonstrated the decline in skeletal muscle strength in old age, however there is no significant correlation between age and 1RM ($r = 0.05$, $p = 0.88$). This can be attributed to the narrow age range of the subjects in the present experimental study (ages ranging from 22 to 34 years old). Meanwhile, there was a significant linear correlation between weight and 1RM ($r = 0.82$, $p = 0.001$), which was in line with the fact that heavier people usually have stronger muscles. Then, linear regression

analyses were performed between the variables of interest and the fatigue-recovery indexes (Table 3.5). Due to the fact that there was a significant difference in 1MinRec between left and right hands (p = 0.03, Table 3.4), the linear regression analyses for 1MinRec were performed for the left and right hand, respectively. Figure 5.10 is a trend line plot of the initial force versus the decreasing slope *k1* and of 1RM versus 1MinRec.

According to Table 3.5, contrary to our hypothesis, a negative linear relationship was found between 1RM and *k1* (r = -0.82, p = 0.001), which means that the average force decreased faster in subjects with higher 1RM. This can be explained by the fact that a stronger subject would experience a greater initial force in the experiment, which would result in a faster reduction of the average force. A notable negative linear relationship was found between initial force and *k1* (r = -0.84, $p < 0.001$). That is to say, in stronger subjects, the average force decreases much faster, simply because they have sustained a greater absolute force in the experiment. Therefore, it can be reasonably concluded that the absolute initial force may be a more important variable affecting the decrease in average force compared to 1RM. In addition, a notable positive linear relationship was found between 1RM and 1MinRec. This is in line with our assumption that stronger people are more likely to recover from fatigue. All the above indicate that when designing resistance training programs, special attention needs to be paid to the absolute initial force and recovery ability difference, rather than focusing on the muscle strength of the trainee.

Table 3.5 Linear regression analysis results. A bigger correlation coefficient means a higher linear relationship between two variables. A negative correlation coefficient indicates a negative correlation between two variables. Data are expressed as correlation coefficient (p-value). Data belongs to left hand* and right hand**.

	Age	Weight	1RM	Initial force
k1	0.02(0.95)	-0.73(0.008)	**-0.82(0.001)**	**-0.85(0.0004)**
k2	0.54(0.07)	-0.30(0.34)	-0.52(0.08)	-0.38(0.22)
1MinRec	-0.33(0.52)* -0.18(0.73)**	0.67(0.15)* 0.67(0.14)**	0.77(0.07)* **0.92(0.009)****	0.71(0.11)* 0.76(0.08)**

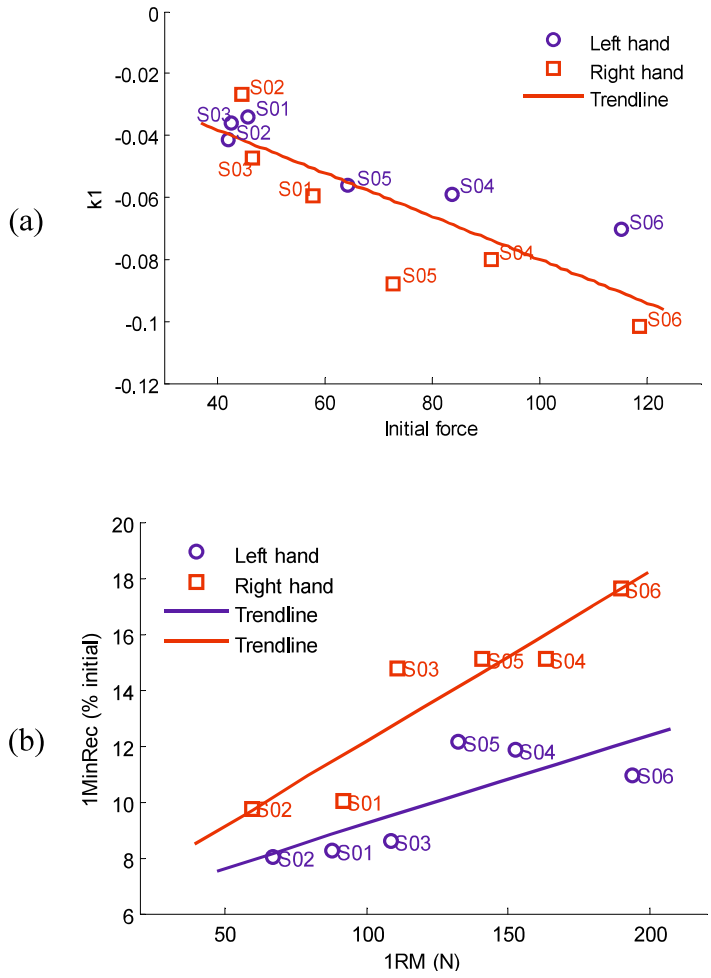

Figure 5.10 Trend line plot for (a): initial force versus *k1* (y = -0.0007x - 0.0103). (b): 1RM versus 1MinRec (y = 0.032x + 6.03 for left hand; y = 0.061x + 6.11 for right hand). The subject's label is marked near each data point.

4. Support system for elbow flexor resistance training

4.1 Support system for active training with dumbbell and resistance band

In this section, we describe the support system used for active elbow flexor resistance training. The first training exercise is biceps curl with a dumbbell. As illustrated in Figure 5.11, a subject is standing in front of a screen with his forearm flexing and extending to lift a dumbbell. Some real-time training results were displayed on the screen. A accelerometer sensor was attached to the lateral side of his forearm and sensor signals were measured and processed by a wireless transmission module and sent to the desktop. A Graphical User Interface (GUI) was built in MATLAB which includes three parts: the musculoskeletal

model (MSM), training plan and the real-time result of time duration during holding parts. The MSM is a detailed, three-dimensional muscle model of human upper-limb and the subject can interact with it in real-time with the accelerometer sensor. At the training plan panel, subject can choose different training intensity according to his training goal.

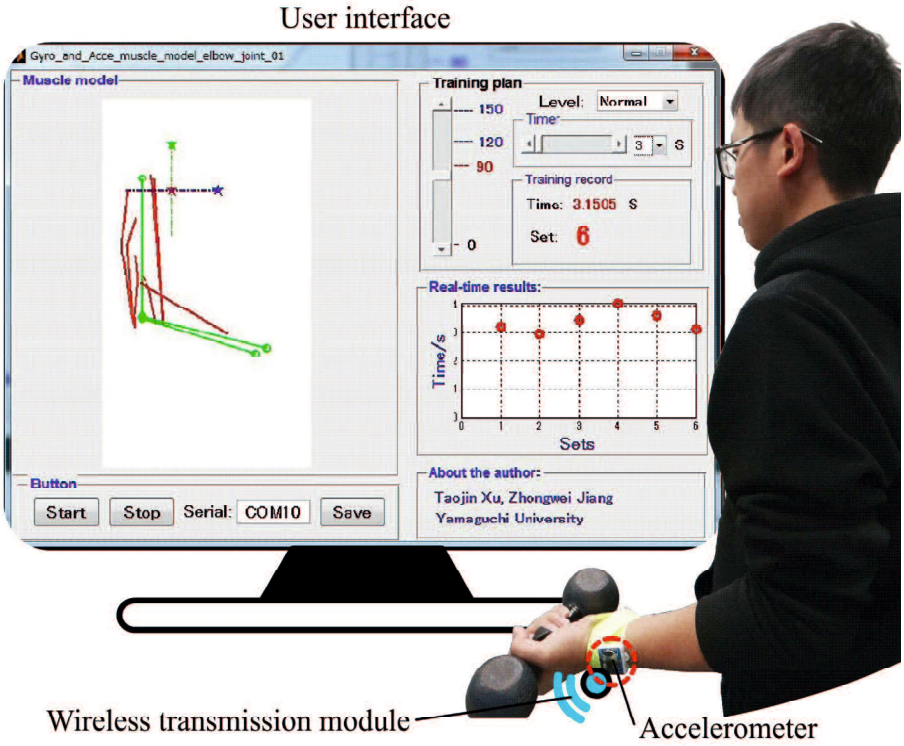

Figure 5.11 Support system for elbow flexor resistance training with a dumbbell.

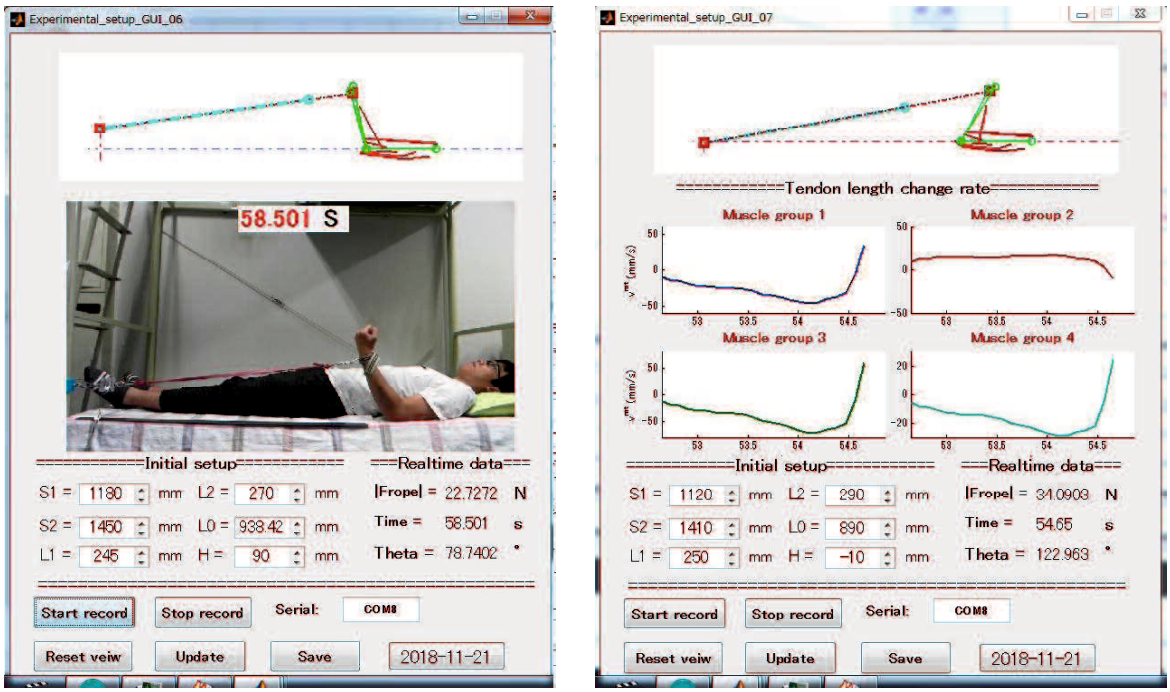

(a) (b)

Figure 5.12 The GUI which is built to show the MSM, muscle velocity (v^{mt}), initial setup and some real-time results. A subject was extending his forearm and the muscle velocity changes over time were showed to users (Muscle velocity reflects state of muscle shortening and stretching. Less than 0 means muscle shortening, and more than 0 means muscle stretching). Muscles were divided into four groups, and the muscle velocity of each group is the average muscle velocity. BICS and BICl belong to Group 1. TRClg, TRClt and TRCm belong to Group 2. BRD belongs to group 3 and BRA belongs to group 4.

As illustrated in Figure 5.12, the second training exercise is biceps curl with a custom-made Thera-Band for bedridden patients. The patient is positioned in bed in supine with his forearm flexing or extending to opposes resistance force produced by a custom-made Thera-Band. The thera-Band is connecting with a load cell which is anchored to bed by a lifting hook and utilized to record resistance force posed by the Thera-Band. Force data is converted to digital signal by A/D converter and sent to the desktop using Arduino board. A muscle model built in Chapter 2 was included in the GUI and the measuring system enables real-time interaction between patient and the muscle model. The real-time interaction increases patient's engagement in the training process. Real-time interaction makes the muscle like a sensor that can be used to measure muscle kinematic parameters such as length and length changes of a muscle.

4.2 Kinematics analysis of a passive training support system

In section 4.1 of this Chapter, we present a support system used for active resistance training with a dumbbell or a resistance band. The users of this system need have the ability to actively lift a dumbbell or stretch a resistance band. However, for patients who have completely or almost completely lost their upper limb mobility, a passive training support system is necessary for them to complete the necessary upper limb activities in daily life, like elbow joint flexing and shoulder joint lifting. As illustrated in Figure 5.13 (a and b), a passive upper-limb training support system is designed to help patients perform necessary upper limb activities in daily life. A subject is siting under the slide and is driven by the slide through ropes to perform upper-limb rehabilitation exercises.

(a) (b)

Figure 5.13 A passive training support system for driving patient perform necessary upper limb activities in daily life. a is the CAD design concept and b is the experimental prototype.

For this passive training support system, an important question is how to control the slide moves to driven subject's upper-limb to complete the desired exercise, which is the forward and inverse kinematics analysis. Here, by using the upper-limb muscle model built in Chapter 2, we designed a GUI for the forward and inverse kinematics analysis of the passive training support system. With this GUI system, designer can conveniently change the angle of the shoulder or the elbow joint, and display the coordinates of the slide and the coordinates of the shoulder, elbow and wrist joints in real time. A simulation results are illustrated in Figure 5.15. In the simulation, the elbow joint angle changes from 0 to 120 degree and the x,y,z coordinates of the wrist joint were calculated. From the simulation results, we can see that the GUI system is capable of performing the forward and inverse kinematics analysis of the passive training support system.

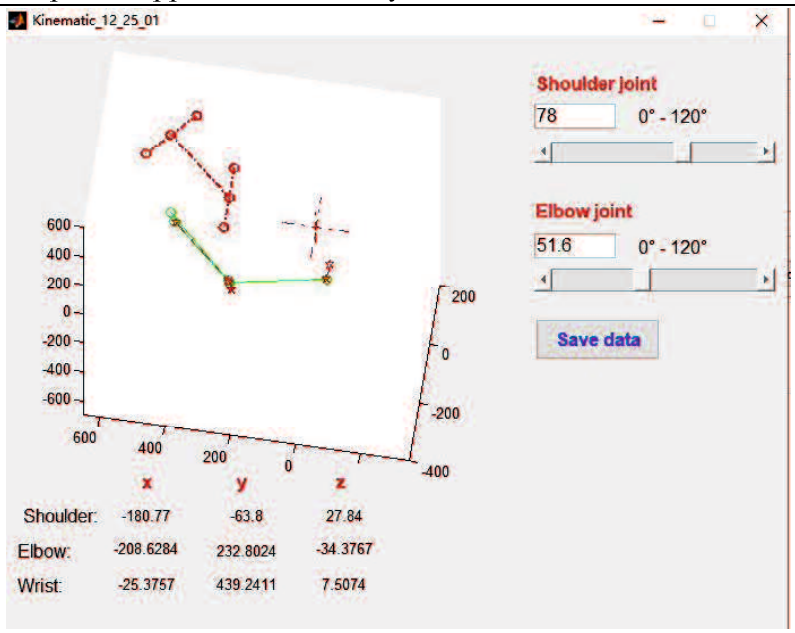

Figure 5.14 The GUI system designed for the forward and inverse kinematics analysis of the passive training support system.

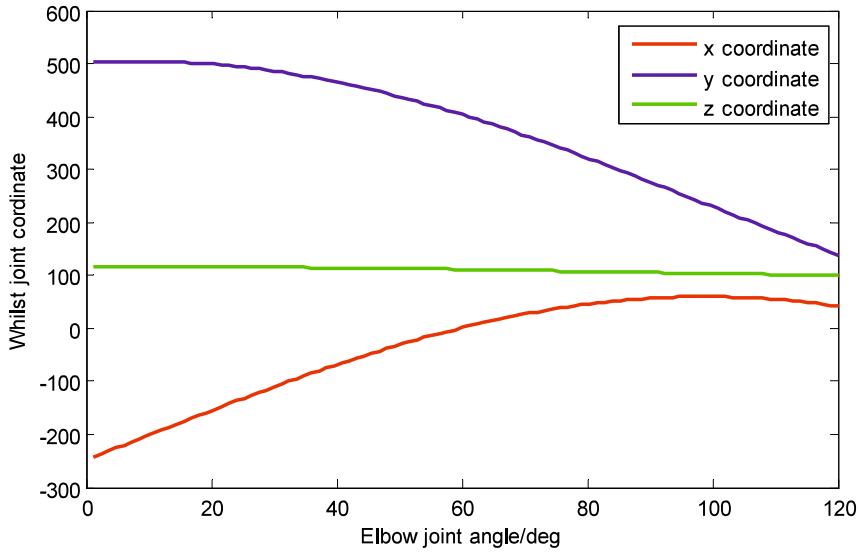

Figure 5.15 The wrist joint coordinates changes with the elbow joint angle.

5. Summary

In this section, we presents the concept of using musculoskeletal modeling to estimate muscular states during elbow flexor resistance training for bedridden patients and it is mainly on the discussion of computational method. We take the elbow flexor RT as a simple example and an integrated system was built for this exercise. The design concepts of the system, the measurement and analysis methods were described in detail. We

recorded the video about the training process and measured the real elbow joint angle by using protractor and compared it with that estimated in EJAEM. Results demonstrate that the measuring system can correctly estimate elbow joint angle when forearm flexes or extends in sagittal plane. The muscle length and muscle moment arms were calculated and compared with results provided in other references to show that the established MSM is adequate to serve as a generic model to analyse muscle kinematics in the case of elbow flexing or extending in sagittal plan. The system offers a simple method to monitor muscle states during elbow flexor RT in bedridden patients, providing coaches or physiotherapists with practical muscle-related information to evaluate the training process. The calculations also demonstrate that the musculoskeletal modeling is a considerable method to vividly analyze the muscular states during training.

In addition, we designed an assistant system for assisting subject do bicep curl resistance training. The training set, period and muscle kinematics parameters were automatically recorded with this system. The measuring system enables real-time interaction between patient and increases patient's engagement in the training process. What's more, we built a GUI system for the forward and inverse kinematics analysis of a passive training support system.

6. References

[1] Rathleff C R, Bandholm T, Spaich E G, et al. Unsupervised progressive elastic band exercises for frail geriatric inpatients objectively monitored by new exercise-integrated technology—a feasibility trial with an embedded qualitative study[J]. Pilot and feasibility studies, 2017, 3(1): 56.

[2] Pollock, Michael L., et al. "The recommended quantity and quality of exercise for developing and maintaining cardiorespiratory and muscular fitness, and flexibility in healthy adults." Medicine and science in sports and exercise 30.6 (1998): 975-991.

[3] Cavanagh P, Evans J, Fiatarone M, et al. Exercise and physical activity for older adults[J]. Med Sci Sports Exerc, 1998, 30(6): 1-29.

[4] Clegg A P, Barber S E, Young J B, et al. Do home-based exercise interventions improve outcomes for frail older people? Findings from a systematic review[J]. Reviews in clinical gerontology, 2012, 22(1): 68-78.

[5] Schutzer, Karen A., and B. Sue Graves. "Barriers and motivations to exercise in older adults." Preventive medicine 39.5 (2004): 1056-1061.

[6] Thiebaud, Robert S., Merrill D. Funk, and Takashi Abe. "Home-based resistance training for older adults: a systematic review." Geriatrics & gerontology international 14.4 (2014): 750-757.

[7] Far, Iman Khaghani, et al. "The interplay of physical and social wellbeing in older adults: investigating the relationship between physical training and social interactions with virtual social environments." PeerJ Computer Science 1 (2015): e30.
[8] Wilson, Richard D., Steven A. Lewis, and Patrick K. Murray. "Trends in the rehabilitation therapist workforce in underserved areas: 1980-2000." The Journal of Rural Health 25.1 (2009): 26-32.
[9] Dong, Haiwei, et al. "Towards whole body fatigue assessment of human movement: A fatigue-tracking system based on combined semg and accelerometer signals." Sensors 14.2 (2014): 2052-2070.
[10] Al-Mulla, Mohamed R., Francisco Sepulveda, and Martin Colley. "A review of non-invasive techniques to detect and predict localised muscle fatigue." Sensors 11.4 (2011): 3545-3594.
[11] Nazmi, Nurhazimah, et al. "A review of classification techniques of EMG signals during isotonic and isometric contractions." Sensors 16.8 (2016): 1304.
[12] Chang, Kang-Ming, Shin-Hong Liu, and Xuan-Han Wu. "A wireless sEMG recording system and its application to muscle fatigue detection." Sensors 12.1 (2012): 489-499.
[13] Al-Mulla, Mohamed R., and Francisco Sepulveda. "Novel feature modelling the prediction and detection of semg muscle fatigue towards an automated wearable system." Sensors 10.5 (2010): 4838-4854.
[14] Callahan, Damien M., Stephen A. Foulis, and Jane A. Kent-Braun. "Age-related fatigue resistance in the knee extensor muscles is specific to contraction mode." Muscle & Nerve: Official Journal of the American Association of Electrodiagnostic Medicine 39.5 (2009): 692-702.
[15] Callahan, Damien M., Brian R. Umberger, and Jane A. Kent. "Mechanisms of in vivo muscle fatigue in humans: investigating age-related fatigue resistance with a computational model." The Journal of physiology 594.12 (2016): 3407-3421.
[16] Sundberg, Christopher W., et al. "Mechanisms for the age-related increase in fatigability of the knee extensors in old and very old adults." Journal of Applied Physiology (2018).
[17] Bloomfield SA. 1997. Changes in musculoskeletal structure and function with prolonged bed rest[J]. Medicine and science in sports and exercise. 29:197-206.
[18] Hoogerduijn JG, Schuurmans MJ, Duijnstee MSH, et al. 2007. A systematic review of predictors and screening instruments to identify older hospitalized patients at risk for functional decline[J]. Journal of clinical nursing. 16:46-57.
[19] Convertino VA, Bloomfield SA, Greenleaf JE. 1997. An overview of the issues: physiological effects of bed rest and restricted physical activity[J]. Medicine and science in sports and exercise. 29:187-190.
[20] Garner BA, Pandy MG. 1999. A kinematic model of the upper limb based on the visible human project (vhp) image dataset[J]. Computer methods in biomechanics and biomedical engineering. 2:107-124.
[21] Garner BA, Pandy MG. 2001. Musculoskeletal model of the upper limb based on the visible human male dataset[J]. Computer methods in biomechanics and biomedical engineering. 4:93-126.
[22] Pigeon P, Yahia LH, Feldman AG. 1996. Moment arms and lengths of human upper limb muscles as functions of joint angles[J]. Journal of biomechanics. 29:1365-1370.
[23] Lemay MA, Crago PE. 1996. A dynamic model for simulating movements of the elbow, forearm, and wrist[J]. Journal of biomechanics. 29:1319-1330.

Chapter 6

Conclusion

6.1 Summary and contribution

As the society ages, the number of elderly people in frailty state or have a risk of being in frailty state increases exponentially, highlighting the importance of assessing frailty and choosing the appropriate intervention for slowing the progress of frailty. According to a survey performed by Ministry of Health, Labour and Welfare of Japan, frailty is the third leading factor that inhibit healthy life expectancy. Therefore, in order to extend people's healthy life expectancy, it is important to recognize the frailty of the body at an early stage and slow its progress through intervention treatment. Focusing on the physical domain of frailty and those people in apparently vulnerable and mildly frail stage, this presents a muscle function evaluation and training support system for the purpose of slowing the progress of frailty.

After searching the common frailty screening criteria, like the Fried Criteria, the J-CHS Criteria, the Kihon checklist and the functional test for upper and lower extremity, we found that the evaluation of physical frailty mainly focus on oral function, mobility and upper limb function. Quantitative indicators like bite force, muscle mass, walking speed and muscle strength are commonly used to quantify physical frailty symptom. The muscle strength, motion control ability and exercise tolerance are important aspect of muscle function and are closely related to the ability to perform activities in daily life. On the other hand, since the comprehensive evaluation indicators of frailty has not been established yet, the means and methods for assessing frailty are highlights of recent research.

To solve the above problems, in this paper, we firstly established an analysis muscle model to estimate muscle strength and established a motion capture system to measure

upper limb movement. Based on the muscle analysis model, a system for evaluating muscle function was developed from the perspective of exercise volume. In addition, based on the evaluation method of muscle function, indexes for frailty evaluation were proposed. Furthermore, in order to delay the progression of muscle frailty, we established a strength training support system that can help trainee perform the appropriate exercise while recording the frailty state.

More detailed, firstly, we presents the concept of using musculoskeletal modeling to estimate muscular states and a detailed three-dimensional model of the upper extremity, including major muscles make up the elbow flexor and extensor, was built base on public references and database. Moreover, the exercise of biceps curl to lift a dumbbell was simulated to provide physiotherapists with good instructions to design the training exercise. The simulation results reveal that: 1. If you want get a more balanced force-sharing of muscle force across the elbow joint, please put your palm faces up; 2. The stretching effect on your BRD muscle is best when you forearm is at neutral position; 3. In order to avoid excessive concentration of muscle force, you'd better not put your palm faces down. The calculation results also demonstrate that musculoskeletal modeling is a considerable method to vividly show the muscular states during the training.

Later, we established a measurement system for muscle function measurement and evaluation. The design concepts and sensor technology are described in detail. The measurement system incorporates an motion capture system and a custom-made Thera-Band. The motion capture system is built based on inertial and visual sensing for recognizing and recording movements of trainee when doing exercise. The Thera-Band is used to help subject do resistance training and the resistance force is recorded through a load cell. In addition, a repetition segmentation and a muscle action segmentation algorithm are proposed to obtain force segments during different contraction phases and the performance of the segmentation algorithm was evaluated. Since during different contraction phase, the role of muscle is different. The force data during different phase can be utilized to quantify subject's muscle function. At last, after obtaining the segmented

force data, indexes for quantifying muscle fatigue and recovery ability, motion control ability and exercise tolerance were proposed to built a muscle function evaluation system.

Furthermore, based on the segmentation algorithm and indexes proposed in Chapter 3, we evaluate physical frailty from the perspective of muscle function. An experiments of multiple subjects was carried out and the muscle motion control ability and exercise tolerance of their elbow flexor were evaluated. We use the quotient of acceleration and deceleration time during flexing stage to quantify motion control ability of elbow flexor. A larger quotient means a longer acceleration phase and a stronger ability of subject to control his flexor muscle. The coefficient of variation of force data during holding phase was used to quantify exercise tolerance. A bigger coefficient of variation means a bigger fluctuation in force, indicating a low ability of subject in keeping the force at a constant value. By using those indexes, the physical frailty state of subject can be determined.

Finally, we describes the application of our system in the field of muscle rehabilitation. We designed an support system for assisting subject do bicep curl resistance training. The training set, period and muscle kinematics parameters were automatically recorded with this system. The measuring system enables real-time interaction between patient and increases patient's engagement in the training process. With the established muscle model in Chapter 2, training results can be displayed to the patient in real-time so that the patient can choose the appropriate training dose based on his feeling or the instruction of physiotherapist.

6.2 Limitations and future work

We lack senior participants in our experiment and we did that with realistic considerations. In Japan, there are some formalities that are required to obtain an ethical license to experiment with older people. Moreover, unlike healthy people, the equipment used by older people needs to be safer and more reliable. There is still some work to be done to make this instrument simple and convenient to use, especially the measurement

system. It is a long way to go to make a smart, cheap, friendly and widely accepted training instrument, especially for the elderly at home. In our research plan, senior participants will be included, after improving our instrument and obtaining permission from the rehabilitation center and Medical Ethics Committee.

Acknowledgement

I would never have been able to finish my dissertation without the guidance of my supervisor, help from friends, and support from my family. First, I would like to gratefully and sincerely thank the most important people in my life, Professor Zhongwei Jiang, for his guidance, unconditional support, understanding, patience, and his friendship during my graduate study at Yamaguchi University. During the study in Japan, he always patiently guided me the professional knowledge, taught me the right way to find and solve problems of the research. Above all and the most needed, he provided me unflinching encouragement in various ways. His truly scientist intuition has made him as a constant oasis of ideas and passions in science, which exceptionally inspire and enrich my growth as a student, a researcher want to be. I also want to show my acknowledgment to Professor Xian Chen, Professor Minami Kazuyuki, Associate Professor Fujii Fumitake and Associate Professor Minoru Morita who are the members of the dissertation committee for evaluating my thesis. Thank you very much for your invaluable comments and suggestions to revise the thesis better.

In addition, I also want to thank all of my colleagues in the Micro-mechatronics laboratory, especially Associate Professor Mamiko Koshiba, Ting Tao, Jingjing Yang, Yu Fang, Yuzhou Luo, Jongyeob Jeong, Hiroyuki Omiya, Jiyao Zhao, Penghao Du, Yunjin Zhang, for your kind help no matter in the research or in life.

The last but not least, deepest appreciations are extended to my beloved parents. They are great inspiration to me, and they invested so much in educating me and always encourage me to cover whatever problems I met. Their selflessly dedicate, support, love, relentless patience, and sacrifices have been a pillar of strength for me whenever I felt exhausted.

Xu Taojin